Three Essays on Environmental and Health Economics

By

Bing Yang Tan

Dissertation

Submitted to the Faculty of the

Graduate School of Vanderbilt University

in partial fulfillment of the requirements

for the degree of

DOCTOR OF PHILOSOPHY

in

Economics

June 30, 2021

Nashville, Tennessee

Approved:

Matthew Zaragoza-Watkins, Ph.D.

Christopher (Kitt) Carpenter, Ph.D.

Mark A. Cohen, Ph.D.

Michelle Marcus, Ph.D.

TABLE OF CONTENTS

LIST OF TABLES

LIST OF FIGURES

Chapter 1

Chapter 2

<center>**Chapter 1**</center>

<center>**Plant a tree and save a life: Estimating the health benefits of urban forests**</center>

1.1 Introduction

More than 100 million people, 30% of the population of the United States, live in urban counties.[1] They share this space with more than a billion trees (Nowak & Greenfield, 2018a). In these densely populated counties, the opportunity cost of tree planting may be high (Pandit, Polyakov, & Sadler, Valuing public and private urban tree canopy cover, 2013); every acre of trees is an acre that cannot be used for office buildings, big box stores or parking lots (Conniff, 2018). For this and other reasons, urban tree cover in the United States has been declining in recent years (Nowak & Greenfield, 2018b).

Is the decline worth reversing? There are many costs to maintaining or increasing urban tree cover. Direct costs, which include the costs of purchasing, planting, maintenance of trees and the removal of dead trees, are substantial – so much so that Gary, Indiana eliminated its whole forestry department due to budget cuts in the wake of the Great Recession (Vogt, Hauer, & Fischer, 2015). Closely related to these costs are the liability risks that trees bring; cities are liable if poorly maintained city trees fall and injure people (Vogt, Hauer, & Fischer, 2015). Finally, the opportunity costs of trees – the alternative uses of the land they take up - are especially salient in urban areas, where high population density means that land is already scarce.

---

[1] These refer to the "large central metro" counties in the NCHS 2013 Urban-Rural Classification Scheme for Counties.

What of the benefits? The most attention has been paid to how trees may reduce the urban heat island effect (Conniff, 2018).[2] Other benefits may include the filtration of air pollution, a moderating effect on local air temperatures (Food and Agriculture Organization of the United Nations, 2016), improved water quality by mitigating stormwater runoff from precipitation (Berland, et al., 2017), reduction in electricity use for heating and cooling (Akbari, 2002) absorption of atmospheric carbon dioxide (Demuzere, et al., 2014) and perhaps even reducing crime (Kondo, Han, Donovan, & MacDonald, 2017).

Nonetheless, it is difficult to estimate the benefits of urban forests; cross-sectional estimates are confounded by the varying preferences and constraints of different city governments and different individuals, which are likely correlated with underlying health behaviors and outcomes. As a result, the benefits of urban forests are likely underappreciated (Conniff, 2018).

My paper is the first to provide robust quasi-experimental evidence on how air pollution and human health respond to urban forest loss caused by the accidental introduction of the emerald ash borer, an insect that eats ash trees. Because tree cover is quantified, I estimate the elasticity of air pollution and mortality to forest loss in cities, rather than, as in previous work, the response of health outcomes to an emerald ash borer infestation of unknown severity. This distinction matters because the policy question is not whether cities should welcome invasive insects that eat urban forests, but whether cities should maintain (or improve) urban forests. Using remotely sensed data, I provide an estimate of how much urban tree cover was lost to this shock and assess the channels

---

[2] The urban heat island effect refers to the phenomenon that urban areas experience higher temperatures than peripheral rural areas (Stone Jr. & Rodgers, 2001)

through which a reduction of urban tree cover of this size (up to 5.5%) affects human health outcomes.

Ultimately, I find increases in ambient levels of air pollution and all-cause mortality, with the size of this effect, at a constant elasticity, implying that the presence of forests reduced all-cause mortality rates in urban counties by 29.3%. This reduction amounted to 290000 deaths in 2014, worth a total of $146 billion in 2014 at the FDA's value of a statistical life year.

1.2   Background and identification

Ash trees (*Fraxinus* sp.) are commonly found as a shade tree in urban areas in the United States (Poland & McCullough, 2006). These trees, which comprise up to 10-40% of many urban forests (Coalition for Urban Ash Tree Conservation, 2011), are now under threat from the emerald ash borer *Agrilus planipennis*, the larvae of which severely damage ash trees by causing dieback[3] and death (McCullough, Schneeberger, Katovich, & Siegert, 2015).

The emerald ash borer (EAB) is a beetle native to north-east Asia whose presence in the United States was first reported in the Detroit area in 2002, although it may have been present for substantially longer, likely introduced by infested shipping material (Muirhead, et al., 2006). The natural spread of the EAB is slow, but as the Detroit introduction suggests, human transport of infested wood may disperse EAB infection over long distances (Muirhead, et al., 2006). Even though a federal quarantine has been in place since 2003, the spread of emerald ash borer has

---

[3] Dieback is defined as "the progressive death of twigs and branches which generally starts at the tips" (Pataky, 1996).

continued, and the quarantine is now being lifted as ineffective (USDA Animal and Plant Health Inspection Service, 2018).

The emerald ash borer does not directly harm humans (Oliver, 2014), the public find it difficult to distinguish ash trees from other tree species (Poland & McCullough, 2006), and the emerald ash borer has proven impossible to eradicate (Herms, et al., 2019) with government officials stating that they have "no adequate tools with which to manage" this insect. (United States Government Accountability Office, 2006). Furthermore, while the emerald ash borer spreads naturally over short distance, the rapid spread of this insect is largely through "*unintentional human agency*" (National Academies of Sciences, Engineering, and Medicine, 2019; emphasis added), occurring when humans transport infested wood products like firewood (Donovan, et al., 2013).

That the spread of emerald ash borer is accidental means there is a significant random component to EAB spread (Jones & McDermott, 2018). It does not mean spread is completely random; as a map of infestation (in Figure 1) shows, locations near the original introduction in Detroit are more likely to be infested. To account for the differences in climate (and other regional differences) caused by this correlation, state by 2012 USDA plant hardiness zone[4] and year fixed effects (to be discussed in more detail in section 3.2) are an important part of my identification strategy. However, conditional on being nearby and having a similar climate, substantial randomness remains even between closely connected regions. For instance, the ash borer was

---

[4] "The 2012 USDA Plant Hardiness Zone Map is the standard by which gardeners and growers can determine which plants are most likely to thrive at a location. The map is based on the average annual minimum winter temperature, divided into 10-degree F zones." (U.S Department of Agriculture Agriculture Research Service, 2012)

found in Fort Worth in 2018 but has not been detected in adjacent Dallas almost 3 years later (Tarrant, 2021) despite that city containing 2 million ash trees (Texas Trees Foundation, 2015). Similarly, it was found in Westchester County, NY (a suburb of New York City) in 2014 but was only detected in the adjacent Bronx 5 years later, a period long enough for the insect to spread from the Midwest to Boulder, CO.

Therefore, the spread of emerald ash borer serves as a natural experiment for the effect of tree cover on human health, which is otherwise confounded by factors such as preferential sorting into neighborhoods with more tree cover.

Existing work about the health benefits of urban afforestation includes Jones & Goodkind, (2019), who look at the effects of an urban afforestation program in New York City, MillionTreesNYC, on infant health, relative to surrounding counties which did not implement such a program. They find reductions in premature births and the probability of low birth rate. That emerald ash borer infestation, as a quasi-random shock to forest health, is a good instrument for forest cover has also been recognized. In the medical literature, Donovan, et al. (2013) used county fixed effects models to find that the presence of the emerald ash borer is associated with increases in mortality from cardiovascular disease and upper respiratory tract illness. However, they control for the ash canopy in the county, estimated by multiplying the total forest cover in the county by the statewide proportion of ash trees. [5] The change in the ash canopy is the channel by which the EAB presumably affects human health, making it unclear what their regression estimates. Donovan, Michael, Gatziolis, Prestemon, & Whitsel (2015) also find that the presence of emerald

---

[5] The ash canopy will be measured with error that covaries with treatment, because ash borer infestation reduces the county fraction of ash trees more than the statewide fraction of ash trees.

ash borer is associated with more cardiovascular illness, but their method only controls for observable differences between counties. In fact, they acknowledge that their result appears to be "influenced by uncontrolled differences between EAB and non-EAB counties".

In the economics literature, Jones & McDermott (2018) find using event study models that the emerald ash borer has caused increases in ambient air pollution of up to 50%. These are accompanied by large increases in cardiovascular mortality of up to 26% cumulatively (given that cardiovascular disease mortality comprises over 30% of deaths, these imply very large increases in all-cause mortality). Similar papers include Jones (2018), which finds that emerald ash borer infestation decreases infant birth weight and increases the likelihood of premature birth, and Jones (2019), which finds that emerald ash borer infestation increases non-winter temperatures. However, their omission of most pre-treatment periods[6] from the event study (Schmidheiny & Siegloch, 2020) materially changes their results,[7] making a causal interpretation of their results uncertain.

A related literature estimates the hedonics of tree cover. The health benefits of tree cover may be incorporated into individuals' preferences for trees. Works in this literature include Polyakov, Pannell, Pandit, Tapsuwan, & Park (2015) and Pandit, Polyakov, & Sadler (2013). These papers find that re-vegetating cities are likely to yield benefits to property owners (in terms of property value), particularly if trees are planted on public land. Exploring the extent to which

---

[6] Specifically, they omit dummies for periods before -3 that are in the sample. This omits 4 balanced (and considerably more unbalanced) pre-periods.
[7] Replication results are available on request.

the health benefits of tree cover are valued by property owners may be a productive line of future enquiry.

These studies look at how air pollution and health outcomes respond to emerald ash borer infestations of unknown severity. Unlike them, my paper is the first to use emerald ash borer infestation to quantify the policy-relevant parameter of how ambient air pollution levels and health outcomes respond to tree loss. Additionally, I focus on all-cause mortality [8] rather than cardiovascular and respiratory disease mortality as in Jones & McDermott, (2018) and Donovan, et al. (2013).

1.3   Data and Methods

I focus on the effects of the negative shock to forest cover, caused by emerald ash borer infestation, in urban counties. The higher temperatures and levels of ambient air pollution in urban areas mean that the potential benefits of trees are likely to have the greatest salience. Unfortunately, the opportunity costs of tree planting may be highest here given tighter space constraints in cities. Finally, the damage that emerald ash borer is likely to be largest in urban areas; urban ash trees are more susceptible to infestation; urban environments are stressful for trees (Poland & McCullough, 2006; Greene & Millward, 2018) and urban ash forests are often planted in single-species stands (Poland & McCullough, 2006) which have low genetic diversity (Greene & Millward, 2018).

---

[8] This is of particular interest because it shows whether cause-specific mortality increases are leading to excess deaths, or whether they are "harvesting" individuals who would soon die of other causes. This phenomenon is also known as mortality displacement.

1.3.1 Data

My estimation sample includes annual county-level data between 1990 and 2014. The dependent variables I analyze fall into several categories. First, I use mean Leaf Area Index [LAI, defined as the ratio of green leaf area to land area]) as a measure of forest cover to assess the damage caused by emerald ash borer.[9] This measure, which has been used to assess ash borer infestation (Tremberger, Sunil, Holden, Marchese, & Cheung, 2012; Murfitt, He, Yang, Mui, & De Mille, 2016), is averaged over July to mid-October, the period in the growing season[10] when emerald ash borer larvae are active (Orlova-Bienkowskaja & Bieńkowski, 2016).[11] This is obtained from the Advanced Very High Resolution Radiometer (AVHRR) instrument installed on a series of National Oceanic and Atmospheric Administration satellites.

Second, there are measures of causal channels by which tree cover may affect human health, including mean annual ambient PM2.5, annual temperature maximums and annual temperature minimums[12] (averaged over county from gridded observations at $\sim 1km^2$, $\sim 16km^2$, $\sim 16km^2$ and $\sim 25km^2$ resolution respectively). The use of gridded PM2.5 measurements, derived from both monitor and satellite information, avoids issues stemming from incomplete and potentially endogenous (Grainger & Schreiber, 2019) county coverage by ground pollution monitors.

As measures of human health, I look at age-standardized mortality rates from all causes, cardiovascular disease, and chronic respiratory disease. As a falsification check, I also look at the age-standardized mortality rate from unintentional injuries.

---

[9] No comprehensive data on the prevalence of ash trees are available (Donovan, 2013).
[10] Leaf area index is only sensitive to green leaf cover.
[11] Emerald ash borer adults do not cause significant damage (McCullough, 2020).
[12] More precisely, the annual maximum (minimum) of mean monthly high (low).

I include median household income, unemployment rate, population density, race/ethnicity, weather controls such as temperatures and squared temperatures, precipitation, wind speed, and NAAQS standards as covariates in different models.

The data source for each variable is listed in Table 1, and summary statistics are available in Table 2.

1.3.2 Methods

Denoting county by i and year by t, I evaluate the effect of emerald ash borer infestation in the continental United States using fully saturated[13] (Clarke & Schythe, 2020) event study[14] models. These estimate dynamic treatment effects, which are the coefficients μ_ℓ associated with indicators for the observations of counties ℓ years after tree death from emerald ash borer starts. To use the notation of Sun & Abraham (2020), the specification is:

$$y_{it} = \alpha_i + U_i Y_t + U_i Y_t + S_i C_i Y_t + \sum_{\ell \neq -1} \mu_\ell \mathbf{1}\{t - E_i = \ell\} + v_{it}$$

All dependent variables y_{it}, with the exception of temperature which is an interval variable, are log-transformed so that I can estimate elasticities (Wooldridge, 2013 p.44) as the policy

---

[13] "Binning" is not necessary because there are never treated units and requires the (unlikely in this context) assumption that treatment effects are constant outside the event window (Schmidheiny & Siegloch, 2020).

[14] A slew of recent papers have discussed potential problems with the weights that event studies assign to different treatment cohorts in the presence of heterogenous treatment effects. In Appendix Table A7 and Figure A3 I show using the Sun and Abraham (2020) decomposition that the weights each event study coefficient places on the corresponding event year in each treatment cohort are reasonable – in particular, they are positive and closely correlated with the number of counties in the cohorts.

parameters of interest.[15] I include fixed effects for county μ_i to account for fixed unobservable differences between infested and unaffected counties in my sample.

I stratify the coefficients μ_ℓ by urban status and at the median first year of tree death (2008) to obtain results specific to urban counties where tree death occurred early (up to and including the median). The first stratification is necessary because urban areas are the focus of my study, but an important part of my estimation strategy is to include fixed effects that interact states S_i with USDA 2012 plant hardiness zones C_i. These are then interacted with year fixed effects Y_t (denoted by $S_i C_i Y_t$ in the equation above). These interactions are included to account for climatic and other regional differences between the affected and unaffected counties (apparent in Table 2) which affect environmental health and may vary over time, particularly over 25 years when climate change is occurring. [16] Since many state by plant hardiness zone fixed effects contain only 1 urban county, [17] this estimation strategy requires the inclusion of all counties. The stratification by urban status is then done to obtain results specific to urban counties.

---

[15] Estimates in levels are in Appendix Table A1. While showing similar patterns, they appear to be confounded by differential trends, which are not present in the log specification. It is not possible for specifications in levels and logs to simultaneously have parallel trends unless the outcomes are the same in the base year (McKenzie, 2020).

[16] The assumption here is that the climate trends similarly over time in locations in the same state and plant hardiness zone. By this logic, outcomes of interest are likely to be correlated in these locations. Therefore, I cluster standard errors by state interacted with plant hardiness zone (127 clusters). This also helps address the potential for overly optimistic standard errors from the inclusion of non-urban countries by dramatically reducing the number of clusters relative to clustering at the level of treatment (county, with 3096 clusters). Results are similar if the standard errors are clustered by state (48 clusters).

[17] This is problematic if the sample is restricted to urban counties because the state by plant hardiness zone fixed effect interacted with year will absorb all variation if the fixed effect contains only 1 urban county.

The second stratification, at the median approximate first year of tree death (2008), [18] allows me to estimate event study coefficients from the same set of counties over a long event window (known as the balanced event window) for urban counties where tree death occurred early. Treatment effects in that window are not confounded by changes in sample composition (Goodman-Bacon, 2019; Clarke & Schythe, 2020). Such a window does not exist without stratifying because detections are continuously occurring. In my results, I focus on the balanced event window for early cohorts after stratifying. However, the results absent stratifying (shown in column (8) of Appendix Tables A2-A6) are similar, with the caveats that the changing sample composition makes the results not directly comparable and causes some loss of statistical power (Schmidheiny & Siegloch, 2020).

I determine E_i, the year when tree death from emerald ash borer starts using information, correct as of May 2021, about when emerald ash borer was detected[19] in a county from the Emerald Ash Borer Information Network[20] and the U.S. Department of Agriculture Animal and Plant Health Inspection Service. [21] However, the treatment of interest is not the detection of the insect *per se*; it is damage to the urban forest caused by the insect. There is usually at least a 4 to 6-year lag between infestation and detection and decline and death usually occurs over a 3 to 5-year period

---

[18] Among counties where tree death started up to 2014; counties where tree death started after that are effectively controls (and are coded as such) since my sample ends in 2014. Results are very similar if they are treated as late cohorts.

[19] Detection methods include insect traps, removing the bark from ash logs, and visually inspecting ash trees (U.S. Department of Agriculture Animal and Plant Health Inspection Service Plant Protection and Quarantine, 2020).

[20] This website is "a collaborative effort of the USDA Forest Service and Michigan State University to provide comprehensive, accurate and timely information on the emerald ash borer" (Emerald Ash Borer Information Network, 2021)

[21] There are inconsistencies between the records of detection status and year in these two sources. To address this conservatively, I treat any county where a detection is listed in either source as detected and use the minimum of detection years.

(Herms, et al., 2019; Arsenault, 2020). Therefore, tree death from emerald ash borer infestation is likely to start around 3 years before detection. Since tree death is the treatment of interest, I set the omitted year (year -1 in event timing) to be 4 years before detection. [22] In this context, the choice of an event study is advantageous because it transparently demonstrates the validity of this choice. Pre-trends (which are generally absent from my results) would be present if significant damage occurred before my choice of omitted year.

I also include county fixed effects α_i, year fixed effects Y_t interacted with urban status, and following controls X_{it} interacted with urban status:[23][24]

- log(median household income), because wealthier neighborhoods can more easily afford to green their neighborhoods (Hoffman, Shandas, & Pendleton, 2020) and are less exposed to pollution (Bell & Ebisu, 2012),

- proportion of population that is non-Hispanic White (Jones & McDermott, 2018), and proportion of population that is Hispanic, because communities of color have less green cover (Hoffman, Shandas, & Pendleton, 2020) and are more exposed to pollution (Banzhaf, Ma, & Timmins, 2019; Bell & Ebisu, 2012).

Therefore, the key identifying assumption is that after controlling for:

- income and race/ethnicity,

---

[22] Based on the 4 to 6-year detection lag and the 3 to 5-year progression of decline and death, the range of start of tree decline is 3 years before detection to 1 year after detection. Based on this range, the omitted year should be 4 years before detection based on the standard normalization (Borusyak & Jaravel, 2018).
[23] Interacting all covariates and year fixed effects with urban status ensures that outcomes of non-urban counties only affect the identification of μ_ℓ through the state by hardiness zone and year fixed effects.
[24] The functional forms for covariates are chosen according to the guidelines in Wooldridge (2013, p.193).

- all other factors that impacted every county in the same climatic zone as the infested county,

- all other county-specific factors that stayed constant over time,

the outcomes of interest (leaf area index, PM2.5 levels, all-cause, cardiovascular, and respiratory disease mortality) in uninfested counties reflect what would have happened in the infested counties if emerald ash borer did not affect them. Some robustness checks, including a variety of controls such as log(population), temperatures and squared temperatures, precipitation and squared precipitation, wind speed and squared wind speed, unemployment rate, and log(upwind Leaf Area Index) and indicators for NAAQS standards, are discussed in Section 3.1 and presented in Appendices Tables A2-A6.

1.3.3 Dynamic treatment effects

One reason why I adopt the event study methodology is to estimate dynamic treatment effects (Sun & Abraham, 2020). There are two reasons why treatment effects are likely to increase in magnitude over time. First, the damage caused by emerald ash borer accumulates over several years (Sadof, Mockus, & Ginzel, 2021). Second, exposure to changes in the environment caused by tree loss may have a cumulative effect on humans in addition to the contemporaneous effect. For instance, we will see later that ambient PM2.5 concentrations increases as tree cover falls. Human mortality caused by air pollutants such as PM2.5 may occur contemporaneously or accumulate over time, and the former may be overstated if the pollutants only "harvest sick individuals who were about to die anyway" (Anderson, 2019). Similar to the analysis in Anderson (2019) of cumulative versus contemporaneous treatment effects, I study the sequence of treatment

13

effects, the maximum treatment effect, and its timing to understand the accumulation of health damage from tree loss.

1.4 Results and discussion

1.4.1 Tree loss

I first discuss the results of my event study for Leaf Area Index to quantify the damage from dieback caused by emerald ash borer infestation to city forests. In Figure 3 I show that urban vegetation cover as measured by remotely sensed Leaf Area Index averaged over July to the first week of October (the part of the growing season where emerald ash borer larvae are active) consistently declines after tree death from emerald ash borer starts, with the largest decline being 5.8% (95% CI -11%, -0.9%) in event year 6. It is worth noting that LAI only captures changes in green leaf area. Leaf loss (and as such, a decline in LAI) occurs with dieback caused by emerald ash borer larvae feeding on the inner bark. Unlike loss of green leaf cover in ash trees (which are deciduous), dieback that involves stems (which also trap air pollutants (Nowak, Crane, & Stevens, 2006)) is likely to persist through the non-growing season months.

One limitation of this analysis is that there is no data with which I can apportion loss of LAI to emerald ash borer or other causes (Jones & McDermott, 2018). As such, the parallel trends assumption requires that any other factors that might affect LAI, such as land clearing, trended the same way in uninfested and infested counties. However, since ash trees comprise up to 10-40% of many urban forests (Coalition for Urban Ash Tree Conservation, 2011) and emerald ash borer eventually kills nearly all ash trees in an infested area (Jones & McDermott, 2018), the reductions of 5-6% that I find after several years seem plausible.

1.4.2 Potential channels by which trees affect human health

One channel by which damage to trees is likely to affect human health is through increases in air pollution. As a measure of air pollution, I look at ambient fine particulate matter (PM2.5) levels in affected counties. PM2.5 is one of the largest threats to air quality in the United States and is well measured even historically. However, PM2.5 is not the only pollutant that is potentially abated by trees, and my findings should be interpreted as an indicator of the effect of tree loss on ambient air pollution more generally, in what Dominici, Peng, Barr, & Bell (2012) describe as "the indicator approach", rather than specifically being the effect on PM2.5 levels.

In Figure 4 I show that there are increases in ambient PM2.5 levels in cities following declines in Leaf Area Index due to emerald ash borer infestation, with a maximal increase in annual mean ambient PM2.5 of 4.4% (95 CI 1.8%, 6.9%) in event year 5. Leaves and bark surfaces of urban trees can filter particulate matter from the atmosphere (Nowak, Crane, & Stevens, 2006), so this result is not unexpected even if some particulate matter is only temporarily trapped by vegetation (Nowak, 2002).

Another potential channel by which urban forests could affect health is by moderating urban temperatures. Unlike with PM2.5, I do not find any meaningful changes in temperature maximums and minimums, shown in Appendix Figures A1a and A1b respectively, with the largest change being well below 1°C. For reference, the temperature "bins" with which Deschenes (2014) shows the "U-shaped" effect of temperature on mortality, and within which mortality is assumed constant, are about 5°C wide. The cooling impact of trees comes from two sources; the shade that the tree cover provides, and evaporative cooling from the transpiration of trees (Wimborne, et al., 2020). As temperature data are interpolated from weather station measurements which should be sited in

the open (World Metereological Organization, 2018), my null finding cannot rule out changes in temperatures from a reduction in tree shade. It does however provide evidence against a reduction in transpiration-related cooling, which affects air temperatures at both the local and regional level (Wimborne, et al., 2020).

Since I cannot definitively isolate a pollutant as the single cause of health effects, I focus on the cautious interpretation (Anderson, 2019) which relates to the reduced-form effect of tree cover on mortality. However, in a later section I explore what can be said about the pollution-mortality relationship under stronger assumptions.

1.4.3   Mortality outcomes

The event study for all-cause mortality is displayed graphically in Figure 5 and numerically in Appendix Table A4. Increases in mortality are gradual and reach a maximum of 1.8% (95% CI 0.2%, 3.4%) in the 5th event year. The increase then falls to 1.1% (95% CI -0.6%, 2.9%) over the base year even as tree cover continues to decline and PM2.5 levels are essentially level, which is suggestive evidence of some "harvesting" of individuals who would have died in a later year, but the point estimates remain positive and with only 1 year of such a dip this evidence is not conclusive. The median elasticity of all-cause mortality to city forest loss implied by the 7 post-treatment coefficients in my event studies is 0.42.

Do these increases come from causes that are consistent with increases in air pollution and potentially heat stress? I look at mortality from the causes most closely linked to these environmental causes – cardiovascular disease and chronic respiratory disease (Deschenes, 2014; Anderson, 2019). In Figures 6a and 6b I show increases in mortality from cardiovascular diseases of up to 3.0% (95% CI 1.0%, 5.0%) in the 5th event year and weaker evidence of increases in

mortality from chronic respiratory diseases of up to 2.5% (90% CI 0.2%, 4.8%). Because these diseases make up 34% and 6% of deaths in affected counties respectively, these two causes account for around 2/3rds of the all-cause mortality increases found earlier.

Treating PM2.5 as an index of ambient air pollution and assuming for the moment that greater exposure to heat stress is not a factor, I combine the PM2.5 ("first stage") and mortality results to obtain a back-of-the-envelope estimate of the elasticity of mortality with respect to air pollution (Anderson, 2019). The median elasticity (again over the 7 post-treatment years) is about 0.45, a value that is larger than comparable estimates of the PM2.5-mortality elasticity, such as Jha & Muller (2018) who find an elasticity of 0.11 in adults for PM2.5 alone. This difference may reflect health effects resulting from exposure to both PM2.5 and pollutant mixtures correlated with PM2.5 (Kim, et al., 2007), or it may reflect the difference in time horizons over which the estimates are calculated (monthly in Jha & Muller (2018), versus up to 7 years in my paper).

1.4.4 Robustness of my results

I perform a variety of robustness checks with different specifications to ensure that my results are not idiosyncratic to the base specification. First, I estimate the event studies in levels rather than logs in Appendix Table A1. I also add a variety of controls such as unemployment rate, weather controls such as temperatures and squared temperatures, precipitation, wind speed, and NAAQS standards to the covariates in the base specification. Finally, I estimate a specification that omits covariates altogether. These robustness checks, displayed in Appendix Tables A2-A6, do not substantially change my results (except potentially for chronic respiratory disease mortality).

As a falsification check, I run the same event study regressions as discussed earlier on mortality from unintentional injuries, an outcome that is unlikely to be affected by pollution exposure (Jha & Muller, 2018) or heat stress. Although it is possible that air pollution increases the likelihood of accidents through harming the nervous system (Guo, et al., 2018), the evidence for this is sparser than that for cardiovascular and respiratory disease mortality. I present these event study estimates in Appendix Figure A2. I do not find any significant changes in mortality from unintentional injuries before and after treatment, suggesting that there are no underlying differential trends common to deaths from unintentional injury and cardiovascular/respiratory causes (such as the quality of the local healthcare system) that are driving my results.

Another concern is that the effect in any given county is overestimated because of the spatial correlation of emerald ash borer infestation. This correlation may mean that there are also fewer trees in nearby counties, so that air pollutants are more easily dispersed to urban areas. The first line of defense against this is the state by plant hardiness zone and year fixed effects, which absorb changes in air quality from pollutants that disperse equally across nearby areas. To eliminate the possibility of asymmetric wind distributions causing unequal dispersion of pollutants across these regions, I add as a robustness check a covariate for the mean late growing season leaf area index (the same variable as described above) in locations upwind[25] of each county, where "upwind" is defined with respect to the prevailing wind direction at each county's centroid in each year, interacted with urban status. The addition of this covariate, which in the presence of fixed effects controls for changes in upwind leaf area index, does not meaningfully change my results, which are shown in column (2) of Appendix Tables A2-A6.

---

[25] Restricted to grid cells up to 100km away.

Yet another potential source of bias, especially with the pollution results, are the contemporaneous imposition of policy changes such as new NAAQS standards (Jones & McDermott, 2018). My results are robust to including controls for the presence of a nonattainment designation for the NAAQS standards for PM10, PM2.5, lead, nitrogen dioxide, sulfur dioxide, carbon monoxide, and ozone. Results with these controls are shown in column (3) of Appendix Tables A2-A6.

1.4.5 Policy implications

The most immediate policy implication is that there are important health costs to uncontrolled emerald ash borer spread. The average excess mortality in early affected urban counties amounted to 189 extra deaths a year in event year 5. At the FDA's value of a statistical life year, $490000 (Viscusi, 2020), these extra deaths came at a cost of $92.6 million per early affected urban county. Therefore, devoting more resources to the control of emerald ash borer seems justifiable.

Although substantial, these estimates are meaningfully smaller than previous literature. The increases in excess deaths of 1.8% that I find are caused by emerald ash borer infestation may be compared to the increases in cardiovascular mortality of 14-26% found by Jones & McDermott (2018), which, given that cardiovascular disease causes about a third of all deaths in the United States, imply increases in all-cause mortality of about 4-9% due to cardiovascular mortality alone.

Extrapolating the constant elasticity of 0.42 to all forests in all urban counties in the continental United States, my results imply that the presence of these forests reduced all-cause mortality rates in urban counties by 29.3%. Across all urban counties in the United States, this reduction implies that urban forests were responsible for preventing a total of 299000 deaths in

2014 alone. At the FDA's value of a statistical life year, the value of the life-years saved thereby was $146 billion.[26] Even ignoring other manifestations of ill-health, the mortality benefit substantially outweighs the direct cost of maintaining urban forests. For instance, the entire budget of the City of Chicago's forestry department in 2020 was about $25 million, substantially smaller than the mortality cost of losing a city's tree cover.

Furthermore, the liability risk from falling trees (Vogt, Hauer, & Fischer, 2015) is insignificant relative to the benefits of retaining tree cover. Schmidlin (2009) finds that there were 407 deaths from wind-related tree failures in the United States between 1995 and 2007, or an average of 31 a year. This is dominated by the 299000 deaths I find that the urban forests in the continental United States prevented in 2014.

My results show that urban afforestation has an important role to play in abating air pollution. Not all means of urban afforestation are equal, however, and the planting of trees should be done with care to maintain biodiversity. One of the reasons for why emerald ash borer has been so damaging has been the low genetic diversity of city ash trees (Greene & Millward, 2018). The experience of the emerald ash borer suggests that maintaining high levels of biodiversity is important for urban forests to stay resilient in the face of yet unknown invasive pests and the more extreme climatic conditions of the future.

1.4.6 Limitations

First, I would like to reiterate that while I have identified one plausible channel by which tree cover improves human health, I cannot rule out some others such as increased heat stress from

---

[26] These rather large numbers should be viewed in the context of being the result of a large treatment, since my results are extrapolated to calculate the effect of the loss of the entire urban forest.

reductions in tree shade. Relatedly, my results are identified off the loss of ash trees due to emerald ash borer infestation and may not be generalizable to urban forests made up of other species of tree. I have not found any evidence that ash trees are more effective in filtering air pollution than any other tree species. However, if changes in tree shade are a relevant channel, its effect may be larger in this context because ash trees were often planted for shade (Poland & McCullough, 2006).

While my analysis is at the county level, there is likely a great deal of within-county variation in tree cover (Kondo, Han, Donovan, & MacDonald, 2017). For instance, "redlining" and its influence on tree cover (Hoffman, Shandas, & Pendleton, 2020) likely occurred at a smaller scale than the county. A more detailed accounting of tree cover will allow for more precise estimates of the relationship between urban tree cover and human health. There are no temporally consistent estimates of tree cover that span the variation I use, but future studies using other sources of variation should explore this source of heterogeneity in treatment.

1.5   Conclusion

In this paper I study the effect of a quasi-experimental negative shock to urban forests, stemming from the introduction of the invasive emerald ash borer, on the health of urban residents. Urban tree cover is quantified by remote sensing data, so my estimates reveal the elasticity of air pollution and health outcomes to urban forest loss, which answers the policy-relevant question of whether cities should invest in their forests.

I find that one channel by which trees benefit urban health is by reducing pollution, with dieback that affects up to 4.2% of city forests being associated with increases in mean PM2.5 of up to 4.4%. These increases in ambient air pollution are one plausible cause for the increase in all-cause mortality I find following tree loss, which gradually increase and peak at 1.8% in affected

cities. The median elasticity (across 7 post-treatment years) of all-cause mortality to urban forest loss of 0.42; extrapolating this elasticity to all urban forests in the continental United States, the presence of these forests reduced all-cause mortality by 29.3%, or 299000 deaths total, in 2014. At the FDA's value of a statistical life year, these avoided deaths had a total value of $146 billion.

My results show that urban afforestation is an important way of abating air pollution and thereby improving human health in urban areas, in addition to its potential benefits for urban livability. Such benefits will only become more important as land suitable for development gets scarcer and the cities of the future get denser.

1.6   References

Akbari, H. (2002). Shade trees reduce building energy use and CO2 emissions from power plants. *Environmental Pollution, 116*, S119-S126. doi:10.1016/S0269-7491(01)00264-0

Anderson, M. L. (2019). As the Wind Blows: The Effects of Long-Term Exposure to Air Pollution on Mortality. *Journal of the European Economic Association, 18*(4), 1886–1927. doi:10.1093/jeea/jvz051

Arsenault, A. (2020, March 23). *Tips for Becoming an Emerald Ash Borer Detective*. Retrieved from University of New Hampshire Cooperative Extension: http://web.archive.org/web/20210103062502/https://extension.unh.edu/blog/tips-becoming-emerald-ash-borer-detective

Banzhaf, H. S., Ma, L., & Timmins, C. (2019). Environmental Justice: Establishing Causal Relationships. *Annual Review of Resource Economics, 11*, 377–398. doi:10.1146/annurev-resource-100518-094131

Bell, M. L., & Ebisu, K. (2012). Environmental Inequality in Exposures to Airborne Particulate Matter Components in the United States. *Environmental Health Perspectives, 120*(12), 1699–1704. doi:10.1289/ehp.1205201

Berland, A., Shiflett, S. A., Shuster, D. W., Garmestani, S. A., Goddard, H. C., Herrmann, D. L., & Hopton, M. E. (2017). The role of trees in urban stormwater management. *Landscape and Urban Planning, 126*, 167-177. doi:10.1016/j.landurbplan.2017.02.017

Borusyak, K., & Jaravel, X. (2018). Revisiting Event Study Designs, with an Application to the Estimation of the Marginal Propensity to Consume. *Working Paper*. Retrieved from https://scholar.harvard.edu/files/borusyak/files/borusyak_jaravel_event_studies.pdf

Clarke, D., & Schythe, K. T. (2020). Implementing the Panel Event Study. *IZA Discussion Paper Series* , IZA DP No. 13524. Retrieved from http://ftp.iza.org/dp13524.pdf

Claverie, M., Vermote, E., & NOAA CDR Program. (2020). NOAA Climate Data Record (CDR) of Leaf Area Index (LAI) and Fraction of Absorbed Photosynthetically Active Radiation (FAPAR), Version 5. doi:10.7289/V5M043BX

Coalition for Urban Ash Tree Conservation. (2011, January 6). Emerald Ash Borer Management Statement. Retrieved from www.emeraldashborer.info/files/conserve_ash.pdf

Conniff, R. (2018, May 7). *U.S. Cities Lose Tree Cover Just When They Need It Most.* Retrieved from Scientific American: http://web.archive.org/web/20200811121120/https://www.scientificamerican.com/article/u-s-cities-lose-tree-cover-just-when-they-need-it-most/

Demuzere, M., Orru, K., Heidrich, O., Olazabal, E., Geneletti, D., Orru, H., . . . Faehnle, M. (2014). Mitigating and adapting to climate change: Multi-functional and multi-scale assessment of green urban infrastructure. *Journal of Environmental Management*, 146: 107-115. doi:10.1016/j.jenvman.2014.07.025

Deschenes, O. (2014). Temperature, human health, and adaptation: A review of the empirical literature. *Energy Economics, 46*, 606-619. doi:10.1016/j.eneco.2013.10.013

Dominici, F., Peng, R. D., Barr, C. D., & Bell, L. M. (2012). Protecting Human Health from Air Pollution: Shifting from a Single-Pollutant to a Multi-pollutant Approach. *Epidemiology, 21*(2), 187-194. doi:10.1097/EDE.0b013e3181cc86e8

Donovan, G. H., Butry, D. T., Michael, Y. L., Prestemon, J. P., Liebhold, A. M., Gatziolis, D., & Mao, M. Y. (2013). The Relationship Between Trees and Human Health: Evidence from the Spread of the Emerald Ash Borer. *American Journal of Preventive Medicine, 44*(2), 139-145. doi:10.1016/j.amepre.2012.09.066

Donovan, G. H., Michael, Y. L., Gatziolis, D., Prestemon, J. P., & Whitsel, E. A. (2015). Is tree loss associated with cardiovascular-disease risk in the Women's Health Initiative? A natural experiment. *Health & Place, 36*, 1-7. doi:10.1016/j.healthplace.2015.08.007

Du, Y., Xu, X., Chu, M., Guo, Y., & Wang, J. (2016). Air particulate matter and cardiovascular disease: the epidemiological, biomedical and clinical evidence. *Journal of Thoracic Disease, 8*(1), E8–E19. doi:10.3978/j.issn.2072-1439.2015.11.37

Duan, J. J., Van Driesche, R. G., Bauer, L. S., Reardon, R., Gould, J., & Elkinton, J. S. (2019). *The role of biocontrol of emerald ash borer in protecting ash regeneration after invasion.* Morgantown, WV: U.S. Department of Agriculture, Forest Service, Forest Health Assessment and Applied Sciences Team.

Dwyer-Lindgren, L., Bertozzi-Villa, A., Stubbs, R. W., Morozoff, C., Kutz, M. J., Huynh, C., & Barber, R. M. (2016). US County-Level Trends in Mortality Rates for Major Causes of Death, 1980-2014. *Journal of the American Medical Association, 316*(22), 2385-2401. doi:10.1001/jama.2016.13645

Emerald Ash Borer Information Network. (2021). About This Site. Retrieved from http://www.emeraldashborer.info/about.php

Emerald Ash Borer Information Network. (2021). State & County Detection Table. Retrieved from https://web.archive.org/web/20210424151613/http://www.emeraldashborer.info/state-dectection-table.php

Evans, W. N., & Moore, T. J. (2011). The short-term mortality consequences of income receipt. *Journal of Public Economics, 95*, 1410-1424. doi:10.1016/j.jpubeco.2011.05.010

Flower, C. E., Dalton, J. E., Knight, S. K., Brikha, M., & Gonzalez-Meler, M. A. (2015). To treat or not to treat: Diminishing effectiveness of emamectin benzoate tree injections in ash trees heavily infested by emerald ash borer. *Urban Forestry & Urban Greening, 14*(4), 790-795. doi:10.1016/j.ufug.2015.07.003

Food and Agriculture Organization of the United Nations. (2016). *Benefits of Urban Trees.* Retrieved from http://www.fao.org/3/a-c0024e.pdf

Goodman-Bacon, A. J. (2019, August 25). Only show coefs from "balanced" event-times. You see some units *way* before/after treatment, but only for the earliest or latest treated ones. Those coefs are partly driven by level diffs b/w units like here. See how weird and noisy things get at the end. Retrieved from https://web.archive.org/web/20210502205008/https://twitter.com/agoodmanbacon/status/1165643423413673987

Grainger, C., & Schreiber, A. (2019). Discrimination in Ambient Air Pollution Monitoring?
American Economic Association: Papers and Proceedings, 277-282.
doi:10.1257/pandp.20191063

Greene, C. S., & Millward, A. A. (2018). The Legacy of Past Tree Planting Decisions for a City
Confronting Emerald Ash Borer (Agrilus planipennis) Invasion. *Frontiers in Ecology and
Evolution, 4*, 1-12. doi:10.3389/fevo.2016.00027

Guo, Y., Lin, H., Shi, Y., Zheng, Y., Li, X., Xiao, J., . . . Wu, F. (2018). Long-term exposure to
ambient PM2.5 associated with fall-related injury in six low- and middle-income
countries. *Environmental Pollution*, 961-967. doi:/10.1016/j.envpol.2017.10.134

Hahn, J. (2018). *Emerald ash borer in Minnesota.* Retrieved from University of Minnesota
Extension: https://extension.umn.edu/tree-and-shrub-insects/emerald-ash-
borers#symptoms-of-eab-infestation-1471661

Herms, D. A., & McCullough, D. G. (2014). Emerald Ash Borer Invasion of North America:
History, Biology, Ecology, Impacts, and Management. *Annual Review of Entomology,
59*, 13-30. doi:10.1146/annurev-ento-011613-162051

Herms, D. A., McCullough, D. G., Smitley, D. R., Sadof, C. S., Miller, F. D., & Cranshaw, W.
(2019). *Insecticide Options for Protecting Ash Trees from Emerald Ash Borer.* North
Central IPM Center. Retrieved from
http://web.archive.org/web/20200908095750/http://www.emeraldashborer.info/docume
nts/Multistate_EAB_Insecticide_Fact_Sheet.pdf

Heutel, G., & Ruhm, C. J. (2016). Air Pollution and Procyclical Mortality. *Journal of the Association of Environmental and Resource Economists, 3*(3), 667-706. doi:10.1086/686251

Hoffman, J. S., Shandas, V., & Pendleton, N. (2020). The Effects of Historical Housing Policies on Resident Exposure to Intra-Urban Heat: A Study of 108 US Urban Areas. *Climate, 8*(12). doi:10.3390/cli8010012

Jha, A., & Muller, Z. N. (2018). The local air pollution cost of coal storage and handling: Evidence from U.S. power plants. *Journal of Environmental Economics and Management, 92*, 360-396. doi:10.1016/j.jeem.2018.09.005

Jones, B. A. (2018). Forest-attacking Invasive Species and Infant Health: Evidence From the Invasive Emerald Ash Borer. *Ecological Economics*, 282-293. doi:10.1016/j.ecolecon.2018.08.010

Jones, B. A. (2019). Tree Shade, Temperature, and Human Health: Evidence from Invasive Species-induced Deforestation. *Ecological Economics, 156*, 12-33. doi:10.1016/j.ecolecon.2018.09.006

Jones, B. A., & Goodkind, A. L. (2019). Urban afforestation and infant health: Evidence from MillionTreesNYC. *Journal of Environmental Economics and Management, 95*, 26-44. doi:10.1016/j.jeem.2019.03.002

Jones, B. A., & McDermott, S. M. (2018). Health Impacts of Invasive Species Through an Altered Natural Environment: Assessing Air Pollution Sinks as a Causal Pathway. *Environmental and Resource Economics*(71), 23-43. doi:10.1007/s10640-017-0135-6

Kim, J., Burnett, R. T., Neas, L., Thurston, G. D., Schwartz, J., Tolbert, P. E., . . . Romieu, I. (2007). Panel discussion review: session two — interpretation of observed associations between multiple ambient air pollutants and health effects in epidemiologic analyses. *Journal of Exposure Science & Environmental Epidemiology, 17*, S83–S89. doi:10.1038/sj.jes.7500623

Kondo, M. C., Han, S., Donovan, G. H., & MacDonald, J. M. (2017). The association between urban trees and crime: Evidence from the spread of the emerald ash borer in Cincinnati. *Landscape and Urban Planning*, 157:193-199. doi:10.1016/j.landurbplan.2016.07.003

McCullough, D. G. (2020). Challenges, tactics and integrated management of emerald ash borer in North America. *Forestry: An International Journal of Forest Research, 93*(2), 197-211. doi:10.1093/forestry/cpz049

McCullough, D. G., Schneeberger, N. F., Katovich, S. F., & Siegert, N. W. (2015). *Pest Alert Emerald Ash Borer NA-PR-02-04.* U.S. Forest Service, Northeastern Area State and Private Forestry. Retrieved from https://www.fs.usda.gov/naspf/sites/default/files/publications/eab.pdf

McKenzie, D. (2020). Revisiting the Difference-in-Differences Parallel Trends Assumption: Part I Pre-Trend Testing. Retrieved from

https://web.archive.org/web/20210310150823/https://blogs.worldbank.org/impactevalua
tions/revisiting-difference-differences-parallel-trends-assumption-part-i-pre-trend

Meng, J., Li, C., Martin, V. R., van Donkelaar, A., Hystad, P., & Brauer, M. (2019). Estimated
Long-Term (1981–2016) Concentrations of Ambient Fine Particulate Matter across North
America from Chemical Transport Modeling, Satellite Remote Sensing, and Ground-
Based Measurements. *Environmental Science & Technology, 53*(9), 5071-5079.
doi:10.1021/acs.est.8b06875

Muirhead, J. R., Leung, B., van Overdijk, C., Kelly, D. W., Nandakumar, K., Marchant, K. R.,
& MacIsaac, H. J. (2006). Modelling local and long-distance dispersal of invasive
emerald ash borer Agrilus planipennis (Coleoptera) in North America. *Diversity and
Distributions, 12*, 71-79. doi:10.1111/j.1366-9516.2006.00218.x

Murfitt, J., He, Y., Yang, J., Mui, A., & De Mille, K. (2016). Ash Decline Assessment in Emerald
Ash Borer Infested Natural Forests Using High Spatial Resolution Images. *Remote
Sensing, 8*(3), 256-273. doi:10.3390/rs8030256

National Academies of Sciences, Engineering, and Medicine. (2019). *Forest Health and
Biotechnology: Possibilities and Considerations.* Washington, DC: The National
Academies Press. doi:https://doi.org/10.17226/25221

National Center for Health Statistics. (n.d.). 2013 NCHS Urban-Rural Classification Scheme for
Counties. Retrieved from https://www.cdc.gov/nchs/data_access/urban_rural.htm

National Centers for Environmental Prediction/National Weather Service/NOAA/U.S. Department of Commerce. (1994, updated monthly). NCEP/NCAR Global Reanalysis Products, 1948-continuing. Research Data Archive at NOAA/PSL: /data/gridded/data.ncep.reanalysis.html.

Nowak, D. J. (2002). *The Effects of Urban Trees on Air Quality.* Syracuse, NY: USDA Forest Service. Retrieved from http://web.archive.org/web/20200709155809/https://www.nrs.fs.fed.us/units/urban/local-resources/downloads/Tree_Air_Qual.pdf

Nowak, D. J., & Greenfield, E. J. (2018a). US Urban Forest Statistics, Values, and Projections. *Journal of Forestry, 116*(2), 164–177. doi:10.1093/jofore/fvx004

Nowak, D. J., & Greenfield, E. J. (2018b). Declining urban and community tree cover in the United States. *Urban Forestry & Urban Greening, 32*, 32–55. doi:10.1016/j.ufug.2018.03.006

Nowak, D. J., Crane, D. E., & Stevens, J. C. (2006). Air pollution removal by urban trees and shrubs in the United States. *Urban Forestry & Urban Greening, 4*(3-4), 115-123. doi:10.1016/j.ufug.2006.01.007

Oliver, M. (2014). Exploring Connections Between Trees and Human Health. *Science Findings*(158). Retrieved from http://web.archive.org/web/20200822130631/https://www.fs.fed.us/pnw/sciencef/scifi158.pdf

Orlova-Bienkowskaja, M. J., & Bieńkowski, A. O. (2016). The life cycle of the emerald ash borer Agrilus planipennis in European Russia and comparisons with its life cycles in Asia and North America. *Agricultural and Forest Entomology, 18*(2), 182-188. doi:10.1111/afe.12140

Pandit, R., Polyakov, M., & Sadler, R. (2013). Valuing public and private urban tree canopy cover. *Australian Journal of Agricultural and Resource Economics, 58*(3), 453-470. doi:10.1111/1467-8489.12037

Pataky, N. R. (1996, April). *RPD No. 641 - Decline and Dieback of Trees and Shrubs.* University of Illinois Extension. Retrieved from https://web.archive.org/web/20200206074652/http://ipm.illinois.edu/diseases/series600/rpd641/

Poland, T. M., & McCullough, D. G. (2006). Emerald Ash Borer: Invasion of the Urban Forest and the Threat to North America's Ash Resource. *Journal of Forestry, 104*(3), 118-124. doi:10.1093/jof/104.3.118

Polyakov, M., Pannell, D. J., Pandit, R., Tapsuwan, S., & Park, G. (2015). Capitalized amenity value of native vegetation in a multifunctional rural landscape. *American Journal of Agricultural Economics, 1*(1), 299-314. doi:10.1093/ajae/aau053

PRISM Climate Group. (2020a). Gridded Climate Data. Retrieved from https://prism.oregonstate.edu/recent/

PRISM Climate Group. (2020b). USDA Plant Hardiness Zone GIS Datasets. Retrieved from
https://prism.oregonstate.edu/projects/plant_hardiness_zones.php

Sadof, C. S., Mockus, L., & Ginzel, M. D. (2021). Factors influencing efficacy of an area-wide
pest management program in three urban forests. *Urban Forestry & Urban Greening*,
126965. doi:10.1016/j.ufug.2020.126965

Schmidheiny, K., & Siegloch, S. (2020). On Event Study Designs and Distributed Lag Models:
Equivalence, Generalization and Practical Implications. *ZEW Discussion Papers*, No. 20-
017.

Schmidlin, T. W. (2009). Human fatalities from wind-related tree failures. *Natural Hazards*(50),
13-25. doi:10.1007/s11069-008-9314-7

Stone Jr., B., & Rodgers, M. O. (2001). Urban form and thermal efficiency: How the design of
cities influences the urban heat island effect. *Journal of the American Planning
Association, 67*(2), 186-198. doi:10.1080/01944360108976228

Sun, L., & Abraham, S. (2020). Estimating dynamic treatment effects in event studies with
heterogeneous treatment effects. *Journal of Econometrics*, In Press.
doi:10.1016/j.jeconom.2020.09.006

Tarrant, D. (2021, January 14). Dallas-area environmentalists warn invasive beetle could be latest
threat to Trinity Forest. *The Dallas Morning News*. Retrieved from
https://web.archive.org/web/20210226195737/https://www.dallasnews.com/news/2021/

01/14/dallas-area-environmentalists-warn-invasive-beetle-could-be-latest-threat-to-trinity-forest/

Texas Trees Foundation. (2015). *State of the Dallas Urban Forest.* Retrieved from https://www.texastrees.org/wp-content/uploads/2019/04/Urban-Forest-report.pdf

Tremberger, G., Sunil, D., Holden, T., Marchese, P., & Cheung, T. (2012). Remote sensing of ash tree health associated with the emerald ash borer via analyses of fluctuations in land-based and satellite-based data indices. *Proc. SPIE 8513, Remote Sensing and Modeling of Ecosystems for Sustainability IX.* San Diego. doi:10.1117/12.929786

U.S Bureau of Labor Statistics. (n.d.). Local Area Unemployment Statistics. Retrieved from https://www.bls.gov/lau/

U.S Department of Agriculture Agriculture Research Service. (2012). USDA Plant Hardiness Zone Map. Retrieved from https://web.archive.org/web/20210502144308/https://planthardiness.ars.usda.gov/PHZMWeb/

U.S. Department of Agriculture Animal and Plant Health Inspection Service. (2021). Emerald Ash Borer Known Infested Counties. Retrieved from https://www.aphis.usda.gov/aphis/maps/plant-health/eab-map

U.S. Department of Agriculture Animal and Plant Health Inspection Service Plant Protection and Quarantine. (2020). Questions and Answers: Changes in the Approach toward Fighting

the   Emerald   Ash   Borer.   Retrieved   from

https://www.aphis.usda.gov/publications/plant_health/fs-eab-transition.pdf

United States Census Bureau. (n.d.). Population and Housing Unit Estimates. Retrieved from

https://www.census.gov/programs-surveys/popest.html

United States Census Bureau. (n.d.). Small Area Income and Poverty Estimates (SAIPE)

Program. Retrieved from https://www.census.gov/programs-surveys/saipe.html

United States Department of Agriculture. (n.d.). Initial County EAB Detections in North America

-          January   4,   2021.   Retrieved   from

https://web.archive.org/web/20210424140648/http://www.emeraldashborer.info/docum

ents/MultiState_EABpos.pdf

United States Government Accountability Office. (2006). *Invasive Forest Pests: Lessons*

Learned from Three Recent Infestations May Aid in Managing Future Efforts. Retrieved

from www.gao.gov/cgi-bin/getrpt?GAO-06-353.

USDA Animal and Plant Health Inspection Service. (2018, September 9). Removal of Emerald

Ash Borer Domestic Quarantine Regulations.

Viscusi, W. K. (2020, Mar 16). Failing to Think Properly About the Value of a Statistical Life.

The   Regulatory   Review.   Retrieved   from

http://web.archive.org/web/20200602202729/https://www.theregreview.org/2020/03/16/

viscusi-failing-think-properly-value-statistical-life/

Vogt, J., Hauer, R. J., & Fischer, B. C. (2015). The Costs of Maintaining and Not Maintaining the Urban Forest: A Review of the Urban Forestry and Arboriculture Literature. *Arboriculture & Urban Forestry*, 41(6): 293–323.

Wimborne, J. B., Jones, T. S., Garvey, S. M., Harrison, J. L., Wang, L., Li, D., . . . Hutyra, L. R. (2020). Tree Transpiration and Urban Temperatures: Current Understanding, Implications, and Future Research Directions. *Bioscience, 70*(7), 576–588. doi:10.1093/biosci/biaa055

Wooldridge, J. M. (2013). *Introductory Econometrics: A Modern Approach* (5th ed.). South-Western, Cengage Learning.

World Metereological Organization. (2018). *Guide to Instruments and Methods: Volume I – Measurement of Meteorological Variables.* Geneva: Publications Board, World Metereological Organization. Retrieved from https://library.wmo.int/doc_num.php?explnum_id=10616

1.7 Tables and Figures

Table 1: Data Sources

Variable	Source
Age adjusted mortality per 100000 population	
All-cause, chronic respiratory disease, cardiovascular disease, injuries	Dwyer-Lindgren, et al., 2016
Weather and environment variables	
Mean annual ambient PM2.5	Meng, et al., 2019
Maximum and minimum temperature, annual mean precipitation	PRISM Climate Group, 2020a
Leaf Area Index	Claverie, Vermote, & NOAA CDR Program, 2020
Wind speed and direction	National Centers for Environmental Prediction/National Weather Service/NOAA/U.S. Department of Commerce, 1994, updated monthly
USDA plant hardiness zone	PRISM Climate Group, 2020b
Year of emerald ash borer detection	Emerald Ash Borer Information Network State & County Detection Table (Emerald Ash Borer Information Network, 2021), USDA APHIS Emerald Ash Borer Known Infested Counties (U.S. Department of Agriculture Animal and Plant Health Inspection Service, 2021)
Other variables	
Median household income	Census Bureau Small Area Income and Poverty Estimates
Unemployment rate	Bureau of Labor Statistics Local Area Unemployment Statistics
Total, White and Hispanic population	Census Bureau Population and Housing Estimates
Urban classification	NCHS 2013 Urban-Rural Classification Scheme for Counties

Table 2: Summary statistics of dependent variables in urban counties by approximate initial year of tree decline

	Full sample			Base year		
Initial year:	Never	1999-2008	2009-2014	Never	1999-2008	2009-2014
No. of counties:	30	17	14	30	17	14
Environment variables						
Jul-early Oct Leaf Area Index	1.15 (0.650)	1.74 (0.595)	1.48 (0.801)	-	1.79 (0.621)	1.55 (0.924)
Annual ambient PM2.5 (μgm^{-3})	9.87 (3.24)	13.2 (3.76)	13.6 (3.61)	-	12.8 (2.83)	9.43 (1.34)
Maximum temperature (°C)	32.7 (4.08)	29.1 (2.11)	30.7 (1.99)	-	29.7 (1.54)	31.2 (1.90)
Minimum temperature (°C)	2.87 (4.97)	-7.98 (4.30)	-4.18 (3.05)	-	-7.29 (3.38)	-3.91 (3.21)
Mortality variables (age adjusted rates per 100000 population)						
All-cause	894 (145)	925 (136)	974 (190)	-	911 (128)	819 (156)
Cardiovascular disease	313 (69.3)	323 (75.3)	355 (85.2)	-	310 (72.5)	271 (49.3)
Chronic respiratory disease	50.6 (9.30)	49.1 (10.8)	45.2 (10.7)	-	50.3 (11.7)	44.0 (11.8)
Unintentional injuries	18.3 (4.70)	20.4 (3.85)	20.6 (5.71)	-	20.3 (3.75)	19.5 (6.21)

This table reports means and standard deviations (in parentheses).

Table 3: Urban counties with emerald ash borer detection by year

Approx. year when tree decline started	County	City	State
1999	Wayne County	Detroit	MI
2000	Kent County	Grand Rapids	MI
	Franklin County	Columbus	OH
2003	Cook County	Chicago	IL
	Cuyahoga County	Cleveland	OH
	Marion County	Indianapolis	IN
2004	Alleghany County	Pittsburgh	PA
	Hamilton County	Cincinnati	OH
2006	Jefferson County	Louisville	KY
	Milwaukee County	Milwaukee	WI
	Ramsey County	St. Paul	MN
2007	Hennepin County	Minneapolis	MN
	Monroe County	Rochester	NY
2008	Alexandria City	Alexandria	VA
	District of Columbia	District of Columbia	DC
	Erie County	Buffalo	NY
2010	Fulton County	Atlanta	GA
	Hartford County	Hartford	CT
	Jackson County	Kansas City	MO
2011	Baltimore City	Baltimore	MD
	Davidson	Nashville	TN
	Suffolk	Boston	MA
2012	St. Louis City	St. Louis	MO
	Wake	Raleigh	NC
	Essex	Newark	NJ
2013	Hudson	Jersey City	NJ
	Philadelphia	Philadelphia	PA
2014	Kings	New York City (Brooklyn)	NY
	Mecklenburg	Charlotte	NC
	Queens	New York City (Queens)	NY

Figure 1: Two emerald ash borers Agrilus planipennis on a leaf

Source: United States Department of Agriculture

Figure 2: Map of counties by status of tree death from emerald ash borer (up to 2014) and urban status

Legend
- No tree death, non-urban
- No tree death, urban
- Likely tree death, non-urban
- Likely tree death, urban
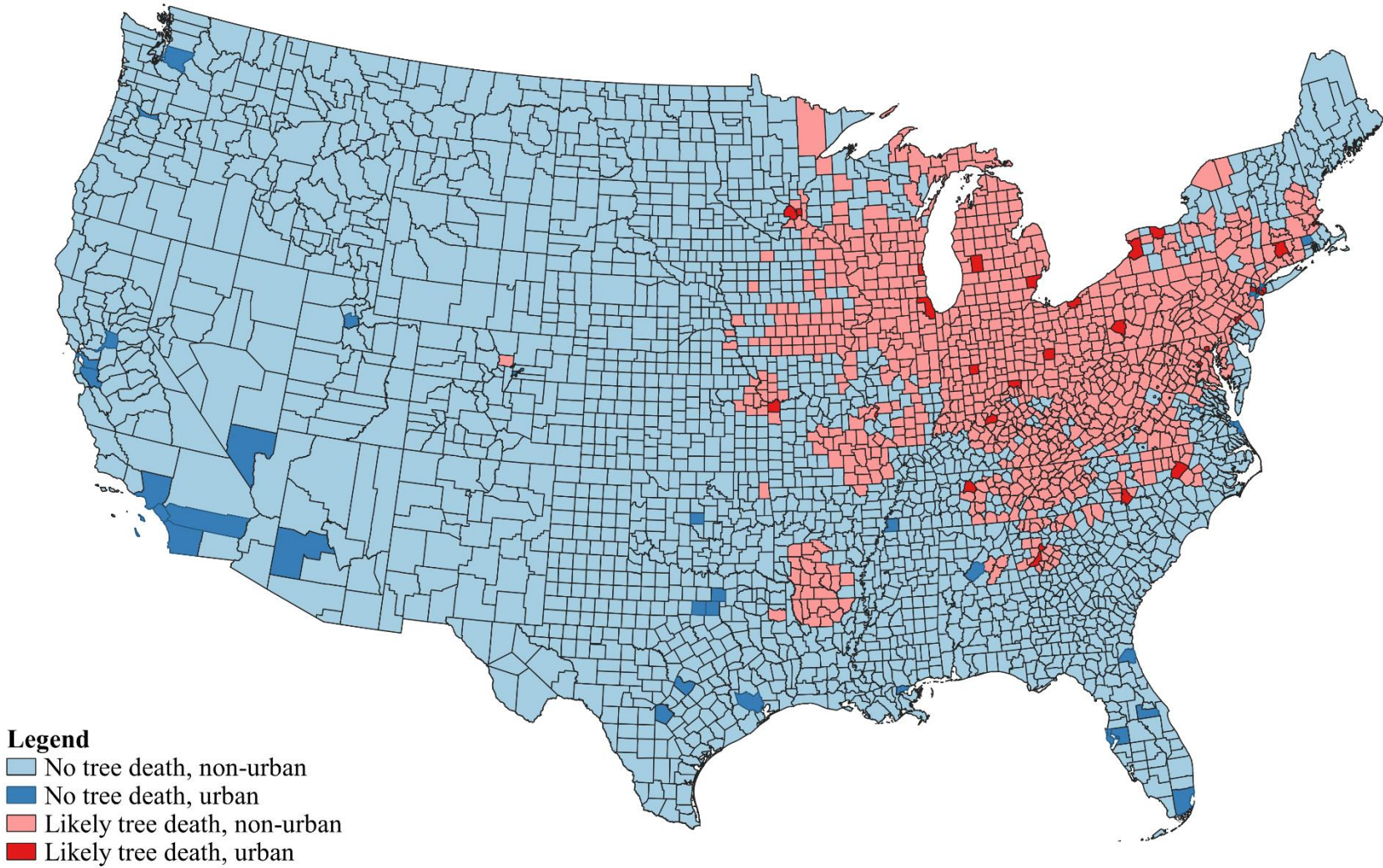
Figure 3: Early emerald ash borer infestation is associated with decreases in late growing season Leaf Area Index after approximate start of tree death in urban counties
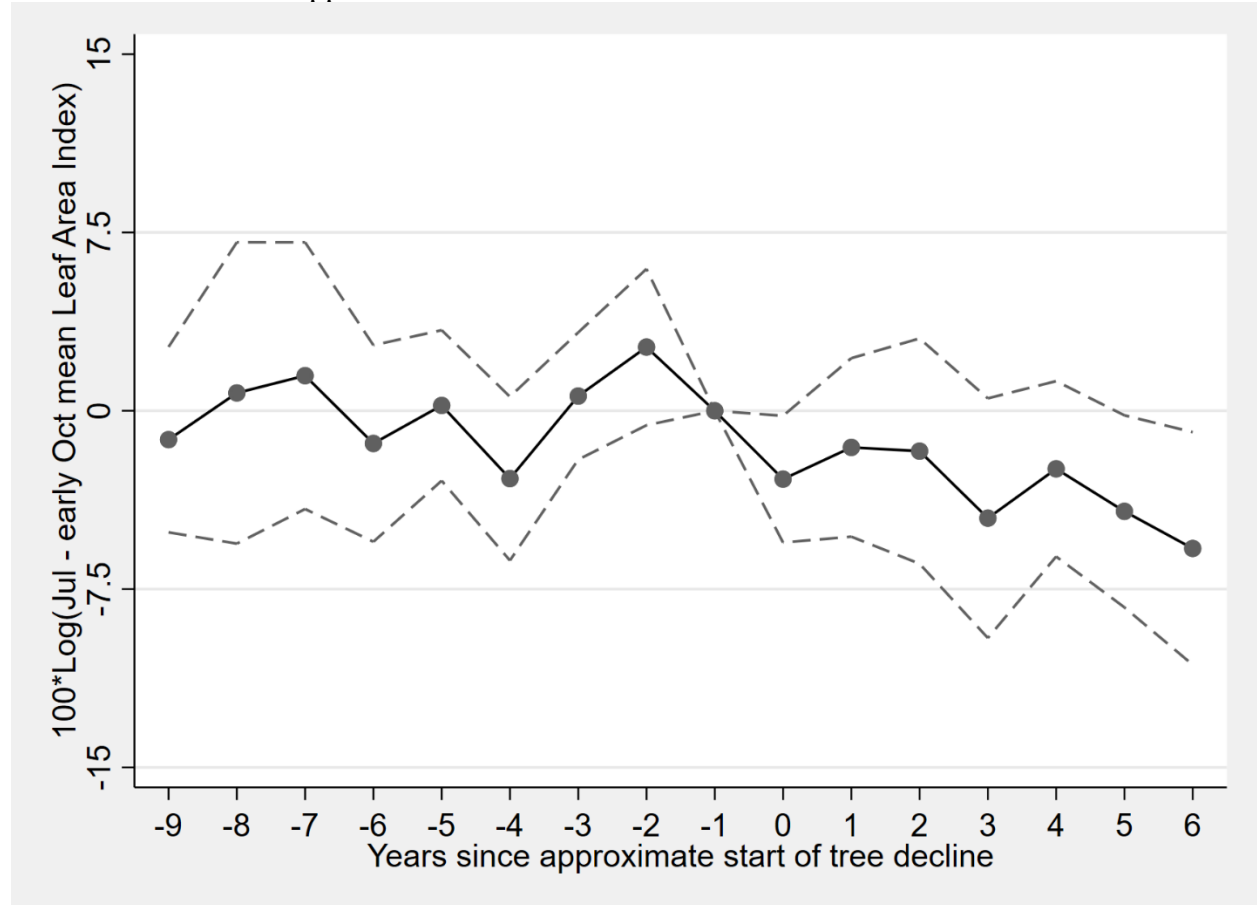
Leaf area index is defined as the ratio of one-sided green leaf area to land area. July to early (the first week of) October is the part of the growing season where emerald ash borer larvae are actively feeding. Standard errors clustered by state interacted with plant hardiness zone; 95% confidence intervals shown. Covariates include log(median household income), log(population density), log(% population that is white), and log(% population that is Hispanic), all interacted with urban status. Fixed effects are county, urban status interacted with year, and state interacted with USDA plant hardiness zone and year. Displayed coefficients are for balanced event years.

Figure 4: Early emerald ash borer infestation is associated with increases in ambient average PM2.5 in urban counties
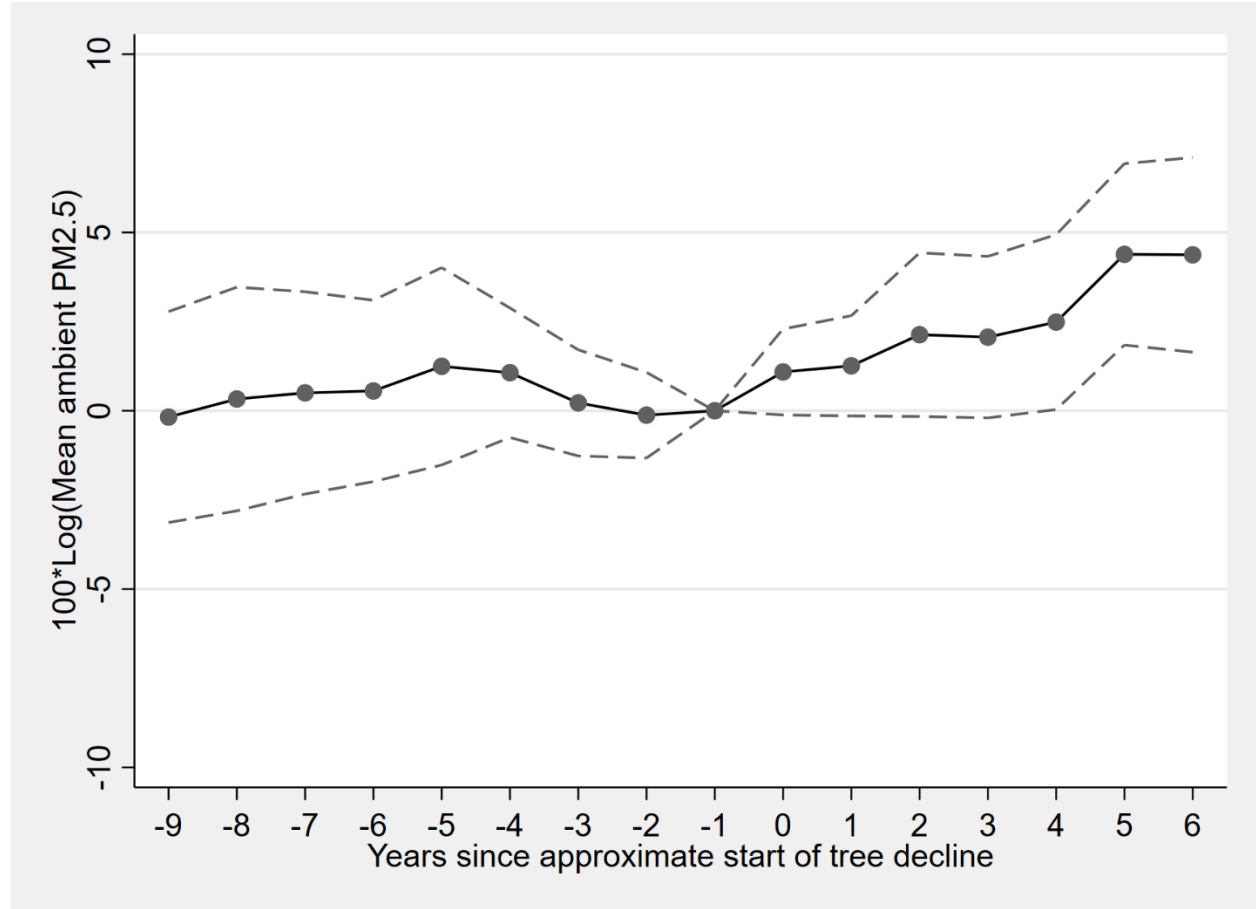
Standard errors clustered by state interacted with plant hardiness zone; 95% confidence intervals shown. Covariates include log(median household income), log(population density), log(% population that is white), and log(% population that is Hispanic), all interacted with urban status. Fixed effects are county, urban status interacted with year, and state interacted with USDA plant hardiness zone and year. Displayed coefficients are for balanced event years.

Figure 5: Early emerald ash borer infestation is associated with increases in all-cause mortality in urban counties
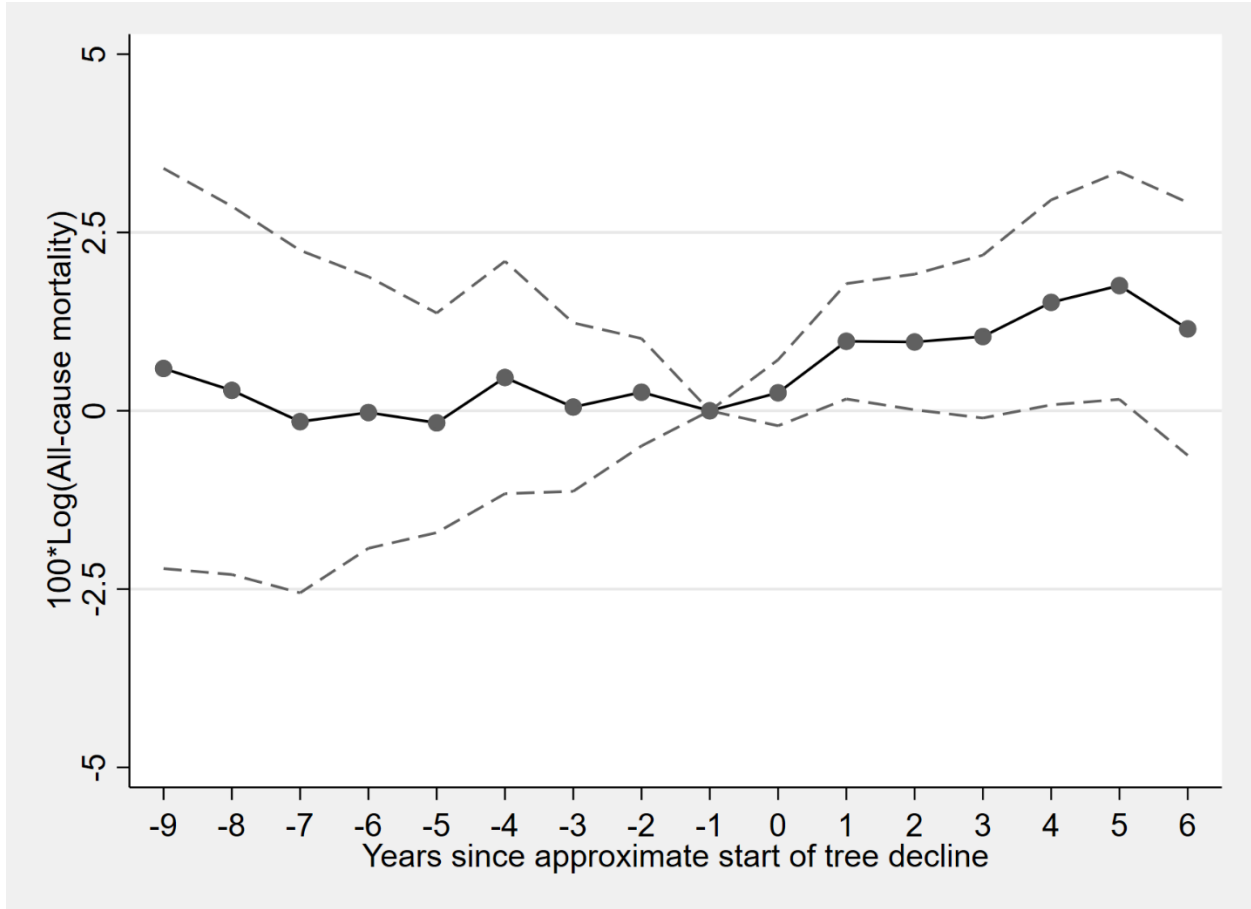
Standard errors clustered by state interacted with plant hardiness zone; 95% confidence intervals shown. Covariates include log(median household income), log(population density), log(% population that is white), and log(% population that is Hispanic), all interacted with urban status. Fixed effects are county, urban status interacted with year, and state interacted with USDA plant hardiness zone and year. Displayed coefficients are for balanced event years for urban counties.

Figure 6: Early emerald ash borer infestation is associated with increases in cardiovascular disease mortality and chronic respiratory disease mortality in urban counties

a) Cardiovascular disease mortality

b)   Chronic respiratory disease mortality
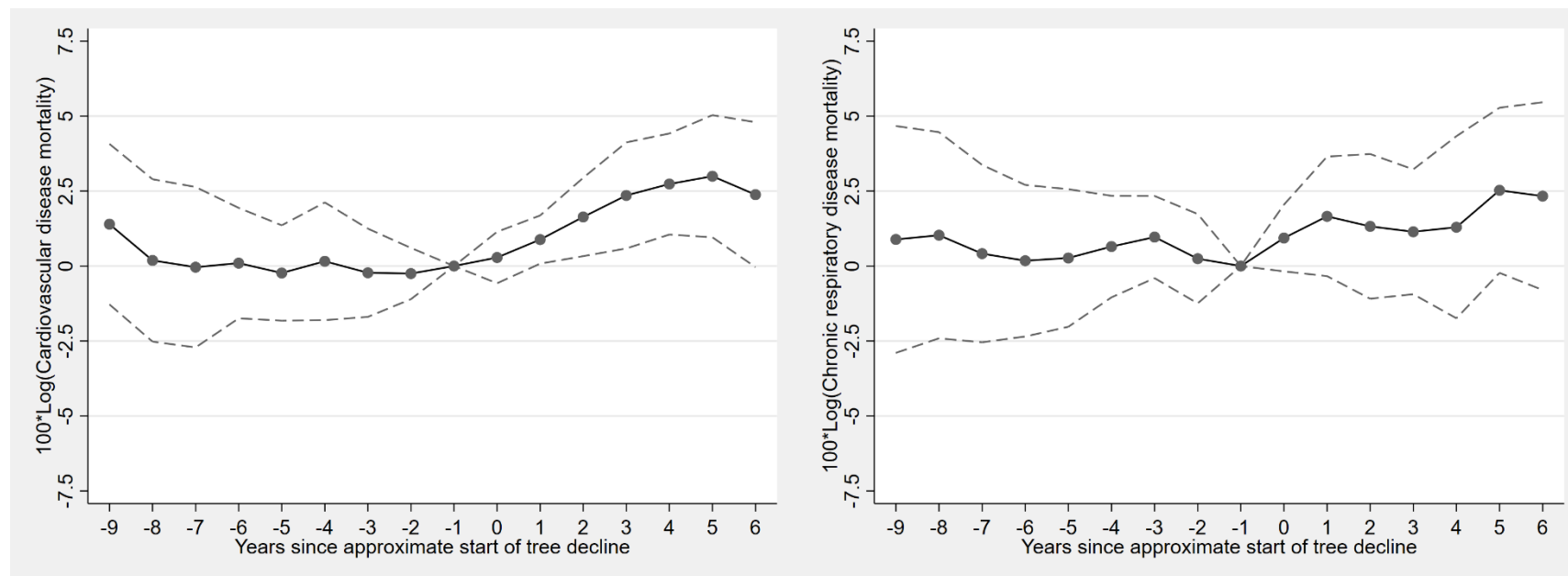
Standard errors clustered by state interacted with plant hardiness zone; 95% confidence intervals shown. Covariates include log(median household income), log(population density), log(% population that is white), and log(% population that is Hispanic), all interacted with urban status. Fixed effects are county, urban status interacted with year, and state interacted with USDA plant hardiness zone and year. Displayed coefficients are for balanced event years for urban counties.

1.8 Appendices

Appendix Table A1: Robustness checks for event study specifications in levels

	(1) July-early Oct Leaf Area Index	(2) Ambient average PM2.5	(3) All-cause mortality	(4) Cardiovascular disease mortality	(5) Chronic respiratory disease mortality
-9	-0.03	-0.01	-2.38	-2.33	0.01
	(-0.97)	(-0.07)	(-0.20)	(-0.55)	(0.01)
-8	0.04	0.07	-3.80	-5.45	0.23
	(0.54)	(0.46)	(-0.33)	(-1.18)	(0.23)
-7	0.02	0.09	-8.37	-6.17	0.04
	(0.50)	(0.56)	(-0.82)	(-1.37)	(0.04)
-6	-0.02	0.10	-6.41	-4.87	-0.09
	(-0.61)	(0.76)	(-0.79)	(-1.55)	(-0.12)
-5	0.01	0.17	-6.58	-5.15*	-0.02
	(0.29)	(1.32)	(-1.05)	(-1.96)	(-0.03)
-4	-0.08***	0.16*	0.85	-2.44	0.21
	(-2.65)	(1.78)	(0.12)	(-0.74)	(0.44)
-3	0.02	0.07	-2.66	-2.94	0.39
	(0.64)	(0.71)	(-0.58)	(-1.37)	(0.95)
-2	0.05***	-0.03	0.22	-2.07	0.10
	(2.76)	(-0.36)	(0.08)	(-1.56)	(0.25)
-1	0.00	0.00	0.00	0.00	0.00
	(.)	(.)	(.)	(.)	(.)
0	-0.04**	0.03	1.47	0.50	0.47
	(-2.35)	(0.57)	(0.74)	(0.42)	(1.51)
1	-0.01	0.09	9.74***	3.53***	1.04*
	(-0.61)	(1.32)	(2.97)	(3.83)	(1.98)
2	-0.04	0.10	10.36**	6.10***	0.82
	(-1.21)	(0.77)	(2.26)	(3.74)	(1.17)
3	-0.07**	0.03	11.54**	8.42***	0.75
	(-2.10)	(0.25)	(2.55)	(3.73)	(1.14)
4	-0.04	0.02	15.32**	9.26***	0.75
	(-1.46)	(0.15)	(2.61)	(4.36)	(0.84)
5	-0.08**	0.14	18.78***	10.74***	1.57*
	(-2.35)	(1.10)	(2.98)	(4.39)	(1.94)
6	-0.10**	0.15	14.42**	9.33***	1.55*
	(-2.49)	(1.07)	(2.09)	(3.45)	(1.69)
Base covariates	X	X	X	X	X

Standard errors clustered at the state by plant hardiness zone level. t statistics in parentheses, $^{*} p < 0.1$, $^{**} p < 0.05$, $^{***} p < 0.01$

Appendix Table A2: Robustness checks for Jul-early Oct leaf area index event studies

	(1)	(2)	(3)	(4)	(5)	(6)	(7)	(8)
-9	-1.21	-1.50	-1.17	-0.40	-1.41	-1.20	-3.08*	0.50
	(-0.62)	(-0.79)	(-0.60)	(-0.23)	(-0.73)	(-0.61)	(-1.71)	(0.32)
-8	0.75	0.19	0.86	1.23	0.61	0.76	-0.89	2.23
	(0.23)	(0.06)	(0.26)	(0.38)	(0.19)	(0.24)	(-0.26)	(1.01)
-7	1.48	0.87	1.67	1.42	1.39	1.49	-0.12	2.72
	(0.52)	(0.34)	(0.58)	(0.48)	(0.49)	(0.53)	(-0.04)	(1.37)
-6	-1.37	-1.55	-1.58	-0.52	-1.38	-1.35	-2.77	1.75
	(-0.66)	(-0.80)	(-0.74)	(-0.25)	(-0.67)	(-0.64)	(-1.35)	(0.96)
-5	0.22	0.03	-0.06	1.29	0.30	0.24	-0.96	1.47
	(0.14)	(0.02)	(-0.04)	(0.78)	(0.19)	(0.15)	(-0.60)	(0.84)
-4	-2.85	-2.55*	-3.15	-3.03*	-2.84	-2.84	-3.85**	-1.91
	(-1.64)	(-1.67)	(-1.61)	(-1.73)	(-1.63)	(-1.62)	(-2.21)	(-1.44)
-3	0.62	0.57	0.36	1.29	0.68	0.63	-0.24	-0.14
	(0.46)	(0.47)	(0.22)	(0.90)	(0.50)	(0.46)	(-0.17)	(-0.13)
-2	2.68	2.23	2.43	3.27**	2.73*	2.69	2.07	0.53
	(1.61)	(1.29)	(1.62)	(2.02)	(1.66)	(1.61)	(1.36)	(0.34)
-1	-	-	-	-	-	-	-	-
0	-2.88**	-2.64**	-3.11**	-3.44**	-3.03**	-2.86**	-3.02**	-0.62
	(-2.13)	(-2.13)	(-2.02)	(-2.28)	(-2.25)	(-2.14)	(-2.05)	(-0.52)
1	-1.54	-1.28	-2.06	-1.13	-1.57	-1.52	-1.23	0.41
	(-0.81)	(-0.64)	(-1.05)	(-0.57)	(-0.83)	(-0.81)	(-0.66)	(0.28)
2	-1.70	-0.27	-3.13	-1.44	-1.72	-1.67	-1.36	0.01
	(-0.71)	(-0.11)	(-1.19)	(-0.64)	(-0.72)	(-0.70)	(-0.59)	(0.01)
3	-4.52*	-3.46	-5.91**	-3.92	-4.50*	-4.50*	-3.88	-1.70
	(-1.77)	(-1.50)	(-2.22)	(-1.54)	(-1.80)	(-1.78)	(-1.43)	(-0.79)
4	-2.44	-1.88	-4.07*	-3.34	-2.43	-2.41	-1.75	-0.69
	(-1.31)	(-1.07)	(-1.78)	(-1.37)	(-1.36)	(-1.30)	(-0.85)	(-0.40)
5	-4.23**	-2.64	-5.70**	-4.29**	-4.16**	-4.20**	-3.15	-3.35*
	(-2.07)	(-1.34)	(-2.16)	(-2.05)	(-2.05)	(-2.09)	(-1.55)	(-1.82)
6	-5.79**	-4.52*	-7.84**	-5.52**	-5.81**	-5.76**	-4.42	-5.05**
	(-2.34)	(-1.92)	(-2.56)	(-2.33)	(-2.36)	(-2.36)	(-1.63)	(-2.07)
Base covariates	X	X	X	X	X	X		X
Log(upwind LAI)		X						
NAAQS standards			X					
Weather variables				X				
Unemployment					X			
Log(Population)						X		
Do not stratify								X

t statistics in parentheses, * $p < 0.1$, ** $p < 0.05$, *** $p < 0.01$

Appendix Table A3: Robustness checks for PM2.5 event studies

	(1)	(2)	(3)	(4)	(5)	(6)	(7)	(8)
-9	-0.18	-0.19	-0.50	-0.09	-0.09	-0.16	-0.38	-1.01
	(-0.12)	(-0.13)	(-0.32)	(-0.06)	(-0.06)	(-0.11)	(-0.26)	(-0.93)
-8	0.33	0.37	-0.05	0.41	0.39	0.34	0.14	-0.20
	(0.21)	(0.23)	(-0.03)	(0.26)	(0.25)	(0.22)	(0.09)	(-0.18)
-7	0.50	0.50	0.12	0.50	0.53	0.51	0.27	-0.08
	(0.35)	(0.35)	(0.08)	(0.37)	(0.37)	(0.36)	(0.19)	(-0.08)
-6	0.56	0.53	0.27	0.50	0.54	0.57	0.29	-0.00
	(0.43)	(0.41)	(0.19)	(0.43)	(0.42)	(0.45)	(0.23)	(-0.00)
-5	1.25	1.23	0.98	1.26	1.19	1.26	1.00	0.48
	(0.89)	(0.89)	(0.65)	(0.92)	(0.85)	(0.90)	(0.71)	(0.52)
-4	1.07	1.05	0.93	0.91	1.04	1.08	0.82	1.01
	(1.16)	(1.16)	(0.87)	(1.09)	(1.15)	(1.19)	(0.86)	(1.62)
-3	0.22	0.24	0.04	0.30	0.18	0.23	-0.02	0.29
	(0.29)	(0.31)	(0.05)	(0.40)	(0.24)	(0.30)	(-0.02)	(0.52)
-2	-0.12	-0.13	-0.25	-0.15	-0.16	-0.12	-0.34	0.86
	(-0.20)	(-0.22)	(-0.40)	(-0.24)	(-0.26)	(-0.19)	(-0.56)	(1.56)
-1	-	-	-	-	-	-	-	-
0	1.09*	1.13*	1.26**	1.08*	1.18*	1.10*	1.00*	1.02***
	(1.79)	(1.81)	(1.99)	(1.76)	(1.92)	(1.80)	(1.77)	(2.67)
1	1.26*	1.30*	1.32*	1.26*	1.29*	1.28*	1.33*	1.00**
	(1.78)	(1.80)	(1.89)	(1.73)	(1.89)	(1.79)	(1.92)	(2.10)
2	2.13*	2.20*	2.28**	2.23*	2.15*	2.17*	2.20*	2.31***
	(1.84)	(1.86)	(2.41)	(1.87)	(1.92)	(1.86)	(1.83)	(2.75)
3	2.07*	2.11*	2.41**	2.03*	2.06*	2.09*	2.22**	1.78*
	(1.81)	(1.83)	(2.47)	(1.69)	(1.93)	(1.82)	(2.08)	(1.96)
4	2.49**	2.52**	2.86***	2.50*	2.49**	2.52**	2.64**	2.02*
	(2.01)	(2.02)	(2.79)	(1.91)	(2.10)	(2.02)	(2.35)	(1.87)
5	4.39***	4.44***	4.99***	4.51***	4.37***	4.42***	4.69***	3.84***
	(3.41)	(3.42)	(4.46)	(3.40)	(3.57)	(3.41)	(3.82)	(3.47)
6	4.37***	4.42***	5.11***	4.30***	4.41***	4.40***	4.80***	3.82***
	(3.17)	(3.13)	(3.87)	(2.92)	(3.29)	(3.16)	(3.66)	(3.00)
Base covariates	X	X	X	X	X	X		X
Log(upwind LAI)		X						
NAAQS standards			X					
Weather variables				X				
Unemployment					X			
Log(Population)						X		
Do not stratify								X

t statistics in parentheses, * $p < 0.1$, ** $p < 0.05$, *** $p < 0.01$

Appendix Table A4: Robustness checks for all-cause mortality event studies

	(1)	(2)	(3)	(4)	(5)	(6)	(7)	(8)

	(1)	(2)	(3)	(4)	(5)	(6)	(7)	(8)
-9	0.59 (0.42)	0.58 (0.41)	0.95 (0.80)	0.71 (0.51)	0.60 (0.42)	0.63 (0.46)	0.03 (0.02)	0.79 (0.80)
-8	0.29 (0.22)	0.27 (0.21)	0.73 (0.67)	0.43 (0.33)	0.29 (0.22)	0.34 (0.27)	-0.18 (-0.14)	0.46 (0.51)
-7	-0.15 (-0.13)	-0.14 (-0.11)	0.26 (0.25)	-0.02 (-0.02)	-0.16 (-0.13)	-0.13 (-0.11)	-0.61 (-0.53)	0.35 (0.42)
-6	-0.02 (-0.02)	-0.01 (-0.01)	0.30 (0.36)	0.08 (0.08)	-0.03 (-0.03)	-0.07 (-0.07)	-0.43 (-0.48)	0.17 (0.25)
-5	-0.17 (-0.22)	-0.17 (-0.22)	0.03 (0.04)	-0.07 (-0.09)	-0.17 (-0.21)	-0.19 (-0.25)	-0.52 (-0.73)	0.34 (0.60)
-4	0.47 (0.57)	0.49 (0.59)	0.34 (0.51)	0.53 (0.64)	0.46 (0.55)	0.44 (0.57)	0.10 (0.14)	0.72 (1.34)
-3	0.05 (0.09)	0.05 (0.08)	-0.09 (-0.18)	0.19 (0.31)	0.04 (0.06)	0.03 (0.06)	-0.30 (-0.65)	0.16 (0.40)
-2	0.26 (0.68)	0.26 (0.68)	0.18 (0.55)	0.37 (0.91)	0.27 (0.68)	0.22 (0.65)	-0.02 (-0.05)	0.74** (2.30)
-1	-	-	-	-	-	-	-	-
0	0.25 (1.08)	0.26 (1.12)	0.21 (0.68)	0.16 (0.66)	0.23 (0.97)	0.15 (0.71)	0.05 (0.27)	-0.13 (-0.47)
1	0.97** (2.38)	0.98** (2.38)	1.12** (2.34)	1.00** (2.38)	0.94** (2.31)	0.85** (2.11)	0.95** (2.32)	0.39 (0.85)
2	0.96** (2.01)	0.98** (2.03)	1.28* (1.97)	1.06** (2.05)	0.96** (1.98)	0.76 (1.53)	0.82 (1.49)	0.99 (1.34)
3	1.04* (1.80)	1.06* (1.84)	1.35* (1.84)	1.12** (2.01)	1.05* (1.82)	0.85 (1.51)	1.04 (1.59)	1.04 (1.20)
4	1.52** (2.09)	1.54** (2.14)	1.87** (2.36)	1.42* (1.88)	1.50** (2.08)	1.28* (1.81)	1.48** (2.18)	1.54 (1.49)
5	1.76** (2.18)	1.76** (2.20)	2.09*** (2.68)	1.67** (2.02)	1.74** (2.18)	1.53** (2.00)	1.88** (2.51)	2.03* (1.78)
6	1.15 (1.28)	1.15 (1.30)	1.12 (1.33)	1.17 (1.30)	1.14 (1.27)	0.94 (1.11)	1.37* (1.75)	1.43 (1.18)
Base covariates	X	X	X	X	X	X		X
Log(upwind LAI)		X						
NAAQS standards			X					
Weather variables				X				
Unemployment					X			
Log(Population)						X		
Do not stratify								X

t statistics in parentheses, $^{*}\,p < 0.1$, $^{**}\,p < 0.05$, $^{***}\,p < 0.01$

Appendix Table A5: Robustness checks for cardiovascular disease mortality event studies

	(1)	(2)	(3)	(4)	(5)	(6)	(7)	(8)

	(1)	(2)	(3)	(4)	(5)	(6)	(7)	(8)
-9	1.40 (1.03)	1.29 (0.95)	2.01 (1.55)	1.04 (0.79)	1.51 (1.11)	1.49 (1.21)	0.68 (0.55)	1.10 (1.07)
-8	0.19 (0.14)	0.12 (0.09)	0.90 (0.73)	-0.04 (-0.03)	0.27 (0.20)	0.31 (0.25)	-0.42 (-0.34)	0.36 (0.36)
-7	-0.04 (-0.03)	-0.06 (-0.05)	0.63 (0.51)	-0.23 (-0.16)	0.02 (0.01)	0.03 (0.03)	-0.64 (-0.49)	0.47 (0.47)
-6	0.10 (0.10)	0.09 (0.10)	0.72 (0.72)	-0.14 (-0.15)	0.12 (0.13)	0.05 (0.06)	-0.50 (-0.60)	0.38 (0.49)
-5	-0.23 (-0.29)	-0.26 (-0.31)	0.27 (0.36)	-0.31 (-0.37)	-0.23 (-0.28)	-0.24 (-0.33)	-0.71 (-0.98)	0.30 (0.48)
-4	0.16 (0.16)	0.17 (0.17)	0.26 (0.32)	-0.01 (-0.01)	0.16 (0.17)	0.13 (0.15)	-0.26 (-0.30)	0.50 (0.73)
-3	-0.22 (-0.30)	-0.22 (-0.30)	-0.38 (-0.52)	-0.21 (-0.29)	-0.25 (-0.34)	-0.25 (-0.39)	-0.59 (-0.96)	-0.13 (-0.23)
-2	-0.25 (-0.58)	-0.24 (-0.56)	-0.30 (-0.67)	-0.12 (-0.23)	-0.26 (-0.59)	-0.31 (-0.78)	-0.51 (-1.33)	0.35 (0.89)
-1	-	-	-	-	-	-	-	-
0	0.28 (0.66)	0.29 (0.66)	0.17 (0.41)	0.00 (0.01)	0.31 (0.72)	0.12 (0.31)	0.12 (0.37)	-0.30 (-0.76)
1	0.88** (2.18)	0.89** (2.19)	0.74 (1.56)	1.00** (2.32)	0.87** (2.14)	0.68* (1.80)	0.90** (2.22)	0.11 (0.24)
2	1.64** (2.48)	1.66** (2.46)	1.34* (1.75)	2.09*** (2.95)	1.64** (2.49)	1.30** (2.02)	1.60** (2.45)	1.31 (1.39)
3	2.35*** (2.63)	2.34** (2.60)	2.07** (2.08)	2.41*** (2.72)	2.36*** (2.65)	2.05** (2.38)	2.46*** (2.65)	2.01** (2.00)
4	2.74*** (3.21)	2.71*** (3.19)	2.45*** (2.67)	2.76*** (3.08)	2.73*** (3.19)	2.35*** (2.88)	2.85*** (3.52)	2.52*** (2.64)
5	3.00*** (2.91)	2.95*** (2.87)	2.64*** (2.93)	3.43*** (3.35)	2.97*** (2.88)	2.63*** (2.80)	3.29*** (3.46)	2.91** (2.55)
6	2.38* (1.95)	2.32* (1.90)	1.40 (1.28)	2.85** (2.38)	2.39* (1.96)	2.03* (1.85)	2.81** (2.46)	2.28* (1.73)
Base covariates	X	X	X	X	X	X		X
Log(upwind LAI)		X						
NAAQS standards			X					
Weather variables				X				
Unemployment					X			
Log(Population)							X	
Do not stratify								X

t statistics in parentheses, * $p < 0.1$, ** $p < 0.05$, *** $p < 0.01$

Appendix Table A6: Robustness checks for chronic respiratory disease mortality event studies

	(1)	(2)	(3)	(4)	(5)	(6)	(7)	(8)
-9	0.89	1.01	1.53	1.26	0.96	1.05	0.92	0.47

	(0.46)	(0.52)	(0.93)	(0.70)	(0.51)	(0.53)	(0.51)	(0.29)
-8	1.03	1.09	1.72	1.50	1.08	1.21	1.07	0.80
	(0.59)	(0.62)	(1.21)	(0.93)	(0.64)	(0.67)	(0.67)	(0.54)
-7	0.41	0.50	1.04	0.73	0.46	0.53	0.40	0.67
	(0.28)	(0.33)	(0.84)	(0.51)	(0.31)	(0.35)	(0.29)	(0.55)
-6	0.18	0.27	0.59	0.25	0.20	0.17	0.19	-0.04
	(0.14)	(0.21)	(0.50)	(0.21)	(0.16)	(0.12)	(0.16)	(-0.04)
-5	0.27	0.32	0.57	0.25	0.25	0.30	0.20	0.02
	(0.23)	(0.28)	(0.58)	(0.23)	(0.22)	(0.24)	(0.19)	(0.02)
-4	0.65	0.69	0.61	0.77	0.64	0.65	0.48	0.89
	(0.76)	(0.79)	(0.78)	(0.97)	(0.76)	(0.76)	(0.65)	(1.31)
-3	0.97	0.97	0.99	1.06	0.95	0.95	0.78	-0.01
	(1.40)	(1.37)	(1.58)	(1.65)	(1.40)	(1.30)	(1.11)	(-0.02)
-2	0.25	0.25	0.31	0.18	0.21	0.19	0.07	0.55
	(0.33)	(0.33)	(0.46)	(0.26)	(0.28)	(0.25)	(0.09)	(1.05)
-1	-	-	-	-	-	-	-	-
0	0.93*	0.94*	0.61	0.84	1.03*	0.78	0.65	0.35
	(1.66)	(1.68)	(1.01)	(1.40)	(1.84)	(1.45)	(1.22)	(0.70)
1	1.66	1.65	1.56	1.59	1.72*	1.45	1.48	0.42
	(1.65)	(1.63)	(1.50)	(1.51)	(1.67)	(1.40)	(1.40)	(0.43)
2	1.32	1.33	1.31	1.23	1.36	1.01	0.92	0.68
	(1.09)	(1.10)	(0.96)	(1.00)	(1.10)	(0.78)	(0.67)	(0.57)
3	1.14	1.19	0.97	1.05	1.15	0.85	0.80	0.34
	(1.09)	(1.13)	(0.89)	(0.97)	(1.09)	(0.76)	(0.64)	(0.25)
4	1.29	1.35	1.16	1.04	1.34	0.91	0.85	0.57
	(0.84)	(0.89)	(0.82)	(0.68)	(0.85)	(0.59)	(0.54)	(0.31)
5	2.53*	2.59*	2.28	2.13	2.56*	2.16	2.19	2.29
	(1.82)	(1.87)	(1.66)	(1.41)	(1.83)	(1.52)	(1.45)	(1.24)
6	2.33	2.41	1.92	1.93	2.41	1.97	2.00	2.17
	(1.47)	(1.54)	(1.18)	(1.17)	(1.52)	(1.21)	(1.19)	(1.08)
Base covariates	X	X	X	X	X	X		X
Log(upwind LAI)		X						
NAAQS standards			X					
Weather variables				X				
Unemployment					X			
Log(Population)							X	
Do not stratify								X

t statistics in parentheses, * $p < 0.1$, ** $p < 0.05$, *** $p < 0.01$

Appendix Table A7: Correlation between number of urban counties in each early cohort and weight for urban counties

Event year	Correlation between number of counties in cohort and weight assigned to that cohort's observations in the same event year.

|	
-9	0.76
-8	0.78
-7	0.78
-6	0.74
-5	0.75
-4	0.78
-3	0.76
-2	0.75
0	0.80
1	0.75
2	0.73
3	0.73
4	0.75
5	0.76
6	0.76

This table shows the correlation between the "own bin" weight assigned to each cohort and the number of counties in that cohort. Weights are obtained from the "eventstudyweights" package from Sun and Abraham (2020) after partialling out covariates and event study indicators for non-urban counties.

Appendix Figure A1: Early emerald ash borer infestation is associated with little change in maximum and minimum temperatures in urban counties
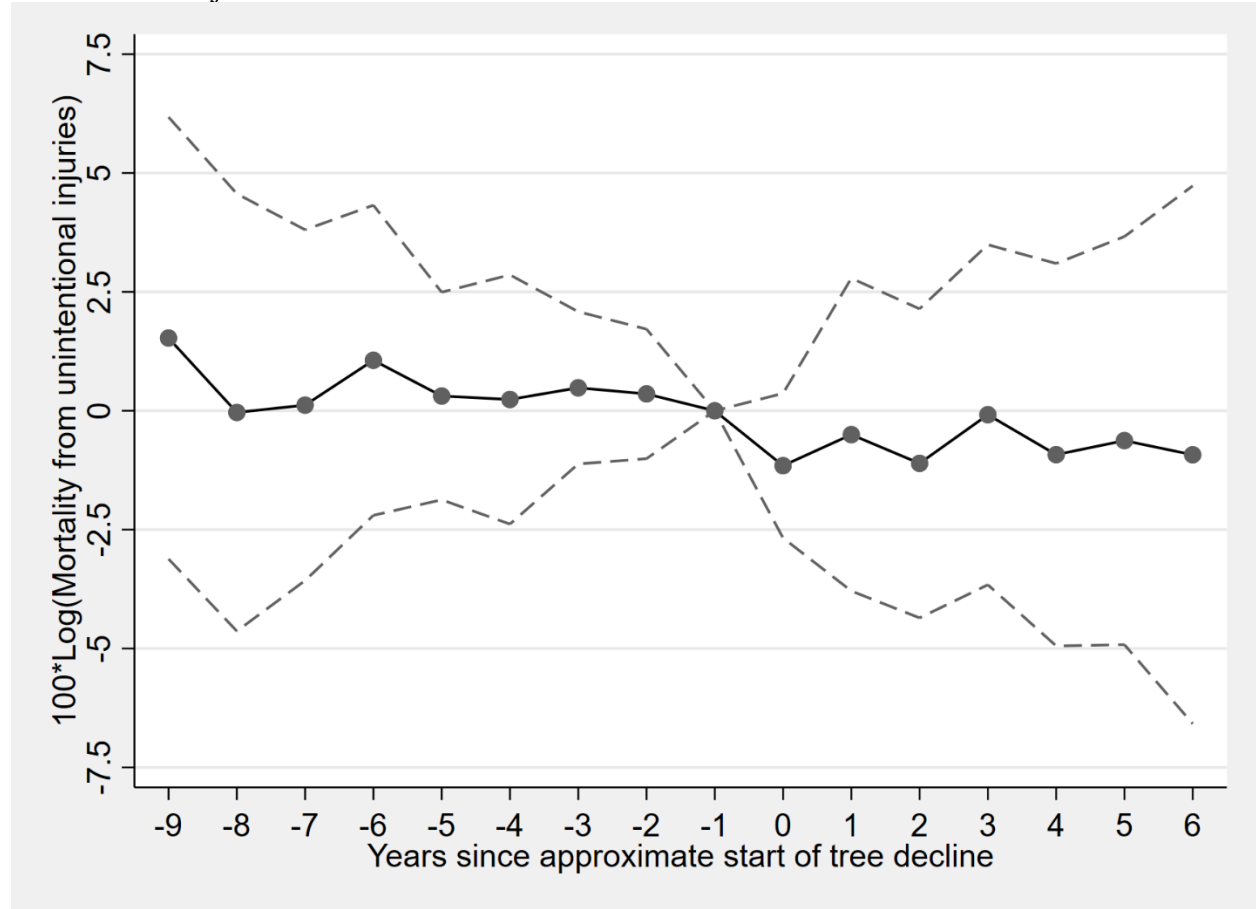
a)   Maximum temperatures
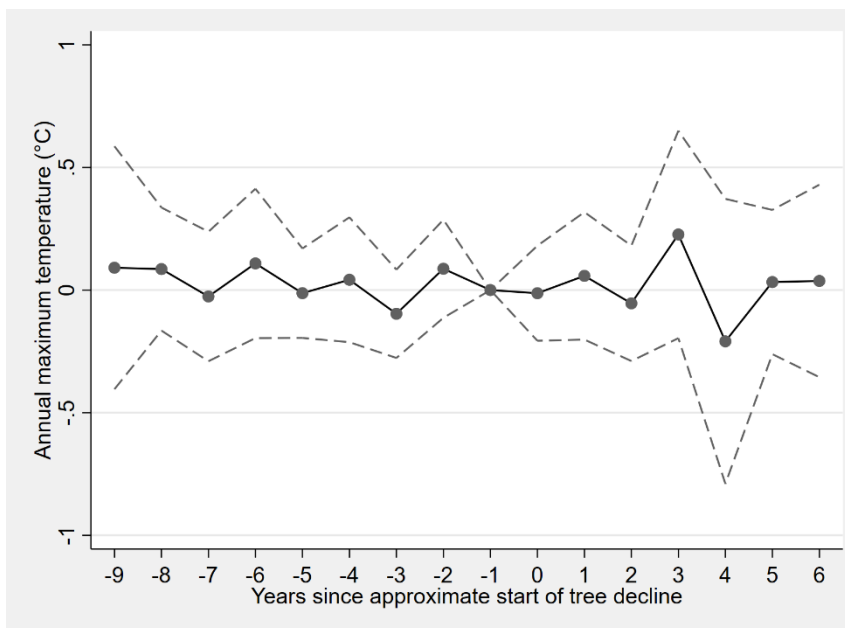
b)   Minimum temperatures
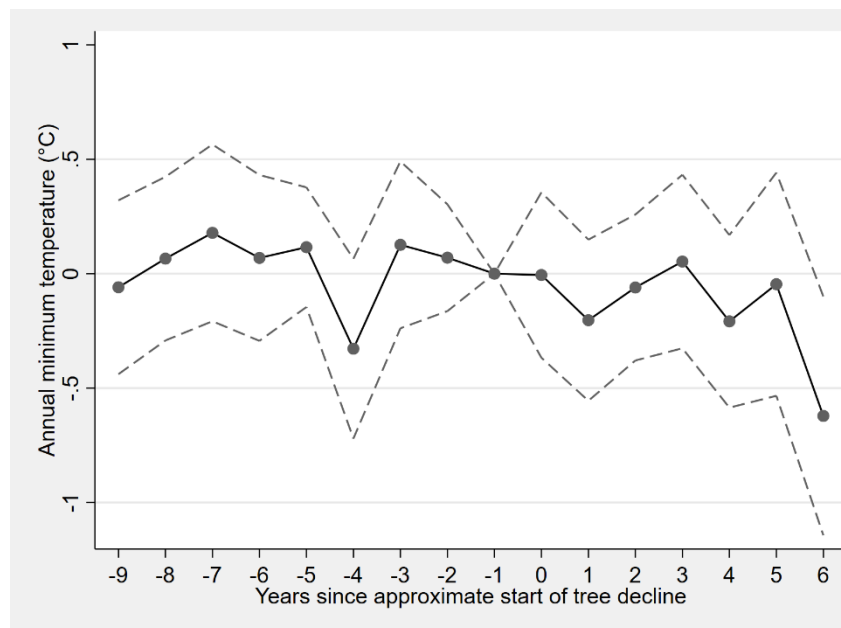
Standard errors clustered by state interacted with plant hardiness zone; 95% confidence intervals shown. Covariates include log(median household income), log(population density), log(% population that is white), and log(% population that is Hispanic), all interacted with urban status. Fixed effects are county, urban status interacted with year, and state interacted with USDA plant hardiness zone and year. Displayed coefficients are for balanced event years for urban counties.

Appendix Figure A2: Early emerald ash borer infestation is not associated with any change in unintentional injuries

Standard errors clustered by state interacted with plant hardiness zone; 95% confidence intervals shown. Covariates include log(median household income), log(population density), log(% population that is white), and log(% population that is Hispanic), all interacted with urban status. Fixed effects are county, urban status interacted with year, and state interacted with USDA plant hardiness zone and year. Displayed coefficients are for balanced event years for urban counties.

Appendix Figure A3: Weights for each event year indicator for urban counties
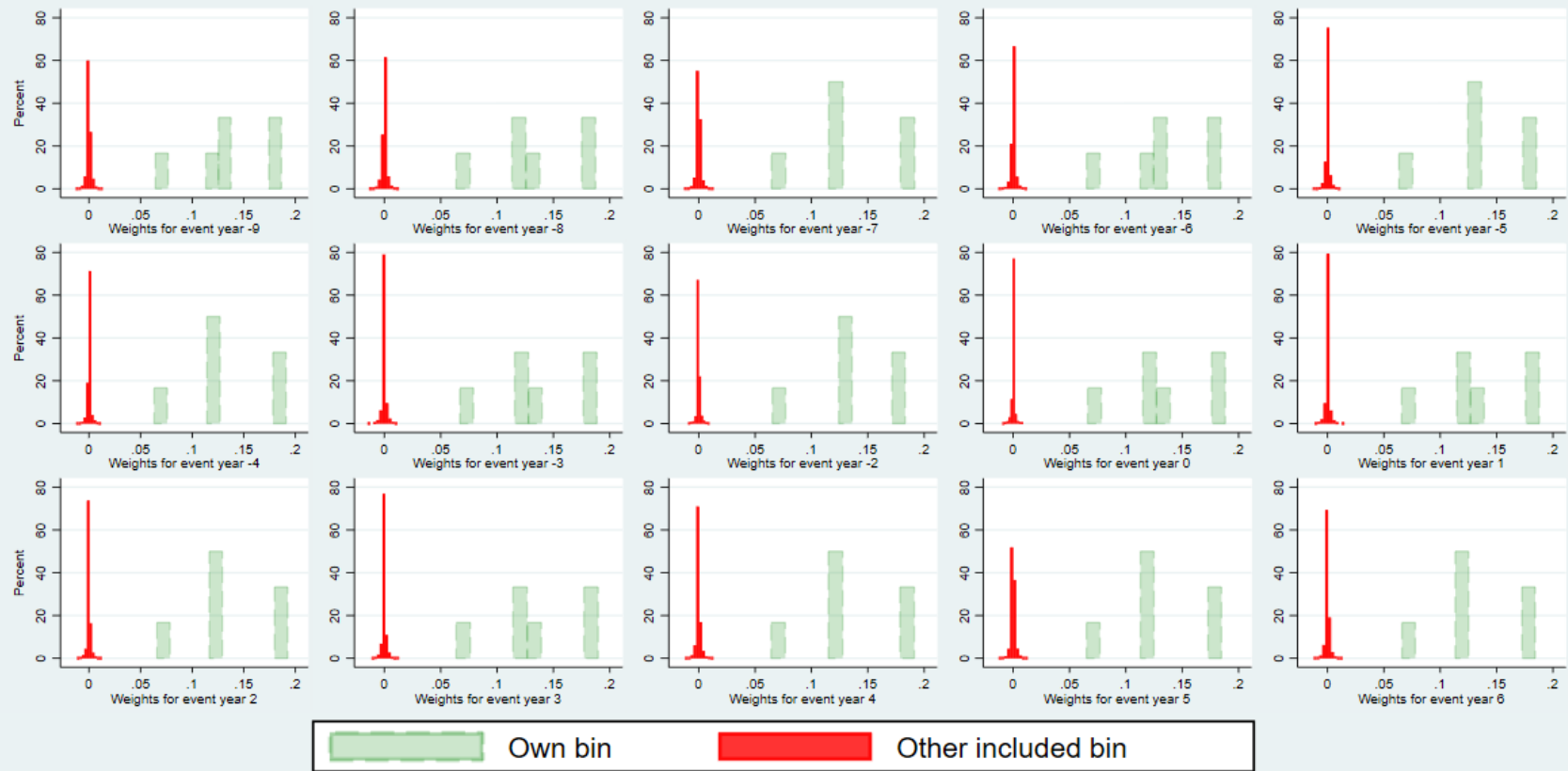
Explanatory text on next page.

These histograms show the distribution of weights for each event study coefficient for urban counties using the "eventstudyweights" package from Sun and Abraham (2020) after partialling out covariates, and the following discussion follows their terminology.

The "own bin" distributions show the weights assigned to each cohort's observations among urban counties in the corresponding event year, where a cohort comprises all counties with the same year of approximate first tree death. For example, the weights in the "own bin" distribution for event time 6 are the weights assigned to each cohort's outcome among urban counties in event year 6. These are, as is desirable, positive and large (Sun & Abraham (2020) show they must sum to 1).

The "other included bin" distributions for event year i reflect the weights assigned to each cohort in other event years $j \neq i$ or urban statuses. Sun and Abraham (2020) show that those weights are, counterintuitively, nonzero; however, in this case they are much smaller than the "own bin" weights, with no overlap, and they are tightly centered around 0, as is desirable so that event year i's estimates are not excessively contaminated by event years $j \neq i$ or by non-urban counties.

Chapter 2

The health co-benefits of carbon pricing in the electricity sector: Evidence from Great Britain

2.1 Introduction

Carbon prices are a powerful tool in limiting greenhouse gas emissions to limit global warming to the "safe" level of 2C or less over pre-industrial temperatures (International Monetary Fund, 2019), a goal that the international community agreed to in the Paris Agreement. The energy sector releases the vast majority - 73% in 2016 (Ge & Friedrich, 2020) - of anthropogenic greenhouse gases, and coal power plants, as a major source of energy, emit a great deal of carbon - 30% of energy-related carbon emissions in 2018 (International Energy Agency, 2019). At the same time, coal plants often release large quantities of local air pollutants such as nitrogen oxides (NO2) (Union of Concerned Scientists, 2017). Therefore, carbon prices, if effective at reducing emissions of carbon from coal combustion, may also benefit local air quality and health.

In this paper, I provide the first quasi-experimental empirical evidence on the effect of imposing a carbon price on local air quality and health outcomes.

2.2 Policy background

In April 2013, the government of the United Kingdom introduced an electricity market reform comprising a carbon price on power plants, known as the Carbon Price Support (CPS), subsidies (contracts for difference) for low-carbon generation, an emissions standard for new plants of 450 gCO_2/kWh, and a capacity market (Grubb & Newbery, 2018). The CPS was imposed on top of a Climate Change Levy, which had been imposed on downstream users of energy -

therefore excluding electricty generators (Pearce, 2005) - since 2001, as well as the European Union Emissions Trading Scheme (EU ETS). Phase-in of the Carbon Price Support was gradual, with the rate being set to £4.94/tCO$_2$[27] between April 2013 and March 2014 (FY 2013/14), rising to £9.55/tCO$_2$ between April 2014 and March 2015 (FY 2014/2015) and £18.08/tCO$_2$ after March 2015 (Hirst, 2018). Since coal is the most carbon-intensive source of electricity generation, the introduction of this carbon tax disadvantages coal generation and has been cited as a reason why the share of coal generation in the UK has plunged.

In this paper I attempt to estimate the effects of the CPS on local air quality and health, focusing primarily on baseload sources of power; coal plants and combined-cycle gas plants. Since coal plants are the largest emitters of both carbon and local air pollutants, a carbon price that disadvantages coal relative to, say, natural gas should improve the local air quality near coal plants. If the reduction in generation from coal plants is made up by natural gas plants, however, there may be an increase in pollution near natural gas power plants.

2.3   Related Work

In the economics literature, the CPS has been studied by Leroutier (2019), Abrell, Kosch & Rausch (2019), and Gugler, Haxhimusa & Liebensteiner (2020). These three papers study the effect of the Carbon Price Support on carbon emissions from the UK power sector, and find that significant reductions in carbon emissions result. A reduction in carbon emissions should be accompanied by reduction in emissions of co-pollutants. All these papers have to grapple with the problem of finding a valid counterfactual for the output of power plants in a setting where every

---

[27] tCO$_2$ stands for ton of carbon dioxide.

other power plant in the same electricity grid is treated by the policy. Abrell, Kosch & Rausch (2019), and Gugler, Haxhimusa & Liebensteiner (2020) do so by using the same plants in the past as counterfactuals; the first uses pre-treatment outcomes to predict future output in the absence of treatment, and the second uses and a discontinuity in time. Leroutier (2019) takes a different approach and uses European power plants as synthetic controls.

Unlike these three papers, which all focus on emissions, I consider ambient air quality and health outcome changes in the vicinity of power plants. Since there are areas near power plants and areas far from power plants, looking at this outcome sidesteps the need for identifying valid counterfactuals for power plants per se. Of course, the link between emissions from large point sources and ambient air quality is unclear in this context as it not only depends on pollutant emissions per se, but also how these pollutants are dispersed into the atmosphere. This dispersion depends on atmospheric circulation and characteristics of the power plant such as the height of its chimney. Unlike the power sector, where it is difficult to find counterfactuals that share a policy background and yet are unaffected by the Carbon Price Support, areas close to a power plant have a natural counterfactual in the form of areas further away from any power plants.

More broadly, greenhouse gas reduction policy has been found to benefit human health, but these papers, at least in economics, generally do not address the electric power sector. These papers include Knittel & Sandler (2011), who find important reductions in pollutants from vehicle Corporate Average Fuel Economy Standards and Renewable Fuel Standards in California, and Holland et al. (2016), who study the local pollution benefits of electric cars. The environmental science literature, such as Dimanchev et al. (2019), forecasts health benefits from the

decarbonization of the electric sector, but these do not as a rule approach this topic from the perspective of causal identification.

A necessary condition for there to be health benefits near coal plants from the imposition of a carbon price is that proximity to coal plants harms human health. Difference-in-difference/event study methods similar to those I will use generally find negative health impacts of living near coal power plants. For example, Barrows, Garg & Jha (2019) find that proximity to coal plants in India is associated with increased child mortality. Likewise, Vyas (2019) finds reductions in height for children living close to coal power plants in India.

2.4   Data and Methods

I adopt an event study framework to study the effect of the carbon price on ambient NO_2 levels and mortality. Excluding from the sample all plants with less than 2MW capacity, which are exempt from this policy, and all CHP plants, which are unlikely to affected by the policy because their electricity load follows their heat load (Denholm et. al, 2018; Jorß et. al, 2013 pp. 149), [28] I obtain the locations of every relevant power plant from from open-power-system-data.org (Wiese et al., 2019) and the Digest of UK Energy Statistics (DUKES) (Department for Business, Energy & Industrial Strategy, 2019a, Table 5.11), and run the following model, which I will refer to as the base specification:

$$Y_{it} = \sum_d CAP_{t,d}^{Coal} \beta_{y,d}^{Coal} + \sum_{j=1}^{7} \sum_d CAP_{t,d}^{j} \beta_{y,d}^{j} + W_{it} + \mu_i + \theta_t$$

---

[28] I do however include Grain CHP, which appears to be primarily operated for electricity generation (Power Technology, 2010).

In this specification[29], Y_{it} is the outcome of interest, i.e, ambient air quality in terms of NO2 levels and mortality, in district i at month t. $CAP_{t,d}^{j}$ is defined as the capacity (in gigawatts) of plants of fuel type j at time t and distance d (in bins) of district i's population-weighted centroid as of the (pre-treatment) 2011 Census. Even though the data are monthly, I run the event studies at the fiscal year level (that is, I interact fiscal year dummies with the capacity variables) because treatment varies by fiscal year. As such, the vector of coefficients $\beta_{y,d}^{Coal}$ are of primary interest; they represent the change (relative to the base period, the 2012-13 fiscal year) in the average effect of having 1GW of coal capacity within distance d of a district on that district's pollution/mortality levels.

Pollution data come from two sources. I primarily use yearly 1km by 1km grids of modelled background pollution (DEFRA, 2019) which I average over each district. Unfortunately, using this alone induces measurement error because these grids are provided for each calendar year, but treatment changes by fiscal year. Therefore, I proxy for each district's distribution of NO_2 over each year by using that district's distribution of tropospheric NO_2[30] in that year from the Aura OMI-NO2 instrument (Krotkov, 2013) on a 0.25°x 0.25°grid (about 25 by 17km at Greenwich's latitude), averaged over the district. This is subject to substantial noise for reasons such as cloud cover[31], so I smooth each district's time series of NO_2 using nonparametric kernel regression. Finally, I calculate the scale factor

---

[29] I run these in a joint model because a district could be within 20km of one coal plant and, say, 35km from another coal plant at the same time.

[30] NO2 is technically one component of NO2, but it is used as an indicator for NO2 (U.S. Environmental Protection Agency, n.d.)

[31] Great Britain is notoriously cloudly; unsurprisingly, excluding pixels with substantial cloud cover leads to district-month combinations with no observations.

$$\frac{Smoothed\ NO2\ for\ month\ i\ of\ year\ y}{\sum_{j=1}^{12} Smoothed\ NO2\ for\ month\ j\ of\ year\ y\ /\ 12}$$

and multiply this scale factor by year *y*'s modelled background NO_2 to get an estimate of each month's ambient NO_2 levels. The monthly means of yearly background NO_2, yearly NO_2 multiplied by a scale factor calculated without smoothing, and yearly NO_2 multiplied by the scale factor calculated with smoothing are plotted in Figure 1 below.

Total death counts by month and lower tier local authority district[32] are obtained from several sources; the Office of National Statistics (2019a) provides them for England and Wales and National Records Scotland (2019a) provides them for Scotland. Cause of death data is only available at the yearly level; for Scotland, from National Records Scotland (2019b); for England and Wales between 2013 and 2017, the Office of National Statistics (2019b); for England before 2013, Office of National Statistics (2019c); and for Wales before 2013, StatsWales (2019). Causes of deaths are only available for the calendar year; as with the pollution data, this is problematic because the treatment (by fiscal year) is not aligned with calendar year. Unfortunately, there are no higher frequency sources of these data, so I assume that the proportion of deaths due to circulatory disease is constant across the calendar year.

Weather variables W_{it} are obtained from MERRA-2 (GMAO, 2015) on a $0.5°$x $0.625°$grid (about 55km by 43km at Greenwich's latitude) and averaged over district. These variables include humidity, temperature, precipitation (all three divided into 10 quantiles), and wind direction

---

[32] There are two levels of local authorities in many parts of England. Multiple lower tier districts are nested in each upper tier district.

(divided into 5 dummies), interacted with district and wind speed (5 quantiles by district and wind direction).

Lower tier local authority districts are small enough that even though there are only 8 coal plants operating throughout the sample period, except for the first 20km, relatively small 10km radii can capture a substantial number of districts. This is shown in Table 1.

Since there are more than two kinds of power plants in Great Britain, I include additional "treatment" dummies to control for districts that are near power plants that are not combined-cycle or coal power plants. The 7 other plant types j are Combined-Cycle, Gas, Other Fossil, time-varying CC, time-varying Coal, time-varying Gas and time-varying Other Fossil;[33] it is is necessary to include all of these simultaneously to control for the fact that most districts are near more than one type of fossil fuel plant.

The choice to partition each fuel type's capacity into "time-varying" and non "time-varying" capacities requires some explanation. The "time-varying" capacity near district i in year y, refers to the capacity of plants near i, that are operating at time t but do not operate through the sample period. Therefore, the "time-varying" capacity at time t comprises plants that started operating after 2009 but before t and plants that retired after t but before 2018. As t increases, the new plants that satisfy these conditions are likely to be newer and therefore cleaner (because the potential start dates are later) and the will-be-retired plants that satisfy these conditions are likely to be more efficient and therefore cleaner (since the potential retirement dates are later). This will

---

[33] Although there are several operational oil plants, they produce a trivial amount of electricity and NO2 emissions

be reflected by the associated coefficient declining over time, which is precisely what I expect will happen to coal plants because of the implementation of the CPS.

This level of aggregation is chosen because it is unlikely that the carbon price will differentially affect plants with the same fuel/technology type, but I expect that the carbon price will impact plants of different fuel types differently. Consider that marginal cost = (Price of fuel * Fuel consumed per unit of electricity), and carbon tax paid = (Tax rate * Carbon intensity per unit of fuel * Fuel consumed per unit of electricity); between plants of the same fuel/technology type, the only differences are in fuel consumed per unit of electricity, so marginal cost is directly proportional to carbon tax paid. Therefore, imposing a carbon tax will not change the cost ordering of plants.

Between plants of different fuel types, however, there are large differences in carbon intensity per unit of fuel, with coal being the most carbon-intensive (pay the most CPS) and combined-cycle natural gas being the least (pay the least CPS). This means that marginal cost is no longer directly proportional to tax paid, so imposing a carbon tax may change the cost ordering. There is likely also treatment effect heterogenity between combined-cycle and open-cycle gas turbines that use the same fuel since open-cycle gas turbines, unlike their combined-cycle brethren, are designed to run for short periods of time and cannot be substitutes for baseload coal plants.

The base specification does not account for several covariates which affect the demand for and supply of electricity from fossil fuel generators. Many of these are applicable to the entire network of electricity generators and therefore have no cross-sectional variation per se, but by

64

affecting the output of generators will disproportionately affect the same locations as those affected by the CPS. These variables are denoted M_t and are interacted with the treatment variable CAP^i_d. The inclusion of these variables means that the event study cannot be done at the quarterly level. In any case, the treatment changes in different fiscal years, so this is the level at which I perform the event studies.

The covariates M_t include log electricity demand net of wind and solar (non-dispatchable resources), log dispatchable[34] generation, and log net imports. In addition, an important factor to consider is the relative prices of different fuels, which determines in large part the location of a power plant on the supply curve and therefore its generation. I obtain the average quarterly gas price paid by electricity producers for natural gas and coal (Department for Business, Energy & Industrial Strategy, 2019b) and include their ratio in the form $g(h(x)) = \text{invlogit}(\ln(\frac{P_{gas}}{P_{coal}}))$ as an interaction term for all plants which run on either natural gas or coal. I additionally control for the log real EU ETS spot price (Quandl, 2019). [35] Since the EU ETS price functions by changing the relative prices of gas and coal, it should should have the largest effect where a change in the price ratio has the largest effect (i.e, where the gradient is highest). Therefore, I interact the EU ETS price with the gradient of the inverse logit function $g'(h(x))$.

---

[34] Nuclear (predominantly) and hydro.

[35] The CPS rates are notionally derived by fixing a target price - the Carbon Price Floor (CPF) - and subtracting the EU ETS price. If that is so, omitting the EU ETS price as a control would give estimates of the effect of whatever level the CPF was set at. In practice, the CPS rates for 2013-14 to 2015-16 were derived by subtracting the 3-years ahead futures price from the CPF, so that interpretation is complicated by the EU ETS price changing after the CPS rate was set. In any case, the CPS was frozen after 2015-16, breaking the link between the CPF and the CPS.

Other variables, X_{it}, exhibit both cross-sectional and time series variation. These include include 16+ employment rate, manufacturing employment rate (Office of National Statistics, 2019d), log real average gross disposable household income (GDHI) (Office of National Statistics, 2019e), total vehicle mileage per area, (Department of Transport, 2019), car mileage per area, [36] population density, and a set of variables controlling for the age distribution in 5-year brackets (Office of National Statistics, 2019f). All these variables are observed at the calendar year level.

The functional form $g(h(x)) = \text{invlogit}(\ln(\frac{P_{gas}}{P_{coal}}))$ is chosen so that at extreme ratios the marginal effect of a change in relative prices is minimal; see Appendix A for further explanation. For example, when gas prices are high enough every coal plant will be at maximum output, so an increase in the gas price will not lead to increased output from coal plants. In practice, the domain of the price ratio in the sample generally falls near the middle of the logistic curve where the gradients are steepest (but to the right of 0; gas prices are generally higher than coal prices), so the results are robust to including $\ln(\frac{P_{gas}}{P_{coal}})$ linearly.

As such, the final specification is of the form:

$$Y_{it} = \sum_d \text{CAP}_{t,d}^{Coal}\left(\beta_{y,d}^{Coal} + M_{t,d}^{Coal}\right) + \sum_{j=1}^{7}\sum_d \text{CAP}_{t,d}^{j}\left(\beta_{y,d}^{j} + M_{t,d}^{j}\right) + X_{it} + W_{it} + \mu_i + \theta_t$$

Standard errors of all specifications are two-way clustered by district and month.

---

[36] Vehicle and car mileages are only available at upper tier local authority districts, so I obtain estimates for each lower tier districts by scaling each upper tier district's mileage by the proportion of the upper tier district's population living in that lower tier district.

2.5   Results and discussion

In the base specification, I find significant reductions in ambient NO2 levels and all-cause mortality rates for any given level of nearby coal capacity in the post-period. Unfortunately, as the significant coefficients in the pre-period suggests, this model is unable to account for all the idiosyncratic variation in that relationship before treatment. Of particular concern are the pollution and health effects of variation in the relative prices of electricity from coal and combined-cycle plants; these depend both on the relative input prices of coal and gas as well as the price of EU ETS permits - increases in the latter disproportionately disadvantages coal plants because coal plants are more carbon intensive. To account for these, as well as other observables that could bias my results, I introduce several covariates as described in the section on the preferred specification above.

Turning our attention to the preferred specification, I start by discussing the effect of the carbon tax on air pollutants. Specifically, I look at nitrogen dioxide (NO_2) levels. NO_2 was a particularly important type of air pollution in Great Britain in the years in question, with its levels exceeding (legally binding) EU ambient air quality standards in most of the country throughout the sample period (DEFRA, 2009-2017). Long-term nitrogen oxide exposure has also been implicated in poor health outcomes up to increases in all-cause mortality (Hoek et al., 2013). As such, I focus my discussion of air quality on NO_2. Ambient NO_2 levels for any given level of nearby coal capacity fall after the carbon tax is implemented, and the largest reductions (in magnitude) in NO_2 near coal plants occur after fiscal years 2015/2016 and beyond when the carbon tax is at its highest value. Such reductions imply that the capacity factor of coal plants has fallen. This is expected because, as described earlier, coal plants are the most carbon-intensive source of

generation, meaning that operating coal plants becomes more expensive relative to all other forms of generation. The reductions in NO_2 tend to tail off beyond a 50km radius, when I fail to find any reductions in all-cause or circulatory disease mortality rates.

If ambient air pollution levels fall for any given amount of nearby coal capacity, mortality for any given level of coal capacity should also decline. Indeed, I find such a decline in most districts up to 50km away from coal plants, with the most significant declines being in districts between 40 and 50km away from coal plants after FY 2016-2017. There are also large declines in mortality in the districts less than 20km from coal plants in the initial years after the introduction of the CPS. Those reductions in death rates amount to drops of around 1.5% to 2.5% from the pre-treatment mean per gigawatt of coal capacity nearby. It appears that mortality reductions do not persist at distances further than 50km away from coal plants; therefore, even though air pollutants from coal plants can travel hundreds of kilometers, I cut the analysis off at a 70km radius.

So far, I have estimated the relationship between coal capacity and mortality rates. This can be converted to an estimate of the changes in mortality rate in affected districts by multiplying the coefficient by the average coal capacity. In the districts between 40 and 50km from a coal plant, the effect of the carbon price was about 1.5 deaths per 100000 per GW of capacity per month in FY2016-2017 and about 2.1 deaths per 100000 per GW of capacity per month in the first 9 months of FY2017-2018. The average coal capacity in these districts was 2.5 GW. Therefore, the average change in mortality was a reduction of 3.8 deaths per 100000 per month in FY2016-2017 and 5.3 deaths per 100000 per month in FY2016-2017.

The information outlined above can also be used to calculate the value of lives lost. The National Institute for Clinical Excellence (NICE) has a recommended value of £20000 for a quality-adjusted life year (Ogden, 2017). [37] There were 37 districts at a distance of 40-50km from a coal plant in those years, with a mean population of 170000. Using these numbers, I estimate that 2850 life-months were saved in FY 2016/2017 and 2950 life-months in the 9 months of FY2017/2018 in the sample. Over these 21 months, there was a total benefit of £9.7 million from mortality reductions stemming from the CPS in addition to the carbon reduction benefit. This is very much a lower bound because it only considers the significant negative mortality coefficients, which ignores the remaining coefficients up to 50km which are negative in every year.

Accompanying the significant reductions in all-cause mortality are significant reductions in mortality from circulatory disease. The reductions in circulatory disease are, on average, a larger proportion of the reductions in all-cause mortality than the proportion of deaths attributable to circulatory disease in those fiscal years. The proportion of reductions seems to be falling over time, suggesting heterogenous short and long-run effects of air pollution from coal plants.

Of course, mortality is not the only negative impact on health that NO_2 exposure brings. Even short-term exposure to NO_2 brings many less than lethal health effects, such as "coughing and choking", "nausea", "headache", "abdominal pain" and "difficulty breathing" (National Institutes of Health, n.d.). Therefore, the effect of this policy on human welfare is larger than the effects on mortality presented here.

---

[37] This is actually a very low valuation; the US EPA's value of a statistical life year is $490000.

I also consider the effect of the CPS on districts near combined-cycle gas plants. These plants are substantially cleaner, particularly at full load, than coal plants (Gonzalez-Salazar et. al, 2018). If NO_2 levels near coal plants have gone down because the carbon price has induced generation to shift from coal plants to combined-cycle gas plants, the capacity factor of combined cycle plants should go up, but increases in the capacity factor from combined cycle plants should not lead to a large increase in the capacity-ambient NO_2/mortality relationship near those plants.

Unlike coal plants, there is no clear movement in the capacity-ambient NO_2 relationship, with perhaps an increase in ambient NO_2 levels at some distances. These increases in ambient pollution do not appear to be accompanied by increases in mortality; in fact, my model finds significant decreases in mortality in districts at 30 to 40km from these plants, but these occur even as the estimates indicate that NO_2 levels are significantly increasing in those districts. The pre-trends and overall larger standard errors (despite there being 4 times as many districts near combined-cycle gas plants as there are near coal plants) do suggest, however, that my model fails to capture some idiosyncratic variation in mortality in the districts near combined-cycle gas plants. Presumably, there is unmodelled cross-sectional or time-varying heterogenity in the mortality response to covariates in the model, which is perhaps inevitable with the large number of districts . Be that as it may, there is no evidence to suggest any (at least, short-run) cost in terms of mortality of substituting from coal plants to combined-cycle gas generation, which is reassuring if that remains necessary for carbon reduction goals until baseload can be provided by zero-GHG resources (Hausfather, 2015).

We may be concerned that these changes have come about due to other changes affecting electricity generation occuring around this time. After all, I described earlier that the carbon price

support was only one of four policies introduced as part of a reform of the electricity market. Since my estimates control for renewable generation, they account for the effects of renewable subsidies on the construction of new low carbon power plants. Capacity payments do not create an incentive that changes the amount of electricity generated or pollutants released from a plant outside of the long-run decision of whether to make the plant available.[38] This means that the estimates I obtain, which are representative of the set of plants that operate throughout the sample period, are only affected by the existence of the capacity market to the extent that capacity payments, which start in October 2018, induce plants to be available not only after October 2018 but also up to 2017.[39] To account for variations in the other carbon tax operating through the sample period, I control for EU ETS permit prices. Although the Climate Change Levy might have affected the demand for electricity from industry, it was constant in real terms through the whole sample period.

2.6   Conclusion

This study shows that the imposition of a relatively small carbon tax in the electricity sector leads to significant reductions in ambient levels of air pollutants such as nitrogen oxides (as NO_2) near coal power plants. Importantly, I show that even in the policy context of a developed economy with an advanced healthcare system, the reductions in air pollution lead to smaller but still significant reductions in all-cause mortality, as well as mortality from circulatory disease. These reductions do not appear to be accompanied by any significant increase in mortality near

---

[38] Winners of capacity auctions were obliged to deliver energy during periods of system stress, but these periods only occurred for 2.5 hours during the sample period (National Grid, 2016). These periods occurred at a time when only certain small-scale generation had a delivery obligation under the Capacity Market (BEIS, 2019)

[39] It is doubtful that the payments necessary to cover costs over this longer period would permit coal to win the auctions given the levels of oversubscription.

competing combined-cycle gas power plants, meaning that the health effects from this policy are unambiguously positive.

When considering the merits of a carbon price, policymakers should consider these health benefits in addition to the carbon reductions that are the direct target of the policy. The existence of these additional health benefits adds weight to the case for increased adoption of carbon prices worldwide. Since the mechanism by which pollution reductions occur is a reduction in the capacity factor of coal, carbon abatement policies that are designed to allow fossil fuel plants to extend their useful lifespan, most notably carbon capture and sequestration, are unlikely to provide similar benefits and should be not be favored.

2.7   References

Abrell, J., Kosch, M., Rausch, S. (2019b) How Effective Was the UK Carbon Tax? A Machine
Learning Approach to Policy Evaluation. CER-ETH Working Paper 19/317.

Central Electricity Generating Board (1969). New construction techniques used in Drax
chimney. Electronics and Power 15(7), 239. https://doi.org/10.1049/ep.1969.0236

Denholm, P., Brinkman, G., & Mai, T. (2018). How low can you go? The importance of
quantifying minimum generation levels for renewable integration. Energy Policy, 115,
249-257.

Department of Business, Energy & Industrial Strategy (2019a).Digest of UK Energy Statistics
(DUKES): electricity (Table 5.11). Retrieved from
https://www.gov.uk/government/statisti cs/electricity-chapter-5-digest-of-united-
kingdom-energy-statistics-dukes

Department of Business, Energy & Industrial Strategy (2019b). Average prices of fuels
purchased by the major UK power producers (QEP 3.2.1). Retrieved from
https://www.gov.uk/governmen t/statistical-data-sets/prices-of-fuels-purchased-by-
major-power-producers

Department of Environment Food and Rural Affairs (2019). Modelled background pollution
data. Retrieved from https://uk-air.defra.gov.uk/data/pcm-data

Department of Environment Food and Rural Affairs (2009-2017). Air Pollution in the UK -

    Compliance Assessment Summary. Retrieved from https://uk-

    air.defra.gov.uk/library/annual report/

Department of Transport (2019).   GB Road Traffic Counts.   Retrieved from

    https://data.g ov.uk/dataset/208c0e7b-353f-4e2d-8b7a-1a7118467acc/gb-road-traffic-

    counts Dimanchev, E. G., Paltsev, S., Yuan, M., Rothenberg, D., Tessum, C. W.,

    Marshall, J. D., & Selin, N. E. (2019). Health co-benefits of sub-national renewable

    energy policy in the US. Environmental Research Letters, 14(8), 085012.

Energy Information Administration (2019).Electric Power Annual.   Retrieved from

    https://www.eia.gov/electricity/annual/

Ge, M. & Friedrich, J. (2020) 4 Charts Explain Greenhouse Gas Emissions by Countries and

    Sectors.

    https://web.archive.org/web/20200802150738/https://www.wri.org/blog/2020/02/green

    house-gas-emissions-by-country-sector

Global Modeling and Assimilation Office (2015), MERRA-2_tavgM_2d_flx_Nx:

    2d,Monthly_mean,TimeAveraged,Single-Level,Assimilation,Surface Flux Diagnostics

    V5.12.4, Greenbelt, MD, USA, Goddard Earth Sciences Data and Information Services

    Center (GES DISC), Accessed: 7 July 2019, 10.5067/0JRLVL8YV2Y4

Gonzalez-Salazar, M. A., Kirsten, T., & Prchlik, L. (2018). Review of the operational

    flexibility and emissions of gas-and coal-fired power plants in a future with growing

renewables. Renewable and Sustainable Energy Reviews, 82, 1497-1513.

https://doi.org/10.1016/j.rser.2017.05.278

Grubb, M., & Newbery, D. (2018). UK electricity market reform and the energy transition:

Emerging lessons. The Energy Journal, 39(6).

Gugler, K., Haxhimusa, A., & Liebensteiner, M. (2020). Carbon Pricing and Emissions: Causal

Effects of Britain's Carbon Tax (Working Paper).

Hausfather, Z. (2015). Bounding the climate viability of natural gas as a bridge fuel to displace

coal. Energy Policy, 86, 286–294. https://doi.org/10.1016/j.enpol.2015.07.012

Hirst, D. (2018). Carbon Price Floor (CPS) and the price support mechanism (Commons

Library Briefing Paper No. 05927). Retrieved from:

https://researchbriefings.parliament.u k/ResearchBriefing/Summary/SN05927

Hoek, G., Krishnan, R. M., Beelen, R., Peters, A., Ostro, B., Brunekreef, B., & Kaufman, J. D.

(2013). Long-term air pollution exposure and cardio-respiratory mortality: a review.

Environmental health, 12(1), 43.

Holland, S. P., Mansur, E. T., Muller, N. Z., & Yates, A. J. (2016). Are there environmental

benefits from driving electric vehicles? The importance of local factors. American

Economic Review, 106(12), 3700-3729.

International Energy Agency (2019). Global Energy & CO2 Status Report 2019. Retrieved

   from https://web.archive.org/web/20200802152552/https://www.iea.org/reports/global-

   energy-co2-status-report-2019/#

International Monetary Fund (2019, October 11). Fiscal Policies to Curb Climate Change.

   Retrieved from

   https://web.archive.org/web/20200625013355/https://blogs.imf.org/2019/1 0/10/fiscal-

   policies-to-curb-climate-change/

Jorß, W., Joergensen, B.H., Loeffler, P., Morthorst, P.E., Uyterlinde, M., van Sambeek, E., &

   Wehnert, T.(2003). Decentralised power generation in the liberalised EU energy

   markets: results from the DECENT research project. Springer.

Leroutier, M. (2019) Carbon Pricing and Power Sector Decarbonisation: Evidence from the

   UK. FAERE Working Paper 2019.12.

Kaplan, S. (2008). Power Plants: Characteristics and Costs. Retrieved from https://fas.or

   g/sgp/crs/misc/RL34746.pdf

Knittel, C. R., & Sandler, R. (2011). Cleaning the bathwater with the baby: The health

   cobenefits of carbon pricing in transportation (No. w17390). National Bureau of

   Economic Research.

Kumar, N., Besuner, P., Lefton, S., Agan, D., & Hilleman, D. (2012). Power Plant Cycling

   Costs. Retrieved from the National Renewable Energy Laboratory:

   https://www.nrel.gov/docs/fy12 osti/55433.pdf

Krotkov, N.A. (2013), OMI/Aura NO2 Cloud-Screened Total and Tropospheric Column L3

> Global Gridded 0.25 degree x 0.25 degree V3, NASA Goddard Space Flight Center,

> Goddard Earth

Sciences Data and Information Services Center (GES DISC), Accessed: 26 June 2018, https:

> //doi.org/10.5067/Aura/OMI/DATA3007

NIH National Library of Medicine (n.d.). What are Nitrogen Oxides?. Retrieved from

> https://web.archive.org/web/20200616110316/https://toxtown.nlm.nih.gov/chemicals-

> and-contaminants/nitrogen-oxides.

National Records Scotland (2019a). Weekly and Monthly Data on Births and Deaths

> Registered in Scotland. Retrieved from https://www.nrscotland.gov.uk/statistics-and-

> data/statistics/statistics-by-theme/vital-events/general-publications/weekly-and-

> monthly-data-on-births-and-deaths-registered-in-scotland

National Records Scotland (2019b).Vital Events Reference Tables.   Retrieved from

> https://www.nrscotland.gov.uk/statistics-and-data/statistics/statistics-by-theme/v ital-

> events/general-publications/vital-events-reference-tables

Office of National Statistics (2019a). Deaths registered monthly in England and Wales.

> Retrieved from

> https://www.ons.gov.uk/peoplepopulationandcommunity/birthsdeathsandmarriages

> /deaths/datasets/monthlyfiguresondeathsregisteredbyareaofusualresidence

Office of National Statistics (2019b). Mortality statistics - underlying cause, sex and age .

    Retrieved from https://www.nomisweb.co.uk/

Office of National Statistics (2019c). Deaths by sex, age group, cause and local authority,

    England, deaths registered 1993 to 2013. Retrieved from:

    https://www.ons.gov.uk/peoplepopulationa

    ndcommunity/healthandsocialcare/causesofdeath/adhocs/004352deathsbysexagegroupc

    a useandlocalauthorityenglanddeathsregistered1993to2013

Office of National Statistics (2019d). Annual Population Survey. Retrieved from https://ww

    w.nomisweb.co.uk/

Office of National Statistics (2019e). Gross disposable household income. Retrieved from

    https://www.nomisweb.co.uk/

Office of National Statistics (2019f). Population Estimates. Retrieved from

    https://www.nomisweb.co.uk/

Ogden, J. (2017). QALYs and their role in the NICE decision-making process. Prescriber,

    28(4), 41-43. Retrieved from https://onlinelibrary.wiley.com/doi/abs/10.1002/psb.1562

Pearce, D. (2005). The United Kingdom Climate Change Levy: A study in political economy.

    Organisation for Economic Co-operation and Development. Power Technology (2008).

    Isle of Grain Combined Heat and Power (CHP) Station, Kent, United Kingdom.

    Retrieved from https://web.archive.org/web/20200607031522/https://www.powe r-

    technology.com/projects/isleofgrain/.

Quandl (2019f). ECX EUA Futures, Continuous Contract #1 (C1) (Front Month). Retrieved
from https://www.quandl.com/data/CHRIS/ICE_C1-ECX-EUA-Futures-Continuous-
Contract-1-C1-Front-Month

StatsWales (2019). Deaths by cause. Retrieved from https://statswales.gov.wales/Catalog
ue/Health-and-Social-Care/Births-Deaths-and-Conceptions/Deaths/Deaths-by-Cause

U.S. Enviromental Protection Agency (n.d.). Basic Information about NO2. Retrieved from
https://web.archive.org/web/20200804054504/https://www.epa.gov/no2-pollution/
basic-information-about-no2.

Union of Concerned Scientists (2017). Coal and Air Pollution. Retrieved from https://web.arch
ive.org/web/20200718021131/https://ucsusa.org/resources/coal-and-air-pollution

Vyas, Sangita, The Child Health Impacts of Coal: Evidence from India's Coal Expansion
(December 28, 2019). Available at SSRN:
https://ssrn.com/abstract=3507883orhttp://dx.doi .org/10.2139/ssrn.3507883

Wiese, F., Schlecht, I., Bunke, W., Gerbaulet, C., Hirth, L., Jahn, M., Kunz, F., Lorenz, C.,
Muhlenpfordt, J., Reimann, J., & Schill, W. (2019). Open Power System Data –
Frictionless data for electricity system modelling. Applied Energy, 236, 401–409.
https://doi.org/10.1016/j.apenergy.2018.11.097

2.8   Tables and figures

Table 1: Summary statistics for districts near coal plants

Distance (km)	Number of districts	Mean coal capacity (GW)	Mean ambient NO_2 (ugm^{-3}) before treatment	Death rate per 100000 before treatment
<20	22	2.22	27.1	76.4
20-30	22	2.29	22.6	81.6
30-40	29	2.54	22.8	79.1
40-50	37	2.47	21.8	81.1
50-60	41	2.58	21.9	81.4
60-70	41	2.28	22.4	80.6

Table 2: Summary statistics for districts near combined-cycle gas plants

Distance (km)	Number of districts	Mean combined-cycle capacity (GW)	Mean ambient NO_2 (ugm^{-3}) before treatment	Death rate per 100000 before treatment
<20	79	.805	28.3	72.4
20-30	87	.872	29.5	69.6
30-40	116	.884	27.3	70.2
40-50	130	.858	27.5	71.4
50-60	150	.990	26.3	72.8
60-70	162	1.06	24.1	74.4

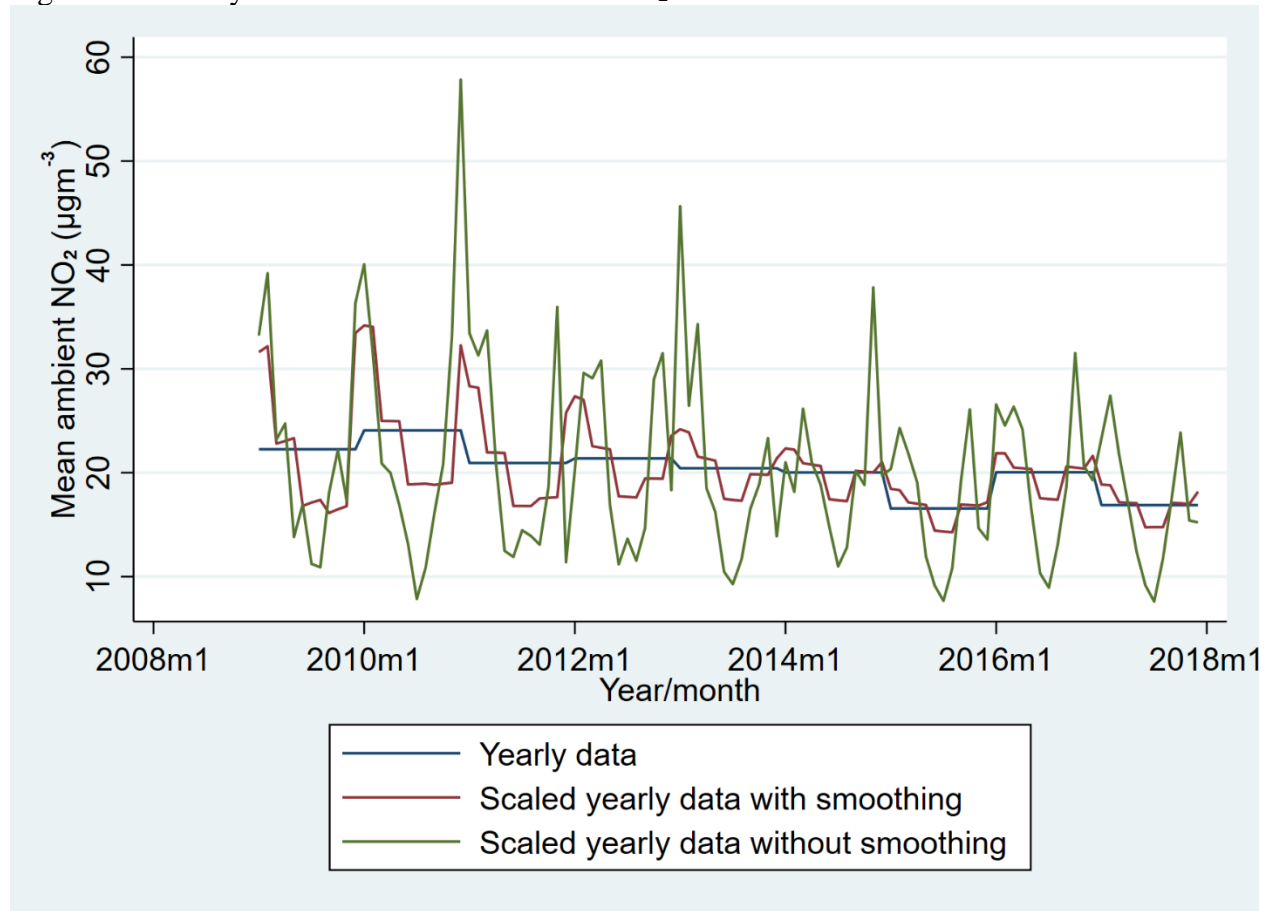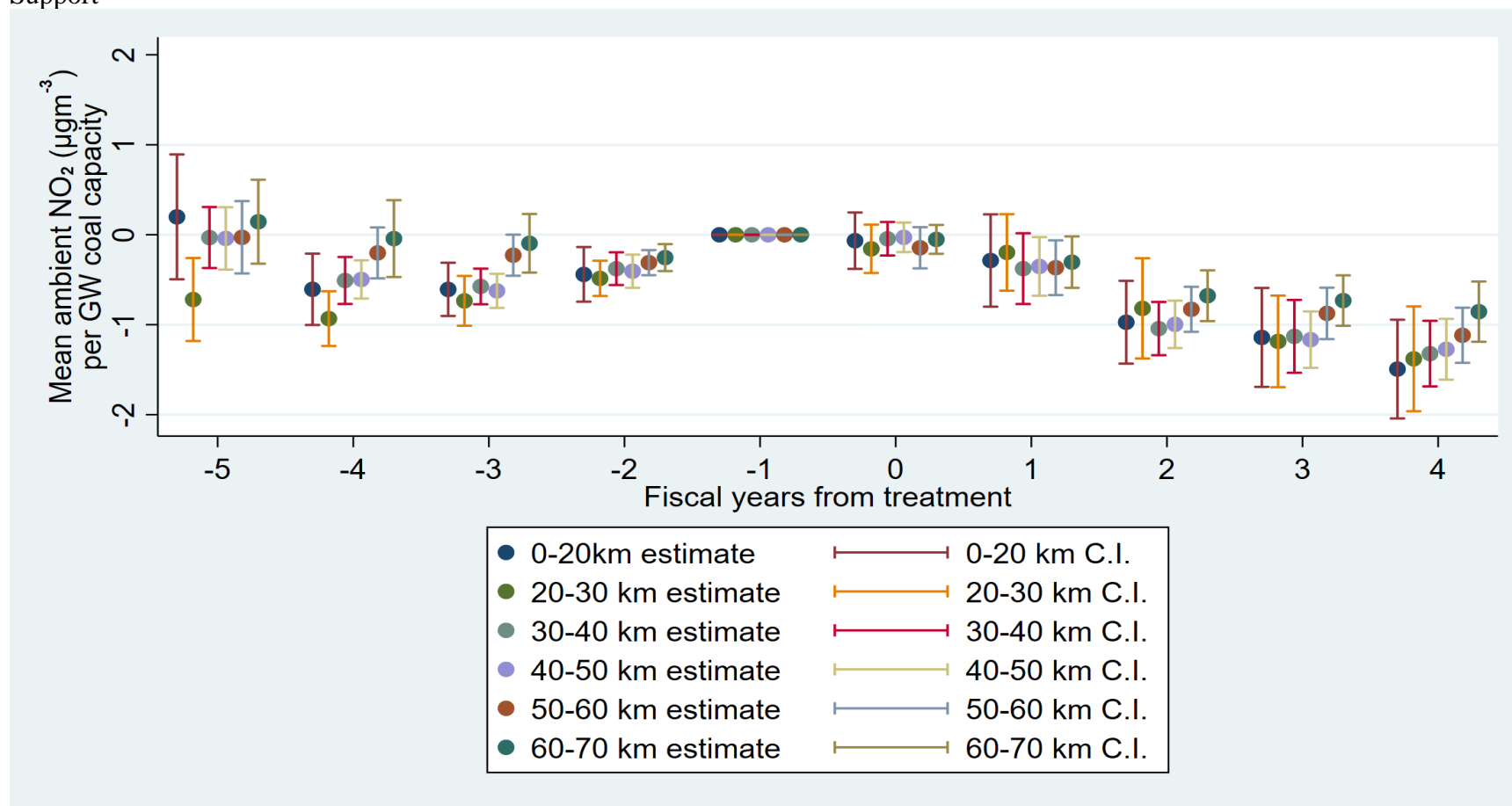Figure 1: Monthly means of three estimates of NO$_2$

Figure 2: Reductions in average ambient surface NO_2 occur near coal power plants after the implementation of the Carbon Price Support
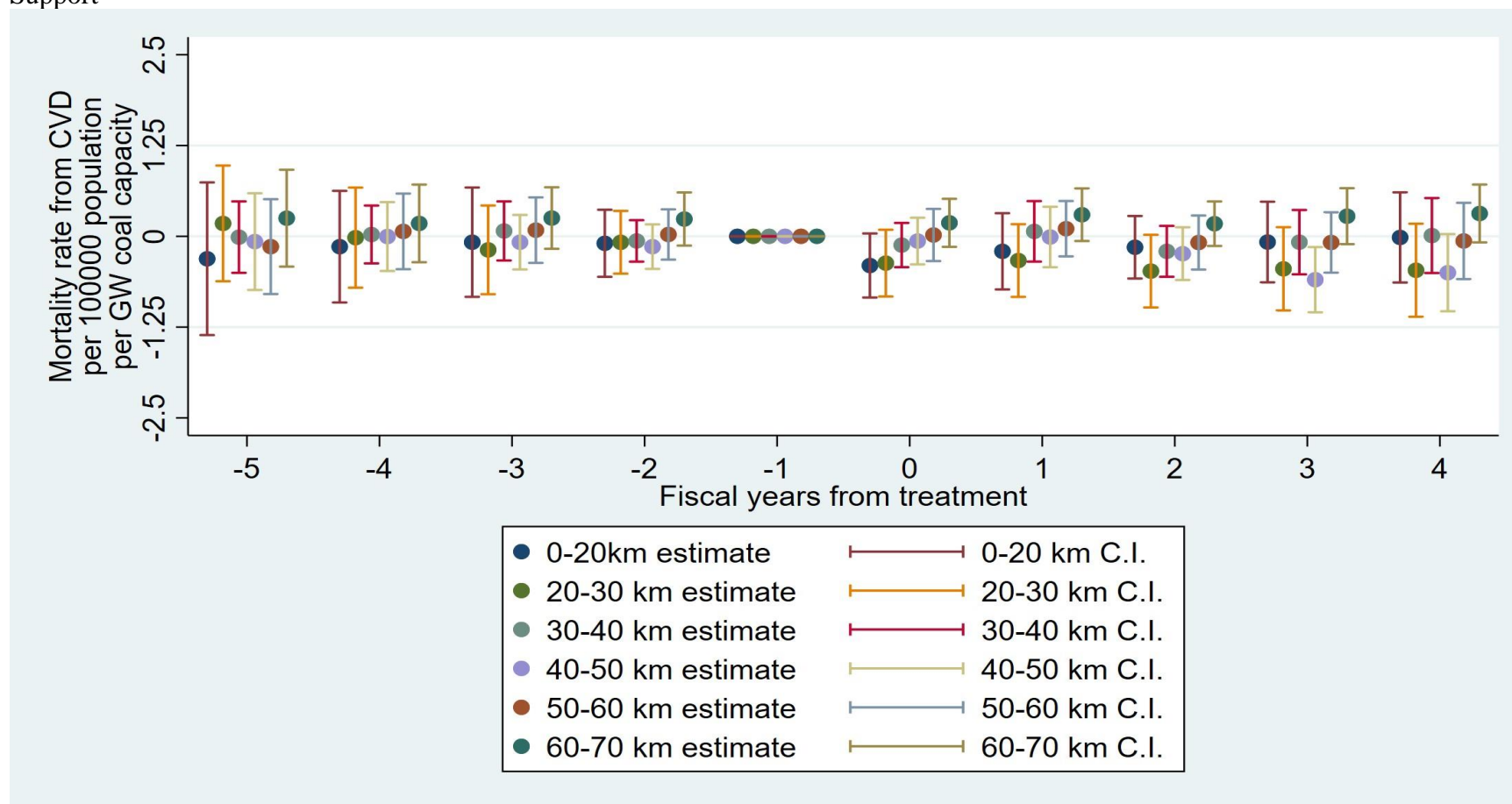

Standard errors are clustered at the (lower tier) local authority level; 95% confidence interval shown.

Figure 3: Reductions in all-cause mortality occur near coal power plants after the implementation of the Carbon Price Support
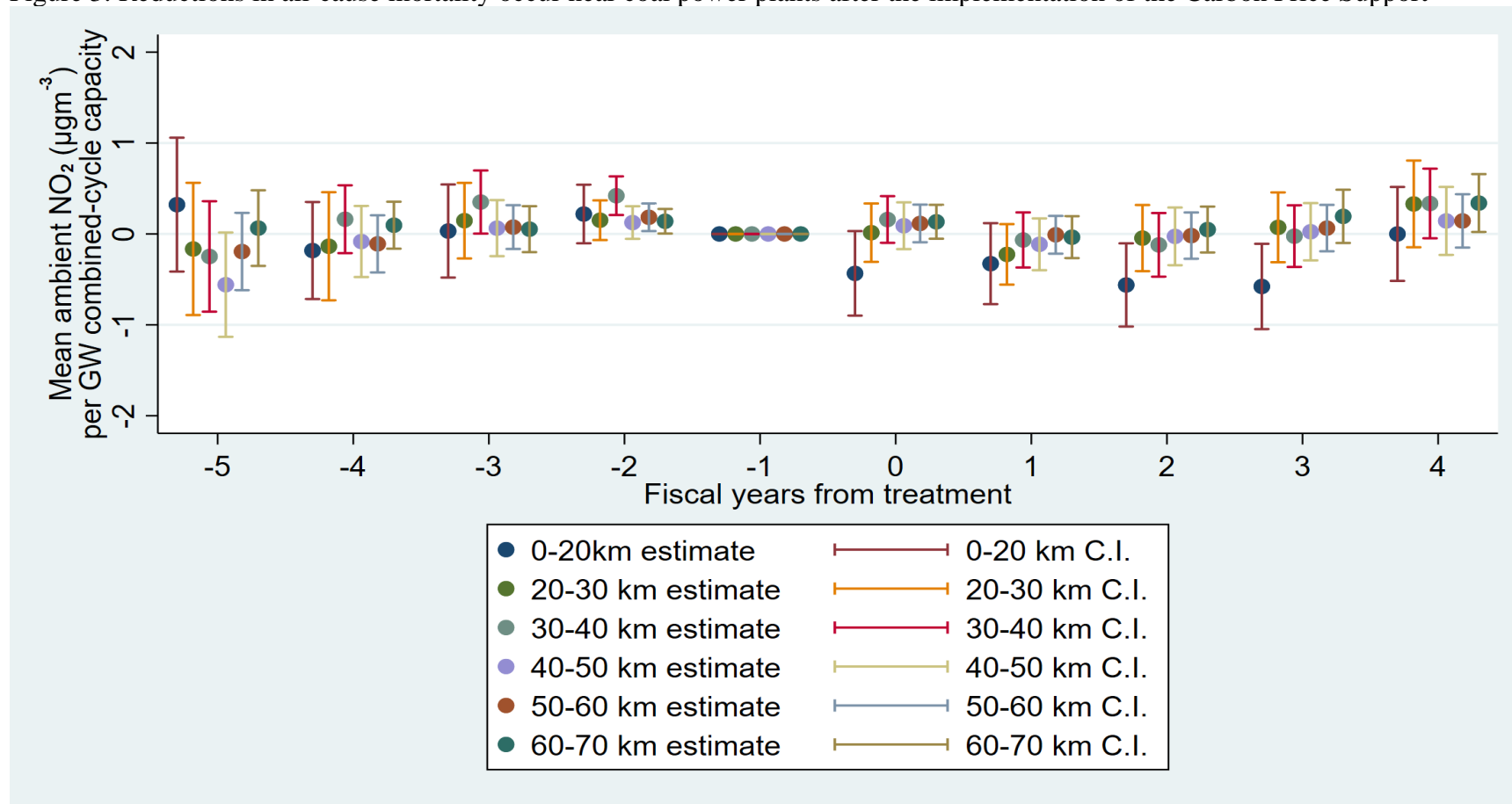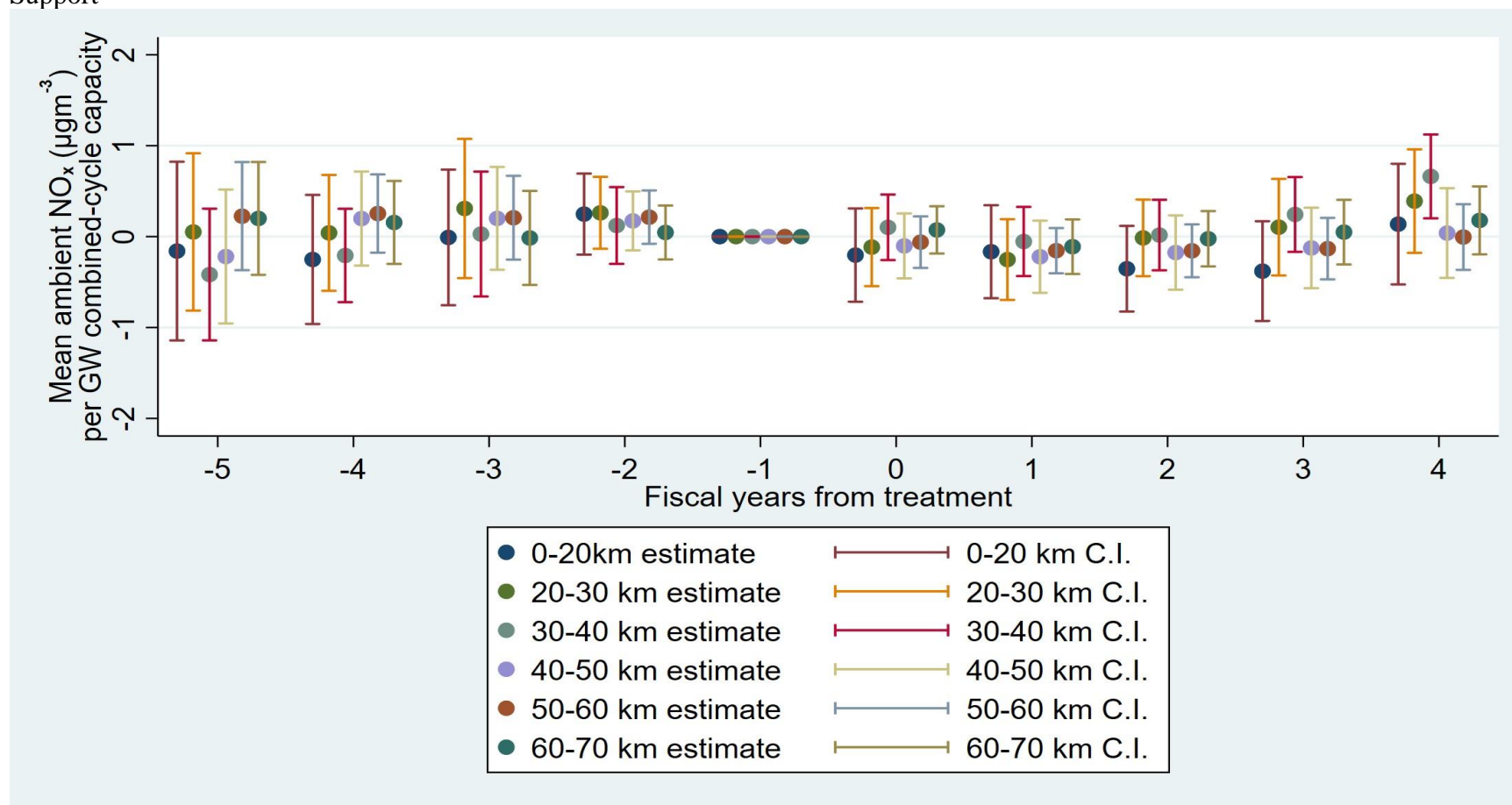

Standard errors are clustered at the (lower tier) local authority level and month; 95% confidence interval shown.

Figure 4: Reductions in cardiovascular disease mortality occur near coal power plants after the implementation of the Carbon Price Support
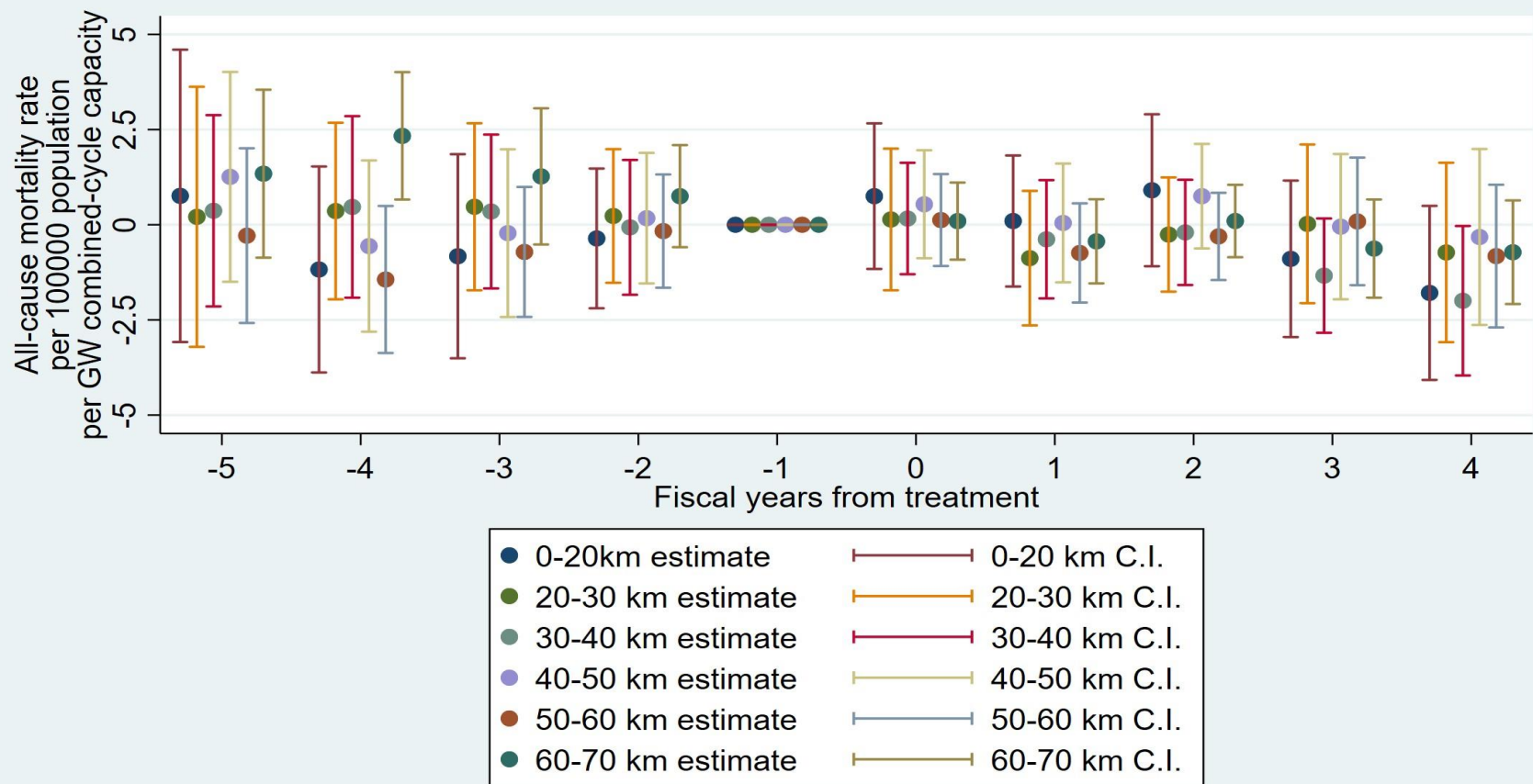

Standard errors are clustered at the (lower tier) local authority level and month; 95% confidence interval shown.

Figure 5: Few changes in ambient NO₂ levels occur near combined-cycle power plants after the implementation of the Carbon Price Support
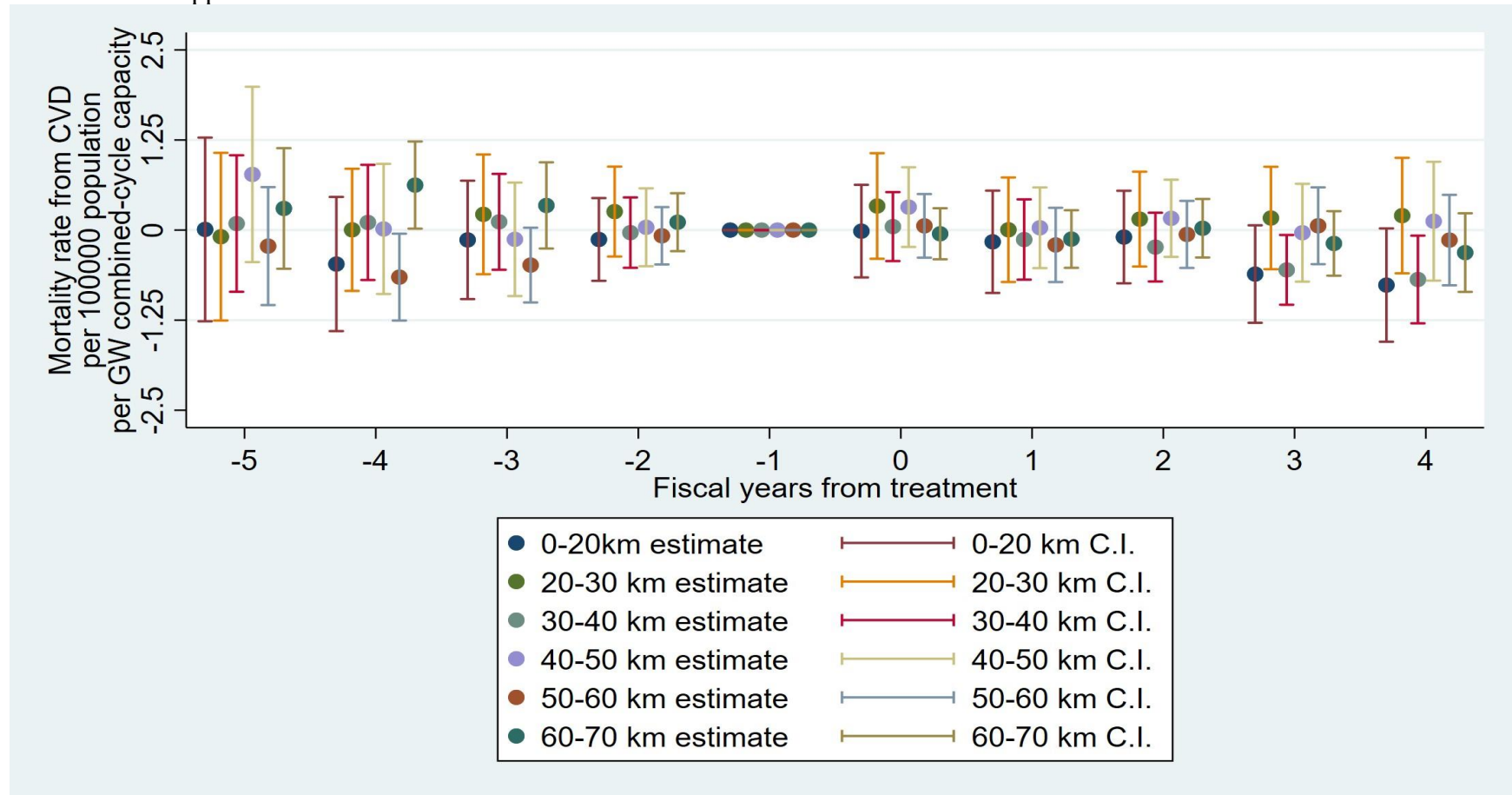

Standard errors are clustered at the (lower tier) local authority level and month; 95% confidence interval shown.

Figure 6: No increases in all-cause mortality occur near combined-cycle power plants after the implementation of the Carbon Price Support

Standard errors are clustered at the (lower tier) local authority level and month; 95% confidence interval shown.

Figure 7: No increases in cardiovascular disease mortality occur near combined-cycle power plants after the implementation of the Carbon Price Support

Standard errors are clustered at the (lower tier) local authority level and month; 95% confidence interval shown.

2.9 Appendix A

I derive the functional form $g(h(x)) = \text{invlogit}(\ln(\frac{P_{gas}}{P_{coal}})) = e^{\ln x}/(1 + e^{\ln x}) = x/$

$(1 + x)$ from the following considerations. The relationship between price ratio and output should follow the shape of the inverse logit function, but the inverse logit has the desired shape over the domain $(-\infty,\infty)$, as opposed to the price ratio which can only take values in the set $(0,\infty)$. Therefore, we need to transform the price ratio with a function $h(x)$ that has domain $(0,\infty)$ and range $(-\infty,\infty)$. The following considerations apply:

- $h(x)$ should have the property that $g(h(1)) - g(h(\frac{1}{x})) = g(h(x)) - g(h(1))$,

to reflect the fact that a price ratio of, say, $\frac{1}{4}$, is as far away from 1 as 1 is to 4.

- Note that $g(0) - g(-h(x)) = g(h(x)) - g(0)$. Comparing this with the desired property $(h(1)) - g(h(\frac{1}{x})) = g(h(x)) - g(h(1))$, the transformation $h(x)$ should have the properties that $h(\frac{1}{x}) = -h(x)$

The natural choice of $h(x)$ is therefore $\ln(x)$, although a logarithm of any base would work. So, $g(h(x)) = g(\ln(x)) = \text{invlogit}(\ln(\frac{P_{gas}}{P_{coal}})) = e^{\ln x}/(1 + e^{\ln x}) = x/(1 + x)$.

Chapter 3

Making up for lost time: The effect of historical pollution on COVID-19 morbidity and mortality

3.1 COVID-19 and air pollution

COVID-19 has wreaked havoc worldwide and in the United States. Unsurprisingly, determining risk factors for COVID-19 infection has been a top priority for the medical and academic communities. Therefore, the relationship between deaths from COVID-19 and levels of air pollution has been a topic of interest.

Understanding the relationship between COVID-19 and air pollution tells policymakers which locations are more vulnerable to COVID-19 and helps them decide how to allocate scarce medical resources. It may also be a mechanism by which other risk factors for COVID-19 operate (Carrington, 7 June 2020). For example, African-Americans have been disproportionately affected by COVID-19 (Yancy, 2020). Since black and Hispanic Americans have also been exposed to higher levels of air pollution (Tessum et al., 2020), a positive relationship between pollution and COVID-19 may be a mechanism by which COVID-19 has disproportionately affected African-Americans.

Exposure to air pollution may increase the likelihood of COVID-19 infection and resulting death. Conticini, Frediani, & Caro (2020) propose a cross-sectional positive correlation between death rates and air pollution in Italy, Wu et. al (2020) find a similar effect for historical air pollution in the United States, and Zhu et al (2020) find a positive association between daily air pollution

and infections in China. In this paper, I build upon these studies by using rich longitudinal variation to identify the COVID-19 – air pollution relationship. Panel data is no panacea, however, and I identify a major omitted variable – the differing times since COVID-19 outbreaks started in each county - that may confound said relationship. I account for this in estimating the effect of historical levels of fine particulate matter (PM2.5) on COVID-19 case rates and death rates. I find that historical levels of PM2.5 increase death rates, but the increase is smaller than previous estimates. At the same time, historical levels of PM2.5 have had no effect on case rates of COVID-19.

In section 2, I discuss the problems arising from ignoring cross-sectional differences when the COVID-19 outbreak started, and solutions to these problems. In section 3, I outline the data and models I use to estimate the COVID-19 – air pollution relationship, and in section 4 I present and discuss the results of these models. I conclude in section 5.

3.2   Issues with modeling the COVID-19 outbreak

Studies of the COVID-19 outbreak in countries like the United States benefit from the ready availability of daily county-level data. The natural way to estimate the effect of policy interventions or protective/risk factors on COVID-19 morbidity and mortality is to run a panel fixed effects regression with county and time fixed effects (Goodman-Bacon & Marcus, 2020). However, this approach comes with certain issues that appear to be underappreciated in the literature.

3.2.1 Date, or time since outbreak started?

It is natural to think of a panel in terms of dates, but this obscures an important issue. Each county's morbidity or mortality rate from COVID-19 depends on how much time has elapsed since the start of the COVID-19 outbreak in that county. Since the outbreak started on different dates in different counties, and because at the time of writing we are still close in time to the start of the COVID-19 outbreak, "time since the start of COVID-19 outbreak" and "date" are substantively different.

This is an important distinction. [40] Consider historical levels of fine particulate matter (mean PM2.5 for each county between 2001 and 2016). By regressing time since first case/death on that variable, we can see that there is a significant correlation between historical mean PM2.5, time since first case was reported, and the time since first death was reported. This correlation is unchanged by the inclusion of date fixed effects because historical mean PM2.5 levels are constant within county. All these estimates are shown in Table 1. This correlation likely exists because polluted urban areas receive more travel – which seeds COVID-19 cases - than rural ones.

This is not solved including a fixed effect for each county which encompasses the (time-constant) date of first case/death (Fowler et al., 2020). [41] The time since date of first case/death is an interaction of the date since first case and the observation date that is not collinear with either.

---

[40] Chowell, Viboud, Hyman and Simonsen (2015) show that the 2014 Ebola outbreak in West Africa grew exponentially over date in the aggregate, but that each district's Ebola outbreak exhibited polynomial growth. If aggregating by date changes the shapes of outbreaks, synthetic control designs that match by calendar date (for instance, Friedson et al. (2020)) may be problematic.

[41] That is impossible for historical mean PM2.5 levels, which do not have time-series variation.

Consider regressing time since first case/death on the presence of state-mandated social distancing measures; results are shown in Table 1. The partial correlation between the implementation of social distancing measures by states and time since first case/death exists after including county and date fixed effects.

In both cases ignoring time since first case/death will lead to omitted variable bias if it is correlated with the outcome of interest. Such a correlation is very likely to exist here. It is hard to think of a variable of interest where a correlation with time since first case/death can be excluded.

A good analogy for the issues caused by COVID-19 outbreaks starting at different times in different places is the event study when the policy of interest starts at different times in different locations. The pre-trends of the event study are checked to identify biases that covary with treatment timing. Because treatment timing is a nonlinear interaction of county and calendar time, these biases are not necessarily eliminated by the inclusion of county and time fixed effects in the event study model.

3.2.2   How should the progression of COVID-19 over time be modeled?

To eliminate the omitted variable bias described above, it is necessary to include time since the outbreak begin in models of COVID-19 spread. But how should this be done? Including time as a covariate only controls for the average partial correlation of time with the dependent variable (Goodman-Bacon & Marcus, 2020), but in this application the partial correlation is likely to vary wildly over time because COVID-19 progression over time is far from linear. Instead, I use parametric models derived from the epidemiology literature.

1.1.1 Morbidity from COVID-19

To model morbidity – the number of cases – of COVID-19, I take inspiration from reduced-form ("phenomenological") epidemiological models of epidemic outbreaks. The progression of COVID-19 cumulative morbidity over time since the start of the outbreak, like many other diseases, is likely best described by a polynomial model (Chowell, Viboud, Simonsen & Moghadas, 2016; Maier & Brockmann, 2020). This is of the form:

$$Cases_{it} = (\frac{r_c}{m_c} t_c + Cases_{i0}^{\frac{1}{m_c}})^{m_c} \qquad (1)$$

Here, $Cases_{it}$ is the cumulative number of cases in county i at time t_c since the first case, r_c is the growth rate per unit of time, and m_c is the polynomial exponent (Chowell, Viboud, Simonsen & Moghadas, 2016). Since the definition of t_c excludes days before the first case was reported, observations before the first case were reported in each county will be dropped from my estimation sample.

Alternatives to the polynomial model are the exponential (Chowell, Viboud, Simonsen & Moghadas, 2016) and logistic (Ma, 2020) models. The polynomial model is a generalization of the exponential model, since as the exponent $m -> \infty$ the polynomial model converges to the exponential one. The logistic model modifies the exponential model to account for saturation, but that is unlikely given that the COVID-19 outbreak will likely go on for decades (Wan and Johnson, 27th May 2020). In Appendix A.1 I show that the polynomial model has the best goodness-of-fit (in terms of adjusted-R^2 and AIC) among these alternatives for US county data.

1.1.2 Mortality from COVID-19

How the severity of COVID-19 infection covaries with historical levels of air pollution is another parameter of interest. The intuitive measure of severity is the case fatality rate (CFR), which is defined as "the proportion of cases of a specified condition that are fatal within a specified time" (Spychalski, Błażyńska-Spychalska & Kobiela, 2020). The natural estimate of CFR with currently available data is:

$$CFR_{it} = Cases_{it}/Deaths_{it} \tag{2}$$

This is, however, subject to potentially severe biases such as time-lag bias (Spychalski, Błażyńska-Spychalska & Kobiela, 2020). Time-lag bias occurs because of the lag between diagnosis and death, so at any time t there are some cases which will progress to death in future but have not died yet.

Instead of trying to estimate CFR, I estimate mortality – the number of deaths – from COVID-19. Rewriting the definition above, we have:

$$Deaths_{it} = CFR_{it} * Cases_{it} \tag{3}$$

Since the proportion CFR_{it} is bounded between 0 and 1 (and in practice is likely much less than 1), $Deaths_{it}$ and $Cases_{it}$ are likely to follow similar shapes over time. In other words, cumulative mortality is likely to follow the process:

$$Deaths_{it} = (\frac{r_d}{m_d}t_d + Deaths_{i0}^{\frac{1}{m_d}})^{m_d} \tag{4}$$

To address time-lag bias, t_d is now defined as the time since first death rather than case. Intuitively, replacing time since first case with time since first death shifts the curve of cases forward by the amount of time it took for the first case in each county to progress to death. As with morbidity, I show in Appendix A.1 that this functional form is preferred over the exponential and logistic models by adjusted-R^2 and AIC. Again, since t_d is undefined before each county's first death, those days are dropped from the estimation sample for deaths.

Using any of these models contrasts with the approach Wu et al. (2020), take. We are estimating different objects; theirs is a snapshot of the effect of historical mean PM2.5 levels on mortality rates at April 22nd, 2020, whereas I estimate how historical mean PM2.5 levels affect the growth rates of COVID-19 morbidity and mortality.

3.3   Data and Methods

3.3.1   Data

My data is a panel of cumulative case counts and deaths for each county of the United States by date up to May 18, 2020, obtained from the New York Times (NYT) COVID-19 tracker (New York Times, 2020). Unlike the alternative Johns Hopkins University Center for Systems Science and Engineering (JHU CSSE) tracker, county-level case and death counts in the NYT tracker are not truncated at March 22, 2020. The confirmed case (deaths) samples comprise all county-day observations with at least 1 confirmed case (death). Summary statistics are available in Table 2.

3.3.2   Model specification

After normalizing morbidity and mortality by 100000 population, I model cumulative morbidity and mortality from COVID-19 as polynomial functions:

$$y_{it} = e^{\alpha}\left(\frac{\beta \log Mean\, PM2.5_i + X_{it}\boldsymbol{\theta}}{m} t + y_{i0}{}^{\frac{1}{m}}\right)^m \varepsilon_{it} \tag{5}$$

Taking the natural logarithm on both sides give us:

$$\log y_{it} = \alpha + m \log\left(\frac{\beta \log Mean\, PM2.5_i + X_{it}\boldsymbol{\theta}}{m} t + y_{i0}{}^{\frac{1}{m}}\right) + \log \varepsilon_{it} \tag{6}$$

I assume the rate of growth r can vary linearly by county-level covariates, and estimate (6) in logged form by nonlinear least squares:

$$\min_{\alpha,m,\beta}\left(\log y_{it} - \left[\alpha + m\left[\log\left(\frac{\beta \log Mean\, PM2.5_i + X_{it}\boldsymbol{\theta}}{m} t + y_{i0}{}^{\frac{1}{m}}\right)\right]\right]\right)^2 \tag{7}$$

Here, y_{it} is county i's cumulative case (death) rate per 100000 population t days since the first day with a non-zero case (death) count. The variable of interest, $Mean\, PM2.5$, is the mean level between 2000 and 2016 of particulate matter less than 2.5 micrometers in diameter. α normalizes the error term to be mean 0, and implies that the first period error term for each county ε_{i0} is normalized to a constant; at $t = 0$, $\log y_{i0} = \alpha + \log y_{i0} + \log \varepsilon_{i0}$, so that $\log \varepsilon_{i0} = -\alpha$ or $\varepsilon_{i0} = e^{-\alpha}$. X is a vector of covariates including 1) an indicator for state-imposed distancing measures, 2) quantiles of population density, 3) % of population aged above 65, aged 45-64 and aged 15-44, 4) % living in poverty, 5) log median house value, 6) log median household income, 7) % black, 8) % Hispanic, 9) % of population with less than a high school education, 10) % of owner-occupied housing, 11) obesity, 12) smoking rate, 13) number of hospital beds per capita, 14) average summer temperatures, 15) average summer relative humidity, 16) average winter

97

temperatures and 17) average winter relative humidity. These 17 variables are the same as those in Wu et al. (2020) and are obtained from their code. [42]

Due to a "laconic" response to COVID-19 by the United States federal government, there have been large differences in response to COVID-19 between different states (Haffajee & Mello, 2020). I include a vector of state-level fixed effects in X to absorb state-level heterogeneity, particularly in COVID-19 policy interventions. Fixed effects for calendar dates are also included to account for the fact that counties enter the sample at different times and the possibility that growth rates change over time.

3.3.3 Robustness checks

To address the possibility that each county's time-series sequence of errors $(\varepsilon_{it})_{t=1}^{T}$ covaries on average with omitted variables, I instrument - using a control function approach - for each county's historical average PM2.5 levels with the fraction of that county experiencing a ground-level thermal inversion at 8 intervals across the day, consistent with the 8 times daily output of the NCEP North American Regional Reanalysis dataset (National Centers for Environmental Prediction/National Weather Service/NOAA/U.S. Department of Commerce, 2005, updated monthly) I use to determine the presence of thermal inversions. Thermal inversions occur when air at higher altitudes is warmer than the air beneath it, preventing convection and trapping pollutants near the ground. I define an inversion as happening when the 2-meter temperature is lower than the temperature at the altitude where air pressure is 25 hectopascals (hPA) lower than surface pressure, except for surface pressures between 700 and 300 hPA where temperatures are

---

[42] https://github.com/wxwx1993/PM_COVID

only available at 50 hPA intervals. A 25 hPA difference corresponds to an altitude difference of about 200 meters.

The control function approach involves first running the "first-stage" regression (Wooldridge, 2012):

$$\log Mean\ PM2.5_i = \boldsymbol{INV_i\theta} + \boldsymbol{Z_{it}\theta} + v_i \tag{8}$$

In this equation, $\boldsymbol{Z_{it}}$ includes all variables in $\boldsymbol{X_{it}}$, as well as t (included as fixed effects) and y_{i0}. Once that equation is estimated, the residuals $\hat{v}_i$ are obtained. These residuals represent the estimated reduced form "endogenous part" of $\log Mean\ PM2.5_i$. Finally, I run a similar polynomial model as earlier:

$$\min_{\alpha,m,\beta,\rho} \left(\log y_{it} - \left[\alpha + \log \left(\frac{\log Mean\ PM2.5_i + \boldsymbol{X_{it}\theta}}{m} t + y_{i0}^{\frac{1}{m}} \right) + p\hat{v} \right] \right)^2 \tag{9}$$

Testing $p = 0$ tests whether $\hat{v}$ appears in the conditional expectation of $\log y_{it}$ (Wooldridge, 2011, p.744). As further robustness checks I interact $\hat{v}$ with t and $\log(t+1)$ to see if $\hat{v}$ has a time-varying effect in the conditional expectation. [43] One requirement for this approach is for thermal inversions to affect mean PM2.5 levels. My instruments are a vector of 8 variables corresponding to the average fraction of each county experiencing a thermal inversion in each 3-hour brackets across the day; the F-stat on the joint test $\boldsymbol{\theta} = 0$ for these instruments in the first stage regression (with standard errors clustered at the state level) is 11. The other requirement, that inversions be independent of omitted variables determining morbidity/mortality, is not testable,

---

[43] These transformations are admittedly ad-hoc. Wooldridge (2011, p.744) notes that testing $\rho = 0$ tests for the presence of $\hat{v}$ in the conditional expectation regardless of how $\hat{v}$ is derived; given the lack of structural assumptions, testing $\rho = 0$ for the interaction term should be similar.

but thermal inversions have frequently been used in the economics literature as instruments for pollution (Arceo, Hanna & Oliva, 2016; Jans, Johansson & Nilsson, 2018; He, Liu & Salvo, 2019; Sager, 2019). It is likely that people disregard the presence of inversions because they have no direct health effects (Arceo, Hanna & Oliva, 2016) and are difficult to observe since they occur hundreds of meters above ground level.

3.4   Results and Discussion

The growth of mortality and morbidity rates follow similar processes; the polynomial exponent m is very similar. These results are reported in Table 3. In either case, m is somewhat above 2, consistent with the values found by Maier and Brockmann (2020) for provinces in China. This result underscores the existence of a correlation between time since first case/death and morbidity/mortality from COVID-19, which in conjunction with the correlations found in Table 1 means that omitted variable bias will be present if time since first case/death is ignored.

The similarity of m for morbidity and mortality is reassuring because it suggests that errors in reporting cases are relatively stable over time. Morbidity rates increasing much faster than mortality rates suggest that the case fatality rate is falling quickly over time. In the absence of a cure for COVID-19, that would presumably be because only the most severe cases were diagnosed with COVID-19 at the start of the outbreak.

I find a significant relationship between historical levels of PM2.5 and mortality rates from COVID-19, with an elasticity of .541, 95% CI (.479, .603) on May 18th, the last day of the sample. [44] Unlike mortality rates, morbidity rates appear, at least in the preferred specification, to be

---

[44] Since the dependent variable is a cumulative rate, averaging over all dates does not produce a meaningful statistic.

unrelated to historical levels of PM2.5. These results are shown in Table 3, where the preferred specification is in the 4th (rightmost) column; the specifications in the other columns give broadly similar results except when state fixed effects are omitted. The coefficients on log(Mean PM2.5), reported above the elasticities, are the effect of an increase in historical mean PM2.5 on the growth rate of cases/deaths. Because of the sample restriction to places with at least one case (death), estimates for morbidity (mortality) only apply to places with at least one case (death); counties with at least one death account for about 91% of the US population. As of May 18th, there were about 90000 deaths from COVID-19 in the United States; if the historical level of pollution were 10% (about 0.85 $\mu g/m^3$) lower, there would have been around 4500 fewer deaths from COVID-19. [45]

Because of the relationship (3), the effect of historical mean PM2.5 levels on log(deaths) can be decomposed as follows:

$$\frac{\partial \log Deaths_{it}}{\partial \log Mean\ PM2.5} = \frac{\partial \log CFR_{it}}{\partial \log Mean\ PM2.5} + \frac{\partial \log Cases_{it}}{\partial \log Mean\ PM2.5} \qquad (10)$$

Since I find an increase in mortality but not morbidity due to historical pollution exposure, my results imply that $\frac{\partial \log Deaths}{\partial \log Mean\ PM2.5}$ is positive and $\frac{\partial \log Cases}{\partial \log Mean\ PM2.5}$ is (statistically) 0. If so, $\frac{\partial \log CFR}{\partial \log Mean\ PM2.5}$ must be positive; pollution exposure makes COVID-19 cases more severe. Such an increase in severity would not be surprising; exposure to PM2.5 is known to damage the respiratory system (Xing et al, 2016).

---

[45] Determining whether these are excess deaths or if these individuals would have died from other conditions in the absence of COVID-19, or the value of the life-years saved, are vexed questions outside the scope of this paper.

The estimates as of May 18th are not comparable with those of Wu et al (2020), which are a snapshot of the effect of mean PM2.5 as of April 22nd, 2020. My estimated elasticity for the same date is .316 (.280, .352). At the (cross-sectional) mean, an increase of $1 \, \mu g/m^3$ in historical PM2.5 averages is about a 12% increase, which implies a 4% mortality increase. This is roughly half of the value Wu et al. (2020) find. Including time since first case in the linear index as a control as in Wu et al. (2020) may not be sufficient to control for the omitted variable bias problem outlined earlier.

I now consider the results of the robustness check using thermal inversions. The control function tests for endogeneity, $\rho=0$, shown in Table 4, are far from rejecting the null of exogeneity of $\log Mean \, PM2.5$, so I do not correct the standard errors for the inclusion of the generated regressor (Wooldridge, 2011 p.412). Although the estimates for the effect of mean PM2.5 are no longer significant, they remain positive and are noisily estimated; the original point estimates are well within the confidence interval. For efficiency reasons, the estimates in Table 3 are therefore preferred.

3.5 Conclusion

Cross-sectional differences in the time the outbreak started are likely to cause omitted variable bias, and this bias remains in panel two-way fixed effects models. This paper estimates the relationship between COVID-19 morbidity and mortality and historical levels of PM2.5 in a panel setting, while identifying and proposing solutions to that bias.

Historical levels of PM2.5 are correlated with when the first COVID-19 case and death was reported in each county. I use polynomial models of disease spread to account for the omitted variable bias. These indicate that historical levels of fine particulate matter have increased death

rates with an elasticity of .541 (.479, .603) as of May 18. These estimates are about half of prior cross-sectional estimates. At the same time, historical PM2.5 levels have had no effect on morbidity rates, suggesting that historical exposure to PM2.5 increases the severity of COVID-19 infection.

It is likely that many variables of interest other than historical PM2.5 levels – for instance, the imposition of social distancing measures - also covary with the start of the COVID-19 outbreak. Omitted variable bias will be present in regressions involving those variables, and controlling for the outbreak-time relationship will be important in making causal inferences.

3.6   References

Arceo, E., Hanna, R., & Oliva, P. (2016). Does the effect of pollution on infant mortality differ between developing and developed countries? Evidence from Mexico City. *The Economic Journal*, 126(591), 257-280. https://doi.org/10 .1111/ecoj.12273

Carrington, D. (2020, June 7). "Omission of air pollution from report on Covid-19 and race 'astonishing'." *The Guardian*. Retrieved from https://www.theguardian.com/environment/2020/jun/07/omission-of-air-pollution-from-report-on-covid-19-and-race-astonishing

Chowell, G., Sattenspiel, L., Bansal, S., & Viboud, C. (2016). Mathematical models to characterize early epidemic growth: A review. *Physics of life reviews*, *18*, 66–97. https://doi.org/10.1016/j.plrev.2016.07.005

Chowell, G., Viboud, C., Hyman, J. M., & Simonsen, L. (2015). The Western Africa ebola virus disease epidemic exhibits both global exponential and local polynomial growth rates. PLoS currents, 7.

Chowell, G., Viboud, C., Simonsen, L., & Moghadas, S. (2016). Characterizing the reproduction number of epidemics with early subexponential growth dynamics. *Journal of the Royal Society, Interface*, 13(123). https://doi.org/10.1098/rsif.2016.0659

Conticini, E., Frediani, B., & Caro, D. (2020). Can atmospheric pollution be considered a co-factor in extremely high level of SARS-CoV-2 lethality in Northern Italy? *Environmental Pollution*, 114465. Advance online publication. https://doi.org/10.1016/j.envpol.2020.114465

Fowler, J.H., Hill, S. J., Obradovich, N., Levin, R. (2020). The Effect of Stay-at-Home Orders on COVID-19 Cases and Fatalities in the United States. medRxiv. https://doi.org/10.1101/2020.04.13.20063628

Friedson, A. I., McNichols, D., Sabia, J. J., & Dave, D. (2020). Did California's shelter-in-place order work? Early coronavirus-related public health effects (No. w26992). National Bureau of Economic Research.

Goodman-Bacon, A. & Marcus, J. (2020). Using Difference-in-Differences to Identify Causal Effects of COVID-19 Policies. *Survey Research Methods*. https://doi.org/10.18148/srm/2020.v14i2.7723

Haffajee, R.L & Mello, M.M (2020). Thinking Globally, Acting Locally — The U.S. Response to Covid-19. *The New England Journal of Medicine*. https://doi.org/10.1056/NEJMp2006740

He, J., Liu, H., & Salvo, A. (2019). Severe air pollution and labor productivity: Evidence from industrial towns in China. *American Economic Journal: Applied Economics*, 11(1), 173-201. https://doi.org/10.1257/app.20170286

Jans, J., Johansson, P., & Nilsson, J. P. (2018). Economic status, air quality, and child health: Evidence from inversion episodes. *Journal of Health Economics*, 61, 220-232. https://doi.org/10.1016/j.jhealeco.2018.08.002

Ma, J. (2020). Estimating epidemic exponential growth rate and basic reproduction number. *Infectious Disease Modelling*, 5, 129–141. https://doi.org/10.1016/j.idm.2019.12.009

New York Times (2020). Coronavirus (Covid-19) Data in the United States. Retrieved from

    https://github.com/nytimes/covid-19-data

Maier, B. F., & Brockmann, D. (2020). Effective containment explains subexponential growth in

    recent confirmed COVID-19 cases in China. *Science*, *368*(6492), 742–746.

    https://doi.org/10.1126/science.abb4557

National Centers for Environmental Prediction/National Weather Service/NOAA/U.S.

    Department of Commerce (2005, updated monthly). NCEP North American Regional

    Reanalysis (NARR). https://rda.ucar.edu/datasets/ds608.0/

Sager, L. (2019). Estimating the effect of air pollution on road safety using atmospheric

    temperature inversions. *Journal of Environmental Economics and Management*, 98,

    102250. https://doi.org/10.1016/j.jeem.2019.102250

Spychalski, P., Błażyńska-Spychalska, A., & Kobiela, J. (2020). Estimating case fatality rates of

    COVID-19. *The Lancet Infectious Diseases*, S1473-3099(20)30246-2. Advance online

    publication. https://doi.org/10.1016/S1473-3099(20)30246-2

Tessum, C. W., Apte, J. S., Goodkind, A. L., Muller, N. Z., Mullins, K. A., Paolella, D. A., ... &

    Hill, J. D. (2019). Inequity in consumption of goods and services adds to racial–ethnic

    disparities in air pollution exposure. *Proceedings of the National Academy of Sciences*,

    116(13), 6001-6006.

Wan, W., Johnson, C. Y. (2020, May 27). "Coronavirus may never go away, even with a vaccine." *The Washington Post.* Retrieved from https://www.washingtonpost.com/health/2020/05/27/coronavirus-endemic/

Wooldridge, J. M. (2011). Econometric Analysis of Cross Section and Panel Data (2nd ed.). MIT Press.

Wooldridge, J. M. (2012). Control Function and Related Methods: Nonlinear Models [PDF slides]. Retrieved from https://www.ifs.org.uk/docs/wooldridge%20session%202.pdf

Wu, X., Nethery, C.N., Sabath, B.M., Braun, D., & Dominici, F. (2020). Exposure to air pollution and COVID-19 mortality in the United States. medRxiv. https://doi.org/10.1101/2020.04.05.20054502

Xing, Y. F., Xu, Y. H., Shi, M. H., & Lian, Y. X. (2016). The impact of PM2.5 on the human respiratory system. *Journal of Thoracic Disease*, *8*(1), E69–E74. https://doi.org/10.3978/j.issn.2072-1439.2016.01.19

Yancy, C.W. (2020). COVID-19 and African Americans. *Journal of the American Medical Association*, 323(19), 1891–1892. doi:10.1001/jama.2020.6548

Zhu, Y.J., Xie, J.G., Huang, F.M,, & Cao, L.Q. (2020). Association between short-term exposure to air pollution and COVID-19 infection: Evidence from China. *Science of The Total Environment*, 138704.

3.7 Tables and Figures

Table 1: Partial correlation between time since first COVID-19 case/death and historical levels of PM2.5

	Time since first case			
Log(Mean PM2.5)	5.82	5.82	-	-
	(3.84, 7.79)	(3.84, 7.79)		
Distancing	32.3	4.50	32.3	4.50
	(30.8, 33.8)	(2.58, 6.42)	(30.8, 33.8)	(2.58, 6.42)
	Time since first death			
Log(Mean PM2.5)	3.92	3.92	-	-
	(2.17, 5.67)	(2.17, 5.67)		
Distancing	13.2	5.25	13.2	5.25
	(11.1, 15.2)	(3.11, 7.38)	(11.1, 15.2)	(3.11, 7.38)
All controls	Y	Y	-	-
State fixed effects	Y	Y	-	-
County fixed effects	-	-	Y	Y
Date fixed effects		Y		Y

Coefficients are from regressions of time since first case and time since first death on log(mean PM2.5 between 2001 and 2016) and an indicator for state-mandated social distancing. Log(mean PM2.5 between 2001 and 2016) does not appear with county fixed effects because it is constant within county. 95% CI in parentheses, all standard errors are clustered at the state level. "All controls' are 1) an indicator for state-imposed distancing measures, 2) quantiles of population density, 3) % of population aged above 65, aged 45-64 and aged 15-44, 4) % living in poverty, 5) log median house value, 6) log median household income, 7) % black, 8) % Hispanic, 9) % of population with less than a high school education, 10) % of owner-occupied housing, 11) obesity, 12) smoking rate, 13) number of hospital beds per capita, 14) average summer temperatures, 15) average summer relative humidity, 16) average winter temperatures and 17) average winter relative humidity.

Table 2: Summary statistics

Dependent variable	Morbidity sample	Mortality sample
	Mean	Mean
	(Standard deviation)	(Standard deviation)
Confirmed cases per 100000 population	128 (352)	236 (501)
COVID deaths per 100000 population	5.10 (15.2)	12.2 (21.6)
Mean PM2.5 (cross-sectional)	8.40 (2.52)	8.40 (2.52)
Mean PM2.5 (sample)	8.78 (2.42)	9.46 (2.21)
Time since first confirmed case	27.7 (17.6)	37.8 (15.6)
Time since first death	9.31 (14.5)	22.0 (14.7)
n	152703	63926
Counties	2876	1658
States	49	49

The morbidity (mortality) samples comprise all county-day observations with at least 1 confirmed case (death). The difference between the cross-sectional and panel PM2.5 means are due to more polluted places spending longer in the sample because they reported their first case earlier.

Table 3: Effect of historical PM2.5 exposure on morbidity and mortality rates using polynomial models

	Log(Morbidity rate)			
Log(Mean PM2.5)	.015	-.010	.081	.028
	(-.093, .124)	(-.082, .062)	(.009, .153)	(-.025, .082)
Average elasticity of Mean PM2.5 on May 18th	.088	-.055	.558	.224
	(-.514, .690)	(-.439, .329)	(.110, 1.01)	(-.176, .625)
m	2.22	2.15	2.38	2.51
	(2.03, 2.41)	(1.94, 2.35)	(2.09, 2.68)	(2.23, 2.79)
	Log(Mortality rate)			
Log(Mean PM2.5)	-.003	.036	.064	.036
	(-.041, .035)	(.008, .064)	(.034, .093)	(.010, .063)
Average elasticity of Mean PM2.5 on May 18th	-.036	.471	.897	.541
	(-.455, .383)	(.122, .821)	(.458, 1.34)	(.479, .603)
m	2.03	2.17	2.30	2.39
	(1.72, 2.33)	(1.86, 2.49)	(1.88, 2.72)	(1.98, 2.81)
All controls	Y	Y		Y
State fixed effects		Y	Y	Y
Date fixed effects			Y	Y

Table shows results from estimating Equation 7. 95% CI in parentheses, all standard errors are clustered at the state level. The coefficients on log(Mean PM2.5), reported above the elasticities, are the effect of an increase in historical mean PM2.5 on the growth rate of cases/deaths. "All controls' are 1) an indicator for state-imposed distancing measures, 2) quantiles of population density, 3) % of population aged above 65, aged 45-64 and aged 15-44, 4) % living in poverty, 5) log median house value, 6) log median household income, 7) % black, 8) % Hispanic, 9) % of population with less than a high school education, 10) % of owner-occupied housing, 11) obesity, 12) smoking rate, 13) number of hospital beds per capita, 14) average summer temperatures, 15) average summer relative humidity, 16) average winter temperatures and 17) average winter relative humidity. Column 3 includes only quantiles of population density, average summer temperatures, average summer relative humidity, average winter temperatures, and average winter relative humidity as covariates.

Table 4: Effect of historical PM2.5 exposure on morbidity and mortality rates in control function polynomial models

	Log(Morbidity rate)		
$\hat{v}$ interacted with:	-	Log(t+1)	t
Log(Mean PM2.5)	-.010	-.017	-.003
	(-.070, .051)	(-.087, .053)	(-.061, .055)
Average elasticity of Mean PM2.5 on May 18th	-.073	-.128	-.023
	(-.526, .379)	(-.648, .392)	(-.452, .405)
ρ	.449	.158	.011
	(-.223, 1.12)	(-.089, .405)	(-.009, .031)
Instrument strength (F-stat)		10.1	
	Log(Mortality rate)		
$\hat{v}$ interacted with:	-	Log(t+1)	t
Log(Mean PM2.5)	.030	.023	.018
	(-.006, .066)	(-.031, .077)	(-.042, .077)
Average elasticity of Mean PM2.5 on May 18th	.440	.341	.259
	(-.071, .952)	(-.438, 1.12)	(-.597, 1.12)
ρ	.130	.079	.012
	(-.518, .778)	(-.256, .413)	(-.029, .054)
Instrument strength (F-stat)		10.6	
All controls	Y	Y	Y
State fixed effects	Y	Y	Y
Date fixed effects	Y	Y	Y

Table shows results from estimating Equation 9. 95% CI in parentheses, all standard errors are clustered at the state level. The coefficients on log(Mean PM2.5), reported above the elasticities, are the effect of an increase in historical mean PM2.5 on the growth rate of cases/deaths. All standard errors are clustered at the state level. "All controls' are 1) an indicator for state-imposed distancing measures, 2) quantiles of population density, 3) % of population aged above 65, aged 45-64 and aged 15-44, 4) % living in poverty, 5) log median house value, 6) log median household income, 7) % black, 8) % Hispanic, 9) % of population with less than a high school education, 10) % of owner-occupied housing, 11) obesity, 12) smoking rate, 13) number of hospital beds per capita, 14) average summer temperatures, 15) average summer relative humidity, 16) average winter temperatures and 17) average winter relative humidity.

3.8   Appendix

Table A.1: Goodness of fit of exponential, sub-exponential and logistic models and effect of historical PM2.5 exposure on morbidity and mortality rates.

	Log(Morbidity rate)		
	Exponential	Sub-exponential	Logistic
Log(Mean PM2.5)	.017	.028	.029
	(.001, .032)	(-.025, .082)	(.009, .049)
Shape parameter	-	2.51	68.0
		(2.23, 2.79)	(51.1, 84.8)
Adjusted R^2	.592	.718	.679
AIC	434458	377701	397482
	Log(Mortality rate)		
	Exponential	Sub-exponential	Logistic
Log(Mean PM2.5)	.046	.037	.051
	(.029, .063)	(.010, .063)	(.033, .069)
Shape parameter	-	2.39	13.4
		(1.98, 2.81)	(8.81, 18.0)
Adjusted R^2	.609	.691	.653
AIC	154962	139923	147469
All controls	Y	Y	Y
State fixed effects	Y	Y	Y
Date fixed effects	Y	Y	Y

95% CI in parentheses, all standard errors are clustered at the state level. The coefficients on log(Mean PM2.5) are the effect of an increase in historical mean PM2.5 on the growth rate of cases/deaths. "All controls' are 1) an indicator for state-imposed distancing measures, 2) quantiles of population density, 3) % of population aged above 65, aged 45-64 and aged 15-44, 4) % living in poverty, 5) log median house value, 6) log median household income, 7) % black, 8) % Hispanic, 9) % of population with less than a high school education, 10) % of owner-occupied housing, 11) obesity, 12) smoking rate, 13) number of hospital beds per capita, 14) average summer temperatures, 15) average summer relative humidity, 16) average winter temperatures and 17) average winter relative humidity.